

KHOVANOV HOMOLOGY AND THE FUKAYA CATEGORY OF THE TRACELESS CHARACTER VARIETY FOR THE TWICE-PUNCTURED TORUS

DAVID BOOZER

ABSTRACT. We describe a strategy for constructing reduced Khovanov homology for links in lens spaces by generalizing a symplectic interpretation of reduced Khovanov homology for links in S^3 due to Hedden, Herald, Hogancamp, and Kirk. The strategy relies on a partly conjectural description of the Fukaya category of the traceless $SU(2)$ character variety of the 2-torus with two punctures. From a diagram of a 1-tangle in a solid torus, we construct a corresponding object (X, δ) in the A_∞ category of twisted complexes over this Fukaya category. The homotopy type of (X, δ) is an isotopy invariant of the tangle diagram. We use (X, δ) to construct cochain complexes for links in S^3 and some links in $S^2 \times S^1$. For links in S^3 , the cohomology of our cochain complex reproduces reduced Khovanov homology, though the cochain complex itself is not the usual one. For links in $S^2 \times S^1$, we present results that suggest the cohomology of our cochain complex may be a link invariant.

CONTENTS

1.	Introduction	1
2.	Preliminary material	6
3.	The Fukaya category of $R^*(T^2, 2)$	8
4.	Twisted complexes corresponding to tangle diagrams	26
5.	Invariance under Reidemeister moves	34
6.	Links in S^3	41
7.	Links in $S^2 \times S^1$	45
Appendix A. The Fukaya category of $R^*(S^2, 4)$		52
Appendix B. Homotopy equivalences		54
References		60

1. INTRODUCTION

Khovanov homology is an invariant of oriented links in S^3 that categorifies the Jones polynomial [16, 17]. An important open problem is to generalize Khovanov homology to links in arbitrary 3-manifolds. Candidate generalizations have been defined for links in certain specific 3-manifolds, including links in I -bundles over arbitrary surfaces by Asaeda, Przytycki, and Sikora [2], links in $S^2 \times S^1$ by Rozansky [22], links in all connected sums of $S^2 \times S^1$ by Willis [25], and links in $\mathbb{R}P^3$ by Gabrovšek [10].

We describe here a strategy for constructing Khovanov homology for links in arbitrary lens spaces. Our strategy is inspired by a symplectic interpretation of Khovanov homology for links in S^3 due to Hedden, Herald, Hogancamp, and Kirk [15], which originated as an outgrowth of their project to construct *pillowcase homology* [13, 14], a symplectic counterpart to Kronheimer and Mrowka's singular instanton link homology [18, 19, 20]. The setup for pillowcase homology is as follows. Given an oriented link L in S^3 , we consider a Heegaard splitting

$$(S^3, L) = (B^3, T_0) \cup_{(S^2, 4)} (B^3, T_1)$$

such that the Heegaard surface $(S^2, 4)$ is a 2-sphere that transversely intersects L in four points, the handlebodies (B^3, T_0) and (B^3, T_1) are closed 3-balls containing 2-tangles T_0 and T_1 , and T_0 is trivial. To the Heegaard surface $(S^2, 4)$ we associate the irreducible locus $R^*(S^2, 4)$ of the traceless $SU(2)$ character variety for the 2-sphere with four punctures, a symplectic manifold known as the *pillowcase*. To the handlebodies

(B^3, T_0) and (B^3, T_1) we associate traceless $SU(2)$ character varieties $R_\pi^{\natural}(B^3, T_0)$ and $R^*(B^3, T_1)$. By pulling back $SU(2)$ representations along the inclusions $(S^2, 4) \hookrightarrow (B^3, T_0)$ and $(S^2, 4) \hookrightarrow (B^3, T_1)$, we obtain maps $R_\pi^{\natural}(B^3, T_0) \rightarrow R^*(S^2, 4)$ and $R^*(B^3, T_1) \rightarrow R^*(S^2, 4)$ of the corresponding character varieties. The images of these maps define Lagrangians L_0 and W_1 in $R^*(S^2, 4)$ that can be viewed as symplectic representations of the tangles T_0 and T_1 . Roughly speaking, and ignoring certain technical complications, the pillowcase homology of (S^3, L) is defined to be the Lagrangian Floer homology of the pair of Lagrangians (L_0, W_1) .

In [15], Hedden, Herald, Hogancamp, and Kirk give a symplectic interpretation of reduced Khovanov homology by modifying the construction used to define pillowcase homology. Instead of working directly with the tangle T_1 , they consider a cube of resolutions of a planar projection of T_1 . The natural setting to symplectically encode this cube of resolutions is the twisted Fukaya category of $R^*(S^2, 4)$. To the cube of resolutions they assign an object (X, δ) of this A_∞ category, where X consists of shifted copies of Lagrangians corresponding to planar tangles at the vertices of the cube and $\delta : X \rightarrow X$ consists of maps of Lagrangians corresponding to saddles at the edges of the cube. They prove:

Theorem 1.1. (*Hedden–Herald–Hogancamp–Kirk [15, Theorem 1.1]*) *Given a planar projection of (B^3, T_1) , there is a corresponding object (X, δ) of the twisted Fukaya category of $R^*(S^2, 4)$. The homotopy type of (X, δ) is an isotopy invariant of T_1 rel boundary.*

To the trivial tangle T_0 they assign an object $(W_0, 0)$ of the twisted Fukaya category. The morphism spaces of the twisted Fukaya category have the structure of cochain complexes, so in particular the space of morphisms from $(W_0, 0)$ to (X, δ) is a cochain complex. They show that this cochain complex is identical to the usual cochain complex for the reduced Khovanov homology $\text{Khr}(L)$ of L , thus proving:

Theorem 1.2. (*Hedden–Herald–Hogancamp–Kirk [15, Corollary 1.2]*) *We have an isomorphism of bigraded vector spaces*

$$\text{Khr}(L) \rightarrow H^*(\text{hom}((W_0, 0), (X, \delta))),$$

where the hom space is taken within the twisted Fukaya category of $R^*(S^2, 4)$.

Theorem 1.2 shows that the Fukaya category of $R^*(S^2, 4)$ knows about Khovanov homology. Our strategy for generalizing Khovanov homology is based on generalizing this observation. Theorem 1.2 is formulated in terms of $R^*(S^2, 4)$ because this is the character variety corresponding to the Heegaard surface $(S^2, 4)$ for the chosen Heegaard splitting of (S^3, L) . More generally, one can split a 3-manifold Y containing a link L along a Heegaard surface (Σ_g, n) of genus g that intersects L in n points. In light of Theorem 1.2, one might hope that the Fukaya category of the corresponding character variety $R^*(\Sigma_g, n)$ contains information that could be used to generalize Khovanov homology to links in Y .

As a first step towards this goal, we consider the case of links in lens spaces. Given an oriented link L in a lens space Y , we consider a Heegaard splitting

$$(Y, L) = (U_0, T_0) \cup_{(T^2, 2)} (U_1, T_1)$$

such that the Heegaard surface $(T^2, 2)$ is a 2-torus that transversely intersects L in two points, the handlebodies (U_0, T_0) and (U_1, T_1) are solid tori containing 1-tangles T_0 and T_1 , and T_0 is trivial. To the Heegaard surface $(T^2, 2)$ we associate the irreducible locus $R^*(T^2, 2)$ of the traceless $SU(2)$ character variety for the torus with two punctures. We project (U_1, T_1) onto the plane to obtain a 1-tangle diagram T in the annulus, as shown in Figure 1. One of the two boundary points of the 1-tangle diagram lies on the inner bounding circle of the annulus and the other lies on the outer bounding circle. We define the *loop number* ℓ of the tangle diagram to be the number of arcs that loop around the annulus. We would like to encode the cube of resolutions of the tangle diagram T as an object (X, δ) of the twisted Fukaya category of $R^*(T^2, 2)$.

Our first task is thus to understand the relevant structure of the Fukaya category of $R^*(T^2, 2)$. We can explicitly describe the Lagrangians that are needed to construct the object X corresponding to the planar tangles at the vertices of the cube of resolutions, and we can describe the morphism spaces for pairs of Lagrangians, the generators of which are needed to construct the endomorphism $\delta : X \rightarrow X$. However, to verify that (X, δ) is indeed an object of the twisted Fukaya category, and to construct cochain complexes from the morphism spaces of the twisted Fukaya category, we also need to know certain A_∞ operations, which are obtained by counting pseudo-holomorphic disks in $R^*(T^2, 2)$, and these operations are more difficult to describe. In the case of $(S^2, 4)$, the character variety $R^*(S^2, 4)$ is two-dimensional, so the relevant A_∞

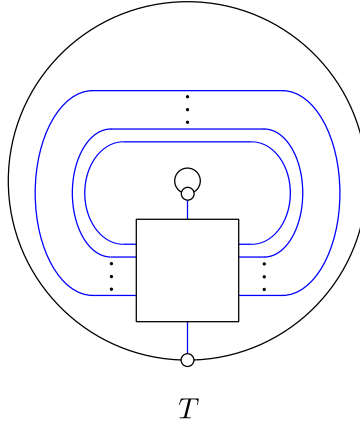


FIGURE 1. A planar projection of (U_1, T_1) yields a 1-tangle diagram T in the annulus. One of the two boundary points of T lies on the inner bounding circle of the annulus and the other lies on the outer bounding circle. For simplicity, we will usually omit these bounding circles when depicting tangle diagrams.

operations can be computed combinatorially using the Riemann mapping theorem. But $R^*(T^2, 2)$ is four-dimensional, and with our current methods we are unable to compute the operations we need. Instead, we conjecture these operations based on the information we do have. One useful guide in this process is that the Fukaya categories of $R^*(T^2, 2)$ and $R^*(S^2, 4)$ appear to be closely related. For example, we show that $R^*(S^2, 4)$ is a symplectic submanifold of $R^*(T^2, 2)$. The A_∞ operations that we conjecture for $R^*(T^2, 2)$ are natural generalizations of the known A_∞ operations for $R^*(S^2, 4)$. Our hope is that the information we have regarding the Lagrangians and morphism spaces, together with the conjectured A_∞ operations, will provide the necessary clues to generalize reduced Khovanov homology.

The first step towards this goal is to generalize Theorem 1.1 for $R^*(S^2, 4)$. We prove:

Theorem 1.3. *If the A_∞ operations of $R^*(T^2, 2)$ are as conjectured, then given a planar projection T of (U_1, T_1) there are two corresponding objects (X, δ_+) and (X, δ_-) of the twisted Fukaya category of $R^*(T^2, 2)$. The homotopy type of (X, δ_\pm) is an invariant of T_1 rel boundary.*

The twisted complex (X, δ_\pm) has several unusual features. The complex is constructed from a cube of resolutions of the 1-tangle diagram T whose vertices are planar 1-tangles. Each planar 1-tangle contains an arc component connecting the boundary points on the outer and inner bounding circles of the annulus. By orienting the arc component so it is directed outer-to-inner, we can distinguish between saddles that split/merge circle components from/with the left and right sides of the arc component. In the twisted complex (X, δ_\pm) , the differentials corresponding to such *left* and *right* saddles are distinct. Also, the circle components that are split or merged by left and right saddles can enclose additional circle components, and the differentials corresponding to left and right saddles act nontrivially on vector space factors corresponding to the enclosed circle components. So, there is a sense in which the differential δ for our twisted complex is *nonlocal*.

Our next task is to generalize Theorem 1.2 by using the twisted objects (X, δ_+) and (X, δ_-) to reproduce the reduced Khovanov homology for links in S^3 . Given an oriented 1-tangle diagram T in the annulus, we can construct links L_{T+} and L_{T-} in S^3 by closing T with an overpass arc A_+ or underpass arc A_- , as shown in Figure 2. The handlebodies for the arcs A_+ and A_- correspond to Lagrangians W_+ and W_- in $R^*(T^2, 2)$, and hence to twisted objects $(W_+, 0)$ and $(W_-, 0)$. We define bigraded cochain complexes

$$(C_\pm, \partial_\pm) = \text{hom}((W_\pm, 0), (X, \delta_\pm)).$$

We use the conjectured A_∞ relations to explicitly construct (C_\pm, ∂_\pm) from the cube of resolutions of T . The cohomology of the cochain complex (C_\pm, ∂_\pm) is shown in [8] to reproduce the reduced Khovanov homology for the link $L_{T\pm}$:

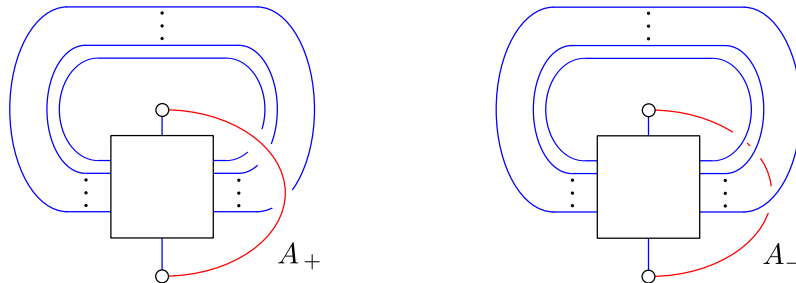


FIGURE 2. We can close a 1-tangle diagram T with an overpass arc A_+ or underpass arc A_- to obtain a link diagram. The link diagram can be interpreted as the planar projection of either a link $L_{T\pm}$ in S^3 or a link L_{T^0} in $S^2 \times S^1$.

Theorem 1.4. (Boozer [8]) *There is an isomorphism of bigraded vector spaces*

$$\text{Khr}(L_{T\pm}) \rightarrow H^*((C_{\pm}, \partial_{\pm})).$$

The cochain complex $(C_{\pm}, \partial_{\pm})$ is typically not the same as the usual cochain complex for the reduced Khovanov homology of $L_{T\pm}$, though the two complexes do agree for tangle diagrams with loop number 0. For example, the complex $(C_{\pm}, \partial_{\pm})$ has *long differentials* corresponding to pairs of successive saddles in the cube of resolutions of T . The complex $(C_{\pm}, \partial_{\pm})$ can be smaller than the usual complex, since crossings between the overpass or underpass arc and the tangle diagram are not included in the cube of resolutions. Example cochain complexes for the unknot and right trefoil are given in Sections 6.3 and 6.4.

From Theorem 1.4, we obtain the following generalization of Theorem 1.2:

Theorem 1.5. *If the A_{∞} operations of $R^*(T^2, 2)$ are as conjectured, then there are isomorphisms of bigraded vector spaces*

$$\text{Khr}(L_{T\pm}) \rightarrow H^*(\text{hom}((W_{\pm}, 0), (X, \delta_{\pm}))).$$

where the hom space is taken within the twisted Fukaya category of $R^*(T^2, 2)$.

We next turn our attention to links in $S^2 \times S^1$. Given an oriented 1-tangle diagram T in the annulus, we can construct links L'_{T+} and L'_{T-} in $S^2 \times S^1$ by closing T with an overpass arc A_+ or underpass arc A_- , as shown in Figure 2. The links L'_{T+} and L'_{T-} are isotopic, since one can isotope A_+ to A_- by moving A_+ around the S^2 factor, and we will let L_{T^0} denote either of these isotopic links. The handlebodies for the arcs A_+ and A_- correspond to the same Lagrangian W_0 in $R^*(T^2, 2)$. We define a bigraded cochain complex

$$(C_0, \partial_0) = \text{hom}((W_0, 0), (X, \delta_-)).$$

For a 1-tangle diagram T with loop number $\ell \in \{0, 2\}$, we use the conjectured A_{∞} relations to explicitly construct (C_0, ∂_0) from the cube of resolutions of T .

One might hope that the cohomology of (C_0, ∂_0) depends only on the isotopy class of the link L_{T^0} and not on its description as the closure of the particular tangle diagram T . From Theorem 1.3, it follows that the cohomology is an isotopy invariant of the tangle diagram T . But it is possible for nonisotopic tangle diagrams T_1 and T_2 to yield isotopic links $L_{T_1^0}$ and $L_{T_2^0}$ in $S^2 \times S^1$, and example calculations show that in this situation the cohomology for T_1 and T_2 need not be the same. In all the examples we have checked, however, the dependence on the tangle diagram is reflected only in the bigradings of generators, and the cohomology does agree if we collapse bigradings from \mathbb{Z} to \mathbb{Z}_2 . Several specific examples are described in Sections 7.3, 7.4, and 7.5. On the basis of such examples, we make the following conjecture:

Conjecture 1.6. *The cohomology of the cochain complex (C_0, ∂_0) with bigradings collapsed from \mathbb{Z} to \mathbb{Z}_2 is an isotopy invariant of the link L_{T^0} .*

We prove an invariance result in support of Conjecture 1.6. Given a 1-tangle diagram T with loop number 2, we define a 1-tangle diagram T_{τ} by adding a full twist to T as shown in Figure 3. The diagrams T and T_{τ} are typically not isotopic, but the corresponding links L_{T^0} and $L_{T_{\tau}^0}$ in $S^2 \times S^1$ are isotopic, since one can

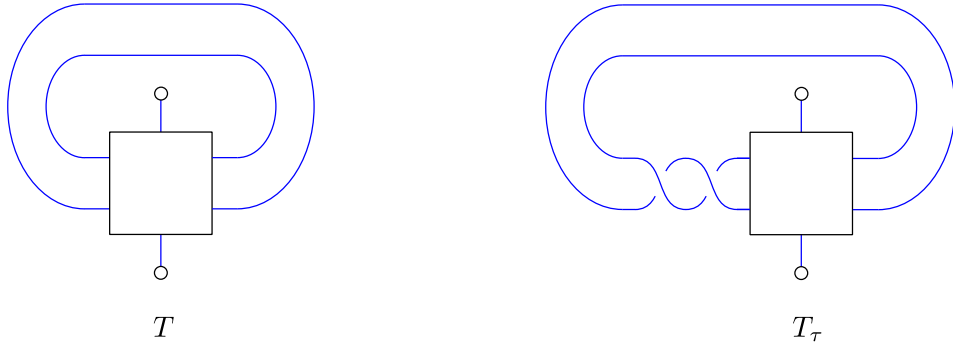


FIGURE 3. Given a 1-tangle diagram T with loop number 2, we add a full twist to obtain a 1-tangle diagram T_τ .

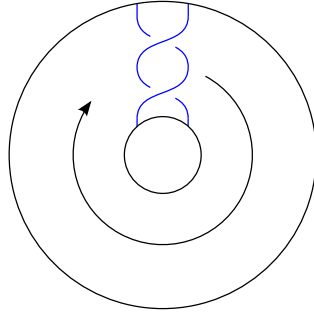


FIGURE 4. The inner and outer circles represent two copies of S^2 that are identified to give $S^2 \times S^1$. We can unwind the full twist in the indicated link in $S^2 \times S^1$ by moving one of the strands around the S^2 factor.

unwind the full twist in T_τ by moving one of the strands around the S^2 factor as shown in Figure 4. Let (C_0, ∂_0) and $(C_0^\tau, \partial_0^\tau)$ denote the cochain complex for T and T_τ . We prove:

Theorem 1.7. *With bigradings collapsed from \mathbb{Z} to \mathbb{Z}_2 , there is an isomorphism of bigraded vector spaces*

$$H^*((C_0, \partial_0)) \rightarrow H^*((C_0^\tau, \partial_0^\tau)).$$

If the cohomology of (C_0, ∂_0) with bigradings collapsed to \mathbb{Z}_2 is indeed an isotopy invariant of L_{T^0} , there is a sense in which it is a natural generalization of the reduced Khovanov homology for links in S^3 . Consider a tangle diagram T with loop number 0. The corresponding link L_{T^0} can be contained inside an open 3-ball in $S^2 \times S^1$. By collapsing the complement of the open 3-ball to a point, we obtain a link L'_{T^0} in S^3 . We prove:

Theorem 1.8. *There is an isomorphism of bigraded vector spaces*

$$V \otimes \text{Khr}(L'_{T^0}) \rightarrow H^*((C_0, \partial_0)),$$

where V is a two-dimensional bigraded vector space.

Theorem 1.8 does not hold at the level of cochain complexes; that is, the cochain complex (C_0, ∂_0) is generally not the tensor product of V with the usual cochain complex for the reduced Khovanov homology of L'_{T^0} .

If the cohomology of (C_0, ∂_0) with bigradings collapsed to \mathbb{Z}_2 is not an isotopy invariant of L_{T^0} , it may still be of interest due to a possible relationship to Kronheimer and Mrowka's singular instanton link homology. Given a knot K in S^3 , Kronheimer and Mrowka show in [18] that there is a spectral sequence whose E_2 page is the reduced Khovanov homology of the mirror knot K^m and that converges to the singular instanton

homology of K . Singular instanton homology is closely related to Lagrangian Floer homology in character varieties of punctured surfaces. For example, generating sets for the singular instanton homology of knots in a 3-manifold Y can be constructed from Lagrangian intersections in $R^*(S^2, 4)$ when $Y = S^3$, as described in [13], and in $R^*(T^2, 2)$ when Y is a lens space, as described in [7]. Thus, one might conjecture that there is a spectral sequence from the cohomology of (C_0, ∂_0) to the singular instanton homology of the corresponding link in $S^2 \times S^1$ that would generalize Kronheimer and Mrowka's spectral sequence for links in S^3 .

The paper is organized as follows. In Section 2, we review the material we will need regarding the group $SU(2)$ and A_∞ categories. In Section 3, we describe the character variety $R^*(T^2, 2)$ and its Fukaya category. In Section 4, we show how to construct an object (X, δ) in the twisted Fukaya category of $R^*(T^2, 2)$ from an oriented 1-tangle diagram T in the annulus. In Section 5, we show that the homotopy type of (X, δ) is an isotopy invariant of the corresponding tangle diagram T . In Section 6, we prove Theorem 1.4 for links in S^3 . In Section 7, we prove Theorems 1.7 and 1.8 for links in $S^2 \times S^1$. In Appendix A, we describe the character variety $R^*(S^2, 4)$ and compare it with $R^*(T^2, 2)$. In Appendix B, we fill in some technical details in the proof of Theorem 1.7.

2. PRELIMINARY MATERIAL

2.1. The group $SU(2)$. We briefly review here some facts about the group $SU(2)$. We define the Pauli spin matrices:

$$\sigma_x = \begin{pmatrix} 0 & 1 \\ 1 & 0 \end{pmatrix}, \quad \sigma_y = \begin{pmatrix} 0 & -i \\ i & 0 \end{pmatrix}, \quad \sigma_z = \begin{pmatrix} 1 & 0 \\ 0 & -1 \end{pmatrix}.$$

We define $SU(2)$ matrices \mathbf{i} , \mathbf{j} , and \mathbf{k} :

$$\mathbf{i} = -i\sigma_x, \quad \mathbf{j} = -i\sigma_y, \quad \mathbf{k} = -i\sigma_z.$$

These matrices satisfy the quaternion multiplication laws:

$$\mathbf{i}^2 = \mathbf{j}^2 = \mathbf{k}^2 = \mathbf{ijk} = -\mathbb{1}.$$

Any $SU(2)$ matrix A can be uniquely expressed as

$$A = t\mathbb{1} + x\mathbf{i} + y\mathbf{j} + z\mathbf{k},$$

where $(t, x, y, z) \in S^3 = \{(t, x, y, z) \in \mathbb{R}^4 \mid t^2 + x^2 + y^2 + z^2 = 1\}$. We can thus identify $SU(2)$ with the unit quaternions. We will refer to $t\mathbb{1}$ and $x\mathbf{i} + y\mathbf{j} + z\mathbf{k}$ as the *scalar* and *vector* parts of the matrix A . Note that $\text{tr } A = 2t$, so traceless $SU(2)$ matrices are precisely those for which the scalar part is zero.

We define a surjective group homomorphism $SU(2) \rightarrow SO(3)$ by $g \mapsto (\hat{v} \mapsto \hat{v}')$, where the unit vectors $\hat{v} = (v_x, v_y, v_z)$ and $\hat{v}' = (v'_x, v'_y, v'_z)$ are related by

$$g(v_x\mathbf{i} + v_y\mathbf{j} + v_z\mathbf{k})g^{-1} = v'_x\mathbf{i} + v'_y\mathbf{j} + v'_z\mathbf{k}.$$

In general, conjugating an arbitrary $SU(2)$ matrix preserves the scalar part of the matrix and rotates the vector part of the matrix:

$$g(t\mathbb{1} + r_x\mathbf{i} + r_y\mathbf{j} + r_z\mathbf{k})g^{-1} = t\mathbb{1} + r'_x\mathbf{i} + r'_y\mathbf{j} + r'_z\mathbf{k},$$

where (r'_x, r'_y, r'_z) is given by multiplying (r_x, r_y, r_z) by the $SO(3)$ matrix corresponding to $g \in SU(2)$.

2.2. A_∞ categories. We briefly review here the material we will need regarding A_∞ categories. For a more extensive discussion of this material, see Section 2 of [15] or the book [23]. We define \mathbb{F} to be the field of two elements.

An A_∞ category consists of a set of objects $\{a_i\}$, for each pair of objects (a_i, a_j) an integer-graded \mathbb{F} -vector space $\text{hom}_{\mathcal{A}}(a_i, a_j)$ called the *space of morphisms from a_i to a_j* , and for each integer $m \geq 1$ a linear *structure map*, also called an *operation*, with grading $2 - m$:

$$\mu_{\mathcal{A}}^m : \text{hom}_{\mathcal{A}}(a_{m-1}, a_m) \otimes \cdots \otimes \text{hom}_{\mathcal{A}}(a_0, a_1) \rightarrow \text{hom}_{\mathcal{A}}(a_0, a_m).$$

The structure maps are required to satisfy certain relations, which we do not describe here. The first relation asserts that the endomorphism $\mu_{\mathcal{A}}^1 : (a_0, a_1) \rightarrow (a_0, a_1)$ squares to zero:

$$\mu_{\mathcal{A}}^1(\mu_{\mathcal{A}}^1(f)) = 0.$$

If $\mu_{\mathcal{A}}^m = 0$ for $m \neq 2$, the relations reduce to a single relation asserting the associativity of $\mu_{\mathcal{A}}^2$:

$$\mu_{\mathcal{A}}^2(\mu_{\mathcal{A}}^2(h, g), f) = \mu_{\mathcal{A}}^2(h, \mu_{\mathcal{A}}^2(g, f)).$$

An important example of an A_∞ category is the category Ch of cochain complexes over \mathbb{F} . The objects of Ch are pairs (C, d) consisting of an integer-graded \mathbb{F} -vector space C and an endomorphism $d : C \rightarrow C$ with grading 1 such that $d \circ d = 0$. We define $\text{hom}_{\text{Ch}}((C_1, d_1), (C_2, d_2))$ to be the graded \mathbb{F} -vector space of all linear maps $C_1 \rightarrow C_2$. We define structure maps μ_{Ch}^1 and μ_{Ch}^2 such that

$$\mu_{\text{Ch}}^1(f) = d_2 \circ f + f \circ d_1, \quad \mu_{\text{Ch}}^2(g, f) = g \circ f$$

for $f : (C_1, d_1) \rightarrow (C_2, d_2)$ and $g : (C_2, d_2) \rightarrow (C_3, d_3)$. We define $\mu_{\text{Ch}}^m = 0$ for $m > 2$.

Given an A_∞ category \mathcal{A} , we define an A_∞ category $\Sigma\mathcal{A}$ called the *additive enlargement* of \mathcal{A} . The objects of $\Sigma\mathcal{A}$ are pairs $(I, \{(a_i, V_i) \mid i \in I\})$, where I is a finite indexing set and for each $i \in I$ the pair (a_i, V_i) consists of an object a_i of \mathcal{A} and an integer-graded \mathbb{F} -vector space V_i . For simplicity, we will denote such an object of $\Sigma\mathcal{A}$ as

$$\bigoplus_{i \in I} (a_i \otimes V_i).$$

The morphism spaces of $\Sigma\mathcal{A}$ are given by

$$\text{hom}_{\Sigma\mathcal{A}}\left(\bigoplus_{i \in I} a_i \otimes V_i, \bigoplus_{j \in J} a_j \otimes V_j\right) = \bigoplus_{i \in I, j \in J} \text{hom}_{\mathcal{A}}(a_i, a_j) \otimes \text{hom}_{\mathbb{F}}(V_i, V_j).$$

The A_∞ operation $\mu_{\Sigma\mathcal{A}}^n$ is given by applying the operation $\mu_{\mathcal{A}}^n$ to the $\text{hom}_{\mathcal{A}}(a_i, a_j)$ factors and composing the $\text{hom}_{\mathbb{F}}(V_i, V_j)$ factors.

Given an A_∞ category \mathcal{A} , we define an A_∞ category $\text{Tw}\mathcal{A}$ called the *category of twisted complexes over* \mathcal{A} . The objects of $\text{Tw}\mathcal{A}$ are pairs (X, δ) , where X is an object of $\Sigma\mathcal{A}$ and $\delta \in \text{hom}_{\Sigma\mathcal{A}}(X, X)$ is homogeneous with grading 1 and satisfies

$$\sum_m \mu_{\Sigma\mathcal{A}}^m(\delta, \dots, \delta) = 0.$$

We also require that X admit a filtration with respect to which δ is strictly lower triangular. The morphism spaces of $\text{Tw}\mathcal{A}$ are given by

$$\text{hom}_{\text{Tw}\mathcal{A}}((X, \delta_X), (Y, \delta_Y)) = \text{hom}_{\Sigma\mathcal{A}}(X, Y).$$

The A_∞ operations $\mu_{\text{Tw}\mathcal{A}}^m$ for $\text{Tw}\mathcal{A}$ can be expressed in terms of the A_∞ operations $\mu_{\mathcal{A}}^m$ for \mathcal{A} . If $\mu_{\mathcal{A}}^m = 0$ for $m \neq 2$, then $\mu_{\text{Tw}\mathcal{A}}^m = 0$ for $m > 2$ and we have

$$\mu_{\text{Tw}\mathcal{A}}^1(F) = \mu_{\Sigma\mathcal{A}}^2(\delta_Y, F) + \mu_{\Sigma\mathcal{A}}^2(F, \delta_X), \quad \mu_{\text{Tw}\mathcal{A}}^2(G, F) = \mu_{\Sigma\mathcal{A}}^2(G, F)$$

for $F : (X, \delta_X) \rightarrow (Y, \delta_Y)$ and $G : (Y, \delta_Y) \rightarrow (Z, \delta_Z)$.

An A_∞ functor $\mathcal{F} : \mathcal{A} \rightarrow \mathcal{B}$ of A_∞ categories \mathcal{A} and \mathcal{B} is an assignment of an object $\mathcal{F}(a_i)$ of \mathcal{B} for each object a_i of \mathcal{A} , and for each integer $m \geq 1$ a linear map of grading $1 - m$:

$$\mathcal{F}^m : \text{hom}_{\mathcal{A}}(a_{m-1}, a_m) \otimes \dots \otimes \text{hom}_{\mathcal{A}}(a_0, a_1) \rightarrow \text{hom}_{\mathcal{B}}(\mathcal{F}(a_0), \mathcal{F}(a_m)).$$

The maps \mathcal{F}^m are required to satisfy certain conditions, which we do not describe here.

Given an object b of an A_∞ category \mathcal{A} , one can define an A_∞ functor $\mathcal{G}_b : \mathcal{A} \rightarrow \text{Ch}$. On objects, we have

$$\mathcal{G}_b(a) = (\text{hom}_{\mathcal{A}}(b, a), \mu_{\mathcal{A}}^1).$$

The linear maps \mathcal{G}_b^m are given by

$$\begin{aligned} \mathcal{G}_b^m &: \text{hom}_{\mathcal{A}}(a_{m-1}, a_m) \otimes \dots \otimes \text{hom}_{\mathcal{A}}(a_0, a_1) \rightarrow \text{hom}_{\text{Ch}}(\mathcal{G}_b(a_0), \mathcal{G}_b(a_m)), \\ x_m \otimes \dots \otimes x_1 &\mapsto \mu_{\mathcal{A}}^{m+1}(x_m, \dots, x_1, -). \end{aligned}$$

One can extend the A_∞ functor $\mathcal{G}_b : \mathcal{A} \rightarrow \text{Ch}$ to an A_∞ functor $\text{Tw}\mathcal{G}_b : \text{Tw}\mathcal{A} \rightarrow \text{Ch}$. On objects, we have

$$(\text{Tw}\mathcal{G}_b)((X, \delta)) = (C, d + \partial),$$

where the graded \mathbb{F} -vector space C and endomorphisms $d, \partial : C \rightarrow C$ are defined as follows. The object X of $\Sigma\mathcal{A}$ has the form

$$X = \bigoplus_{i \in I} a_i \otimes V_i.$$

For each $i \in I$, we define a cochain complex

$$(C_i, d_i) = \mathcal{G}_b(a_i) = (\text{hom}_{\mathcal{A}}(b, a_i), \mu_{\mathcal{A}}^1).$$

We define

$$C = \bigoplus_{i \in I} C_i \otimes V_i, \quad d = \sum_{i \in I} d_i \otimes \mathbb{1}_{V_i}, \quad \partial = \sum_{m=1}^{\infty} \mathcal{G}_b^m(\delta, \dots, \delta) = \sum_{m=2}^{\infty} \mu_{\Sigma\mathcal{A}}^m(\delta, \dots, \delta, -).$$

The differential for the cochain complex $(C, d + \partial)$ combines the differential d , which is due to the structure map $\mu_{\mathcal{A}}^1$ for \mathcal{A} , and the map ∂ , which is due to the endomorphism $\delta : X \rightarrow X$ that constitutes part of the data of the twisted object (X, δ) .

3. THE FUKAYA CATEGORY OF $R^*(T^2, 2)$

3.1. The character variety $R^*(T^2, 2)$. Consider a surface S with n marked points p_1, \dots, p_n . We define a punctured surface $S^\circ = S - \{p_1, \dots, p_n\}$. We define the traceless $SU(2)$ character variety $R(S, n)$ to be the set of conjugacy classes of $SU(2)$ representations of the fundamental group $\pi_1(S^\circ)$ that map loops around the punctures to traceless matrices. We say that a representation $\rho : \pi_1(S^\circ) \rightarrow SU(2)$ is *irreducible* if the image of ρ is a nonabelian subgroup of $SU(2)$ and *reducible* otherwise. We define the *irreducible locus* $R^*(S, n)$ of $R(S, n)$ to be the set of conjugacy classes of irreducible representations. The set $R^*(S, n)$ has the structure of a smooth manifold with a canonical symplectic form.

We consider here the character variety $R(T^2, 2)$, whose topology is described in [7]. We define fundamental cycles A and B of T^2 and loops a and b around the punctures p_1 and p_2 . A presentation of the fundamental group of $T^2 - \{p_1, p_2\}$ is

$$\pi_1(T^2 - \{p_1, p_2\}) = \langle A, B, a, b \mid [A, B]ab = 1 \rangle.$$

We can specify a representation $\pi_1(T^2 - \{p_1, p_2\}) \rightarrow SU(2)$ by specifying the images of the generators (A, B, a, b) . The character variety $R(T^2, 2)$ is thus given by

$$R(T^2, 2) = \{(A, B, a, b) \in SU(2)^4 \mid [A, B]ab = \mathbb{1}, \text{tr } a = \text{tr } b = 0\} / \text{conjugation},$$

where for simplicity we use the same notation for generators of $\pi_1(T^2 - \{p_1, p_2\})$ and their images under a given representation. The character variety $R(T^2, 2)$ and its irreducible locus $R^*(T^2, 2)$ can be also be interpreted as moduli spaces of semistable and stable parabolic bundles over an elliptic curve with two marked points. Using this interpretation, one can show that $R(T^2, 2)$ and $R^*(T^2, 2)$ can be given the structure of complex manifolds isomorphic to $(\mathbb{C}\mathbb{P}^1)^2$ and the complement of a holomorphically embedded elliptic curve in $(\mathbb{C}\mathbb{P}^1)^2$, respectively [24]. In particular, the irreducible locus $R^*(T^2, 2)$ has the structure of a smooth manifold of real dimension 4.

It is useful to define a subset

$$R_3(T^2, 2) = \{ab = \mathbb{1}\}$$

of $R(T^2, 2)$. Note that $ab = \mathbb{1}$ is invariant under conjugation, so $R_3(T^2, 2)$ is well-defined. We define $R_3^*(T^2, 2)$ to be the irreducible locus of $R_3(T^2, 2)$. As we will see, the set $R_3^*(T^2, 2)$ has the structure of a submanifold of $R^*(T^2, 2)$ of real dimension 3.

We define coordinates on $R_3(T^2, 2)$ as follows. Given a point $[A, B, a, b]$ of $R_3(T^2, 2)$, we can always choose a representative of the form

$$(1) \quad A = \cos \alpha \mathbb{1} + \sin \alpha \mathbf{k}, \quad B = \cos \beta \mathbb{1} + \sin \beta \mathbf{k}, \quad a = b^{-1} = \cos s \mathbf{i} + \sin s \mathbf{k}.$$

The parameters (α, β, s) are subject to 2π -periodicity identifications, as well as the identifications

$$(\alpha, \beta, s) \sim (-\alpha, -\beta, -s), \quad (\alpha, \beta, s) \sim (\alpha, \beta, \pi - s),$$

which follow from the fact that we can conjugate (A, B, a, b) by \mathbf{i} or \mathbf{k} to obtain an equivalent representative. Conjugation by \mathbf{j} does not yield an independent identification, since $\mathbf{ijk} = -\mathbb{1}$. For points (α, β, s) for which $\sin \alpha = \sin \beta = 0$, we have the additional identification

$$(\alpha, \beta, s) \sim (\alpha, \beta, 0),$$

since in this case we can conjugate (A, B, a, b) so as to force $a = b^{-1} = \mathbf{k}$. We will use (α, β, s) , subject to these identifications, as standard coordinates on $R_3(T^2, 2)$.

It is also useful to define a subset

$$R_2(T^2, 2) = R_3(T^2, 2) \cap \{s = 0\}$$

of $R(T^2, 2)$. We define $R_2^*(T^2, 2)$ to be the irreducible locus of $R_2(T^2, 2)$. Setting $s = 0$ in equation (1) for the standard coordinates (α, β, s) on $R_3(T^2, 2)$, we find that points $[A, B, a, b]$ of $R_2(T^2, 2)$ have the form

$$(2) \quad A = \cos \alpha \mathbb{1} + \sin \alpha \mathbf{k}, \quad B = \cos \beta \mathbb{1} + \sin \beta \mathbf{k}, \quad a = b^{-1} = \mathbf{i}.$$

The standard coordinates (α, β, s) on $R_3(T^2, 2)$ restrict to coordinates (α, β) on $R_2(T^2, 2)$. The identifications for (α, β, s) restrict to 2π -periodicity identifications for (α, β) , as well as the identification

$$(\alpha, \beta) \sim (-\alpha, -\beta).$$

From the identifications on the coordinates (α, β) , it follows that $R_2(T^2, 2)$ is homeomorphic to S^2 . From equation (2), it follows that the reducible locus of $R_2(T^2, 2)$ is the set $\{\sin \alpha = \sin \beta = 0\}$, which consists of four points. Thus the irreducible locus $R_2^*(T^2, 2)$ is diffeomorphic to a sphere minus four points, as shown in Figure 7.

To visualize $R_3(T^2, 2)$, we define a homeomorphic space Y :

$$Y = \{(\alpha, \beta, z) \mid \alpha \in [0, 2\pi], \beta \in [0, \pi], |z| \leq \sin^2 \alpha + \sin^2 \beta\} / \sim,$$

where the equivalence relation \sim is defined such that

$$(\alpha, 0, z) \sim (2\pi - \alpha, 0, -z), \quad (\alpha, \pi, z) \sim (2\pi - \alpha, \pi, -z), \quad (0, \beta, z) \sim (2\pi, \beta, z).$$

A specific homeomorphism $R_3(T^2, 2) \rightarrow Y$ is given by

$$(\alpha, \beta, s) \mapsto (\alpha, \beta, (\sin^2 \alpha + \sin^2 \beta)(\sin s)).$$

We note that Y , hence $R_3(T^2, 2)$, is compact with boundary homeomorphic to T^2 . A specific homeomorphism $T^2 \rightarrow \partial R_3(T^2, 2)$ is given by $(e^{i\alpha}, e^{i\beta}) \mapsto [A, B, a, b]$, where

$$A = \cos \alpha \mathbb{1} + \sin \alpha \mathbf{k}, \quad B = \cos \beta \mathbb{1} + \sin \beta \mathbf{k}, \quad a = b^{-1} = \mathbf{k}.$$

From equation (1), it follows that the reducible and irreducible loci of $R_3(T^2, 2)$ are its boundary and interior.

We would like to extend the standard coordinates (α, β, s) on $R_3^*(T^2, 2)$ to a system of coordinates defined on a neighborhood of $R_3^*(T^2, 2)$ in $R^*(T^2, 2)$. There are two natural extensions:

Theorem 3.1. *We have coordinates $(\alpha_1, \beta_1, s_1, t_1)$ defined on a neighborhood of $R_3^*(T^2, 2) \cap \{\sin \alpha \neq 0\}$:*

$$\begin{aligned} A &= \cos \alpha_1 \mathbb{1} + \sin \alpha_1 \mathbf{k}, \\ B &= \cos t_1 \cos \beta_1 \mathbb{1} + \sin t_1 \mathbf{i} + \cos t_1 \sin \beta_1 \mathbf{k}, \\ a &= \cos s_1 \cos \theta_1 \mathbf{i} + \cos s_1 \sin \theta_1 \mathbf{j} + \sin s_1 \mathbf{k}, \\ b &= (ABA^{-1}B^{-1}a)^{-1}, \end{aligned}$$

where

$$\theta_1 = \alpha_1 + \beta_1 - \arcsin(\cos \alpha_1 \tan s_1 \tan t_1).$$

Proof. A calculation shows that the matrices (A, B, a, b) satisfy the constraint $[A, B]ab = \mathbb{1}$ and thus represent a point in $R(T^2, 2)$. Comparing the above matrices with the definition of the standard coordinates (α, β, s) on $R_3^*(T^2, 2)$ in equation (1), we see that if $t_1 = 0$ then $[A, B, a, b]$ lies in $R_3^*(T^2, 2)$ and

$$(\alpha, \beta, s) = (\alpha_1, \beta_1, s_1).$$

It follows that $\{\partial_{\alpha_1}, \partial_{\beta_1}, \partial_{s_1}\}$ are linearly independent on $R_3^*(T^2, 2)$. Since irreducibility is an open condition, for sufficiently small values of $|t_1|$ the point $(\alpha_1, \beta_1, s_1, t_1)$ lies in $R^*(T^2, 2)$. Define a function $f^4 : R(T^2, 2) \rightarrow \mathbb{R}$:

$$f^4 = -\frac{1}{4}(\text{tr } Aa + \text{tr } Ab).$$

A calculation shows that the first derivatives of f^4 are given by

$$\begin{aligned} (\partial_{\alpha_1} f^4)(\alpha, \beta, s, 0) &= 0, & (\partial_{\beta_1} f^4)(\alpha, \beta, s, 0) &= 0, \\ (\partial_{s_1} f^4)(\alpha, \beta, s, 0) &= 0, & (\partial_{t_1} f^4)(\alpha, \beta, s, 0) &= \sin^2 \alpha \cos s. \end{aligned}$$

So $\{\partial_{\alpha_1}, \partial_{\beta_1}, \partial_{s_1}, \partial_{t_1}\}$ are linearly independent on $R_3^*(T^2, 2) \cap \{\sin \alpha \neq 0\}$. \square

Theorem 3.2. *We have coordinates $(\alpha_2, \beta_2, s_2, t_2)$ defined on a neighborhood of $R_3^*(T^2, 2) \cap \{\sin \beta \neq 0\}$:*

$$\begin{aligned} A &= \cos t_2 \cos \alpha_2 \mathbb{1} + \sin t_2 \mathbf{i} + \cos t_2 \sin \alpha_2 \mathbf{k}, \\ B &= \cos \beta_2 \mathbb{1} + \sin \beta_2 \mathbf{k}, \\ a &= \cos s_2 \cos \theta_2 \mathbf{i} + \cos s_2 \sin \theta_2 \mathbf{j} + \sin s_2 \mathbf{k}, \\ b &= (ABA^{-1}B^{-1}a)^{-1}, \end{aligned}$$

where

$$\theta_2 = \alpha_2 + \beta_2 - \arcsin(\cos \beta_2 \tan s_2 \tan t_2).$$

Proof. The proof is similar to the proof of Theorem 3.1, only we now define a function $h^4 : R(T^2, 2) \rightarrow \mathbb{R}$:

$$h^4 = \frac{1}{4}(\text{tr } Ba + \text{tr } Bb).$$

A calculation shows that the first derivatives of h^4 are given by

$$\begin{aligned} (\partial_{\alpha_2} h^4)(\alpha, \beta, s, 0) &= 0, & (\partial_{\beta_2} h^4)(\alpha, \beta, s, 0) &= 0, \\ (\partial_{s_2} h^4)(\alpha, \beta, s, 0) &= 0, & (\partial_{t_2} h^4)(\alpha, \beta, s, 0) &= \sin^2 \beta \cos s. \end{aligned}$$

So $\{\partial_{\alpha_2}, \partial_{\beta_2}, \partial_{s_2}, \partial_{t_2}\}$ are linearly independent on $R_3^*(T^2, 2) \cap \{\sin \beta \neq 0\}$. \square

For both systems, the coordinates $(\alpha_k, \beta_k, s_k, t_k)$ are subject to 2π -periodicity identifications together with the identifications

$$(3) \quad (\alpha_k, \beta_k, s_k, t_k) \sim (-\alpha_k, -\beta_k, -s_k, t_k), \quad (\alpha_k, \beta_k, s_k, t_k) \sim (\alpha_k, \beta_k, \pi - s_k, -t_k),$$

which follow from the fact that we can conjugate (A, B, a, b) by \mathbf{i} or \mathbf{k} to obtain an equivalent representative. Conjugation by \mathbf{j} does not yield an independent identification, since $\mathbf{ijk} = -\mathbb{1}$.

3.2. The character variety $R^*(S^2, 4)$. The Fukaya category of $R^*(T^2, 2)$ appears to be closely related to the Fukaya category of the pillowcase $R^*(S^2, 4)$. We review here some well-known results regarding $R^*(S^2, 4)$ and describe its relationship to $R^*(T^2, 2)$.

The topology of $R(S^2, 4)$ is discussed in [13]. As a set, the character variety $R(S^2, 4)$ consists of conjugacy classes $SU(2)$ representations of the fundamental group of $S^2 - \{p_1, p_2, p_3, p_4\}$ that map loops around the punctures to traceless matrices. We define loops a, b, c, d around the punctures p_1, p_2, p_3, p_4 . A presentation for the fundamental group of $S^2 - \{p_1, p_2, p_3, p_4\}$ is

$$\pi_1(S^2 - \{p_1, p_2, p_3, p_4\}) = \langle a, b, c, d \mid ba = cd \rangle.$$

The character variety $R(S^4, 4)$ is thus given by

$$R(S^2, 4) = \{(a, b, c, d) \in SU(2)^4 \mid ba = cd, \text{tr } a = \text{tr } b = \text{tr } c = \text{tr } d = 0\} / \text{conjugation},$$

where for simplicity we use the same notation for generators of $\pi_1(S^2 - \{p_1, p_2, p_3, p_4\})$ and their image under a given representation. The character variety $R(S^2, 4)$ and its irreducible locus $R^*(S^2, 4)$ can also be interpreted as moduli spaces of semistable and stable parabolic bundles over \mathbb{CP}^1 with four marked points. Using this interpretation, one can show that $R(S^2, 4)$ and $R^*(S^2, 4)$ can be given the structure of complex

manifolds isomorphic to \mathbb{CP}^1 and the complement of four points in \mathbb{CP}^1 , respectively. In particular, the irreducible locus $R^*(S^2, 4)$ has the structure of a smooth manifold diffeomorphic to S^2 minus four points.

We define coordinates on $R(S^2, 4)$ as follows. Given a point $[a, b, c, d]$ of $R(S^2, 4)$, one can always choose a representative of the form

$$(4) \quad a = \mathbf{i}, \quad b = \cos \gamma \mathbf{i} + \sin \gamma \mathbf{j}, \quad c = \cos \theta \mathbf{i} + \sin \theta \mathbf{j}, \quad d = c^{-1}ba.$$

The parameters (γ, θ) are subject to 2π -periodicity identifications, as well as the identification

$$(\gamma, \theta) \sim (-\gamma, -\theta),$$

which follows from conjugation by \mathbf{i} . We will use (γ, θ) as standard coordinates on $R(S^2, 4)$. From the identifications on the coordinates (γ, θ) , it follows that $R(S^2, 4)$ is homeomorphic to S^2 . From equation (4) it follows that the reducible locus of $R(S^2, 4)$ is the set $\{\sin \gamma = \sin \theta = 0\}$, which consists of four points.

Since the identifications imposed on the coordinates (γ, θ) for $R(S^2, 4)$ are the same as the identifications imposed on the coordinates (α, β) for $R_2(T^2, 2)$, we can define a homeomorphism $R(S^2, 4) \rightarrow R_2(T^2, 2)$, $(\gamma, \theta) \mapsto (\alpha, \beta)$. The homeomorphism restricts to a diffeomorphism $R^*(S^2, 4) \rightarrow R_2^*(T^2, 2)$ of the irreducible loci.

3.3. Symplectic form on $R^*(T^2, 2)$. The irreducible locus $R^*(S, n)$ of the character variety $R(S, n)$ for a surface S with n marked points is a smooth manifold with a canonical symplectic form [12]. The existence of the canonical symplectic form is due to the fact that the character variety can be interpreted as the Hamiltonian reduction of the space of connections on a trivial rank two complex vector bundle over the surface with respect to the action of a group of gauge transformations. The space of connections has the structure of an infinite-dimensional symplectic manifold, as was first noted by Atiyah and Bott [3]. To compute the symplectic form on $R^*(T^2, 2)$, we will use the formalism of *quasi-Hamiltonian reduction* described in [1]. For our purposes, it will suffice to compute the restriction of the symplectic form to the submanifold $R_3^*(T^2, 2)$.

Theorem 3.3. *The restriction of the canonical symplectic form on $R^*(T^2, 2)$ to $R_3^*(T^2, 2) \cap \{\sin \alpha \neq 0\}$ is*

$$\omega = d\alpha_1 \wedge d\beta_1 + \sin \alpha_1 ds_1 \wedge dt_1.$$

The restriction of the canonical symplectic form on $R^(T^2, 2)$ to $R_3^*(T^2, 2) \cap \{\sin \beta \neq 0\}$ is*

$$\omega = d\alpha_2 \wedge d\beta_2 - \sin \beta_2 ds_2 \wedge dt_2.$$

Proof. A general expression for the symplectic form on the character variety $R^*(S, n)$ is given in Theorem 9.3 of [1]. We apply this formula to the case of $R^*(T^2, 2)$. For our application we use the Lie group $G = SU(2)$ and its Lie algebra $\mathfrak{g} = \mathfrak{su}(2)$. Define the Killing form $(-, -)$ on \mathfrak{g} such that

$$(x, y) = -\frac{1}{2} \operatorname{tr} xy.$$

Define left-invariant and right-invariant Maurer-Cartan forms $\theta, \bar{\theta} \in \Omega^1(G, \mathfrak{g})$. At the point $g \in G$, we have

$$\theta_g = g^{-1} dg, \quad \bar{\theta}_g = dg g^{-1}.$$

From Theorem 9.3 of [1], it follows that the canonical symplectic form on $R^*(T^2, 2)$ is given by

$$\omega = \frac{1}{2}(A^*\theta, B^*\bar{\theta}) + \frac{1}{2}(A^*\bar{\theta}, B^*\theta) + \frac{1}{2}((AB)^*\theta, (A^{-1}B^{-1})^*\bar{\theta}) + \frac{1}{2}(b^*\theta, (ABA^{-1}B^{-1})^*\bar{\theta}).$$

We substitute for the matrices (A, B, a, b) using the coordinate systems described in Theorems 3.1 and 3.2 to obtain the result. \square

A similar computation gives the canonical symplectic form on $R^*(S^2, 4)$ that is used in [15]:

Theorem 3.4. *The canonical symplectic form on $R^*(S^2, 4)$ is $d\gamma \wedge d\theta$.*

In Section 3.2 we defined a diffeomorphism $R^*(S^2, 4) \rightarrow R_2^*(T^2, 2)$, $(\gamma, \theta) \mapsto (\alpha, \beta)$. Theorems 3.3 and 3.4 give:

Theorem 3.5. *The diffeomorphism $R^*(S^2, 4) \rightarrow R_2^*(T^2, 2)$ is a symplectomorphism.*

3.4. Hamiltonian perturbation. We will want to perturb Lagrangians in $R^*(T^2, 2)$ by applying a small Hamiltonian flow, which we refer to as a *Hamiltonian pushoff*. We define a Hamiltonian function $H : R^*(T^2, 2) \rightarrow \mathbb{R}$ by

$$(5) \quad H = \frac{1}{2}(\text{tr } A + \eta \text{tr } B).$$

On the submanifold $R_3^*(T^2, 2)$, we can express the Hamiltonian in terms of the standard coordinates (α, β, s) :

$$H|_{R_3^*(T^2, 2)} = \cos \alpha + \eta \cos \beta.$$

We note that the Hamiltonian flow fixes the symplectic submanifold $R_2^*(T^2, 2)$ as a set. From the expression for the Hamiltonian given in equation (5) and the symplectic form given in Theorem 3.3, it follows that the Hamiltonian flow equations for the coordinates (α, β) on $R_2^*(T^2, 2)$ are

$$\dot{\alpha} = \partial_\beta H = -\eta \sin \beta, \quad \dot{\beta} = -\partial_\alpha H = \sin \alpha.$$

We will choose $\eta = 0.2$ and evolve in time by $\tau = -0.2$ for each Hamiltonian pushoff.

3.5. The mapping class group. Given an orientable surface S with n distinct marked points p_1, \dots, p_n , we define the *mapping class group* $\text{MCG}_n(S)$ to be the group of isotopy classes of orientation-preserving homeomorphisms of S that fix $\{p_1, \dots, p_n\}$ as a set. We define the *pure mapping class group* $\text{PMCG}_n(S)$ to be the subgroup of $\text{MCG}_n(S)$ that fixes the individual points p_1, \dots, p_n .

The mapping class group $\text{MCG}_n(S)$ acts on the character variety $R(S, n)$ and its irreducible locus $R^*(S, n)$. The action is defined as follows. Choose a basepoint $x_0 \in S^\circ = S - \{p_1, \dots, p_n\}$. We first define a homomorphism from $\text{MCG}_n(S)$ to $\text{Out}(\pi_1(S^\circ, x_0))$, the group of outer automorphisms of the fundamental group $\pi_1(S^\circ, x_0)$. Given an element $[\phi] \in \text{MCG}_n(S)$ represented by a homeomorphism $\phi : S^\circ \rightarrow S^\circ$, we have an induced homomorphism $\phi_* : \pi_1(S^\circ, x_0) \rightarrow \pi_1(S^\circ, \phi(x_0))$, $[\alpha] \mapsto [\alpha \circ \phi]$. We choose a path $\gamma : I \rightarrow S^\circ$ from x_0 to $\phi(x_0)$ and define an induced isomorphism $\pi_1(S^\circ, x_0) \rightarrow \pi_1(S^\circ, \phi(x_0))$, $[\alpha] \mapsto [\gamma \alpha \bar{\gamma}]$. We now define $f : \text{MCG}_n(S) \rightarrow \text{Out}(\pi_1(S^\circ, x_0))$, $[\phi] \mapsto [\gamma_* \phi_*]$. One can show that f is independent of the choice of representative ϕ and path γ , and is hence well-defined, and is a homomorphism. We define a left action of $\text{MCG}_n(S)$ on the character variety $R(S, n)$ by

$$[\phi] \cdot [\rho] = [\rho \circ \tilde{f}([\phi])^{-1}],$$

where $\tilde{f}([\phi])$ is an automorphism of $\pi_1(S^\circ, x_0)$ representing $f([\phi])$. The action fixes the irreducible locus $R^*(S, n)$ of $R(S, n)$ as a set, so we can restrict the action to $R^*(S, n)$. One can show that the action of $\text{MCG}_n(S)$ on $R^*(S, n)$ is symplectic.

Here we describe the group $\text{MCG}_2(T^2)$ and its action on $R(T^2, 2)$. Presentations for mapping class groups are described in [9, 11, 21], and more details regarding the case $(T^2, 2)$ can be found in [7]. For our purposes it will suffice to consider the pure mapping class group $\text{PMCG}_2(T^2)$. The pure mapping class group is generated by Dehn twists about the simple closed curves a, A, b , and B shown in Figure 5. For simplicity, we will use the same notation for the curves and the corresponding Dehn twists. We denote the inverse Dehn twists by $\bar{a}, \bar{A}, \bar{b}, \bar{B}$. We have:

Theorem 3.6. *The pure mapping class group $\text{PMCG}_2(T^2)$ is generated by the Dehn twists a, A, b , and B , with relations*

$$\bar{a}b\bar{a} = \bar{b}a\bar{b}, \quad \bar{A}B\bar{A} = \bar{B}A\bar{B}, \quad aA = Aa, \quad (\bar{b}aA)^4 = 1, \quad \bar{a}Ba = \bar{A}bA.$$

The relations in Theorem 3.6 can be used to derive the additional relation in $\text{PMCG}_2(T^2)$:

$$bB = Bb.$$

The fact that b and B commute is intuitively clear, since b and B describe Dehn twists around nonintersecting cycles.

The pure mapping class group is closely related to the pure braid group, which we define as follows. Given a surface S , we define the *configuration space for n ordered points*

$$\text{Conf}_n(S) = \{(x_1, \dots, x_n) \in S^n \mid x_i \neq x_j \text{ if } i \neq j\}.$$

Given a surface S and n distinct marked points p_1, \dots, p_n , we define the *pure braid group* $\text{PB}_n(S)$ to be the fundamental group of $\text{Conf}_n(S)$ with basepoint (p_1, \dots, p_n) . Presentations for braid groups are described in

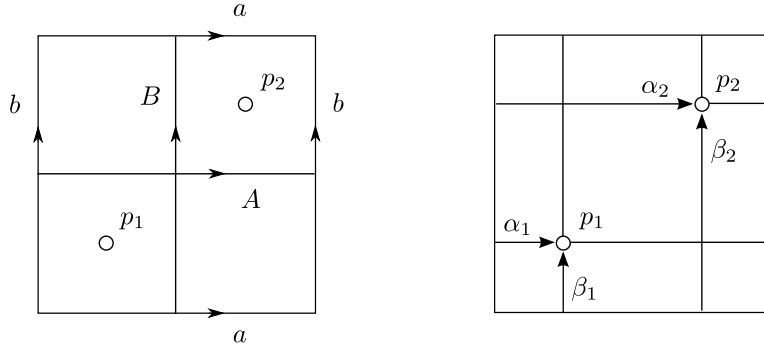


FIGURE 5. Dehn twists a , A , b , and B that generate $\text{PMCG}_2(T^2)$ and braids α_1 , α_2 , β_1 , and β_2 that generate $\text{PB}_2(T^2)$.

[6]. The pure braid group $\text{PB}_2(T^2)$ is generated by braids α_i and β_i for $i = 1, 2$ that drag the marked point p_i rightward and upward around cycles parallel to a and b , as shown in Figure 5.

We have a group homomorphism $\text{PB}_2(S) \rightarrow \text{PMCG}_2(S)$ called the *push map*. Intuitively, to obtain the image of a braid under the push map we view S as an elastic membrane and push the marked points along the braid until they return to their starting locations. The map from the initial to the final state of the membrane gives a homeomorphism of S that represents image of the braid under the push map. The push map $\text{PB}_2(T^2) \rightarrow \text{PMCG}_2(T^2)$ is given by

$$\alpha_1 \mapsto a\bar{A}, \quad \beta_1 \mapsto b\bar{B}, \quad \alpha_2 \mapsto \bar{a}A, \quad \beta_2 \mapsto \bar{b}B.$$

For simplicity, we will use the same notation for elements of $\text{PB}_2(T^2)$ and their images in $\text{PMCG}_2(T^2)$ under the push map.

We define an element s of $\text{PMCG}_2(T^2)$ by

$$s = \alpha_1 \bar{a} b \bar{a} = \bar{A} b \bar{a}.$$

Roughly speaking, if we view T^2 as a square with opposite edges identified, the element s rotates the square counterclockwise by $\pi/2$. We can use the relations in Theorem 3.6 to derive the following relations:

$$s^4 = 1, \quad s\alpha_1 s^{-1} = \beta_1, \quad s\beta_1 s^{-1} = \alpha_1^{-1}.$$

The action of $\text{PMCG}_2(T^2)$ on $R(T^2, 2)$ is described explicitly in [7]. Using this description, one can show:

Lemma 3.7. *The action of α_1^2 fixes $R_2^*(T^2, 2)$ as a set. The action of α_1^2 on the coordinates (α, β) is given by*

$$(\alpha, \beta) \mapsto (\alpha, \pi + \beta - 2\alpha).$$

3.6. Lagrangians. Our goal in this section is to define Lagrangians in $R^*(T^2, 2)$ corresponding to solid tori containing trivial 1-tangles. Given a trivial 1-tangle that winds n times around the solid torus, we will define a corresponding noncompact embedded Lagrangian W_n and a compact immersed Lagrangian L_n . In Section 4 we will use these Lagrangians to construct objects in the twisted Fukaya category of $R^*(T^2, 2)$ corresponding to planar 1-tangle diagrams in the annulus.

Consider a solid torus U_1 containing the trivial tangle T_1 shown in Figure 6(a). We define the *unperturbed character variety* $R(U_1, T_1)$ to be the set of conjugacy classes of homomorphisms $\pi_1(U_1 - T_1) \rightarrow \text{SU}(2)$ that map loops around T_1 to traceless matrices. We define $R^*(U_1, T_1)$ to be the irreducible locus of $R(U_1, T_1)$. The set $R(U_1, T_1)$ has the structure of a smooth manifold with boundary, as described by the following result:

Theorem 3.8. (Boozer [7, Theorem 3.11]) *The unperturbed character variety $R(U_1, T_1)$ is diffeomorphic to the closed unit disk D^2 . The reducible and irreducible loci of $R(U_1, T_1)$ are its boundary and interior.*



FIGURE 6. (a) Handlebody corresponding to the unperturbed Lagrangian W_0 . (b) Handlebody corresponding to the unperturbed Lagrangian W_1 .

An explicit diffeomorphism $R(U_1, T_1) \rightarrow D^2 = \{(x, y) \in \mathbb{R}^2 \mid x^2 + y^2 \leq 1\}$ is given in [7]. We define coordinates $(\chi, \psi) \in (0, \pi) \times (-\pi/2, \pi/2)$ on the irreducible locus $R^*(U_1, T_1)$ by

$$\chi = \pi - \cos^{-1} x \in (0, \pi), \quad \psi = \sin^{-1} \left(\frac{y}{\sqrt{1-x^2}} \right) \in (-\pi/2, \pi/2).$$

We define a map $R^*(U_1, T_1) \rightarrow R^*(T^2, 2)$ by pulling back representations along the inclusion $T^2 - \{p_1, p_2\} \hookrightarrow U_1 - T_1$. We define the *unperturbed Lagrangian* W_0 to be the image of this map. We define $W_0(\chi, \psi) \in R^*(T^2, 2)$ to be the image of the point in $R^*(U_1, T_1)$ with coordinates (χ, ψ) .

Theorem 3.9. (Boozer [7, Theorem 3.13]) *The map $R^*(U_1, T_1) \rightarrow R^*(T^2, 2)$ is an injective immersion. The Lagrangian W_0 lies in $R_3^*(T^2, 2)$ and is given by*

$$W_0 = \{B = \mathbb{1}\} = R_3^*(T^2, 2) \cap \{\beta = 0\}.$$

The point $W_0(\chi, \psi) = [A, B, a, b] \in R^*(T^2, 2)$ is given by

$$A = \cos \chi + \sin \chi \mathbf{k}, \quad B = \mathbb{1}, \quad a = b^{-1} = \cos \psi \mathbf{i} + \sin \psi \mathbf{k}.$$

The point $W_0(\chi, \psi)$ lies in $R_3^*(T^2, 2)$ and has coordinates

$$(\alpha, \beta, s)(W_0(\chi, \psi)) = (\chi, 0, \psi).$$

The Lagrangian W_0 is an open disk, and hence noncompact. We will often prefer to work with compact Lagrangians. To obtain a compact Lagrangian, we first modify the unperturbed character variety $R(U_1, T_1)$ by introducing additional structure. We introduce an *earring* and a *holonomy perturbation* to yield a *perturbed character variety* $R_\pi^\natural(U_1, T_1)$. These modifications are motivated by considerations from gauge theory and are discussed in [7]; the precise details will not be needed here. The set $R_\pi^\natural(U_1, T_1)$ has the structure of a smooth manifold described by the following result:

Theorem 3.10. (Boozer [7, Theorem 3.15]) *The perturbed character variety $R_\pi^\natural(U_1, T_1)$ is diffeomorphic to S^2 . All points of $R_\pi^\natural(U_1, T_1)$ are irreducible.*

An explicit diffeomorphism $R_\pi^\natural(U_1, T_1) \rightarrow S^2 = \{(x, y, z) \in \mathbb{R}^3 \mid x^2 + y^2 + z^2 = 1\}$ is given in [7]. We define spherical-polar coordinates $(\phi, \theta) \in [0, \pi] \times [0, 2\pi]$ on $R_\pi^\natural(U_1, T_1)$ by

$$x = \sin \phi \cos \theta, \quad y = \sin \phi \sin \theta, \quad z = \cos \phi.$$

We define a pullback map $R_\pi^\natural(U_1, T_1) \rightarrow R^*(T^2, 2)$ and define the *perturbed Lagrangian* L_0 to be its image. We define $L_0(\phi, \theta) \in R^*(T^2, 2)$ to be the image of the point in $R_\pi^\natural(U_1, T_1)$ with coordinates (ϕ, θ) . We define the *double-point* $p_D \in R^*(T^2, 2)$ to be the point $[A, B, a, b] = [\mathbf{k}, \mathbb{1}, \mathbf{i}, -\mathbf{i}]$. The point p_D lies in $R_3^*(T^2, 2)$ and has coordinates

$$(\alpha, \beta, s)(p_D) = (\pi/2, 0, 0).$$

Theorem 3.11. (Boozer [7, Theorem 3.17]) *The map $R_\pi^{\natural}(U_1, T_1) \rightarrow R^*(T^2, 2)$ is an immersion and is injective except at the north pole ($\phi = 0$) and south pole ($\phi = \pi$) of $R_\pi^{\natural}(U_1, T_1) = S^2$, which are both mapped to the double-point p_D . The point $L_0(\phi, \theta) = [A, B, a, b] \in R^*(T^2, 2)$ is given by*

$$\begin{aligned} A &= (\cos^2 \nu + \sin^2 \nu \sin^2 \theta)^{-1/2} (\cos \nu \mathbf{i} + \sin \nu \sin \theta \mathbf{k}) (\cos \phi + \sin \phi (\cos \theta \mathbf{i} + \sin \theta \mathbf{j})), \\ B &= \cos \nu + \sin \nu (\cos \theta \mathbf{i} + \sin \theta \mathbf{j}), \\ a &= \mathbf{k}, \\ b &= (\cos^2 \nu + \sin^2 \nu \sin^2 \theta)^{-1} (\sin 2\nu \sin \theta \mathbf{i} - (\cos^2 \nu - \sin^2 \nu \sin^2 \theta) \mathbf{k}), \end{aligned}$$

where

$$\nu = \epsilon \sin \phi$$

and $\epsilon > 0$ is a small control parameter that determines the strength of the holonomy perturbation. The point $L_0(\phi, \theta)$ lies in $R_3^*(T^2, 2)$ if and only if $\theta \in \{0, \pi\}$, and the coordinates of such points are

$$(\alpha, \beta, s)(L_0(\phi, 0)) = (\phi + \pi/2, \nu, 0).$$

In the limit $\epsilon \rightarrow 0$ in which the holonomy perturbation goes to zero, we can relate the perturbed Lagrangian L_0 to the unperturbed Lagrangian W_0 . Recall that we have explicit diffeomorphisms $R(U_1, T_1) \rightarrow D^2$ and $R_\pi^{\natural}(U_1, T_1) \rightarrow S^2$. If we view D^2 as the equatorial disk of S^2 , we can define a map $R_\pi^{\natural}(U_1, T_1) \rightarrow R(U_1, T_1)$ by orthogonally projecting S^2 to D^2 along the z -axis. Using the results of Theorems 3.9 and 3.11, a straightforward calculation gives the following result:

Theorem 3.12. *In the limit $\epsilon \rightarrow 0$ in which the holonomy perturbation goes to zero, we have a commutative diagram*

$$\begin{array}{ccc} R_\pi^{\natural}(U_1, T_1) & & \\ \downarrow & \searrow & \\ R(U_1, T_1) & \longrightarrow & L_0 = W_0. \end{array}$$

We define an unperturbed Lagrangian W_n and a perturbed Lagrangian L_n by acting on W_0 and L_0 with the braid group element α_1^n :

$$W_n = \alpha_1^n \cdot W_0, \quad L_n = \alpha_1^n \cdot L_0.$$

The Lagrangians W_n and L_n correspond to a trivial 1-tangle that winds n times around the solid torus. We define maps $R^*(U_1, T_1) \rightarrow W_n$ and $R_\pi^{\natural}(U_1, T_1) \rightarrow L_n$ by post-composing $R^*(U_1, T_1) \rightarrow W_0$ and $R_\pi^{\natural}(U_1, T_1) \rightarrow L_0$ with α_1^n .

Theorem 3.13. *The point $W_2(\chi, \psi)$ lies in $R_2^*(T^2, 2)$ if and only if $\psi = 0$. The coordinates of such points are*

$$(\alpha, \beta)(W_2(\chi, 0)) = (\chi, \pi - 2\chi).$$

Proof. This follows from Theorem 3.9 for W_0 and the fact that α_1^2 fixes $R_2^*(T^2, 2)$ as a set. \square

Theorem 3.14. *The point $L_2(\phi, \theta)$ lies in $R_2^*(T^2, 2)$ if and only if $\theta \in \{0, \pi\}$. The coordinates of such points are*

$$(\alpha, \beta)(L_2(\phi, 0)) = (\phi + \pi/2, \nu - 2\phi).$$

Proof. This follows from Theorem 3.11 for L_0 and the fact that α_1^2 fixes $R_2^*(T^2, 2)$ as a set. \square

We depict the intersection of the Lagrangians W_0 , W_2 , L_0 , and L_2 with $R_2^*(T^2, 2)$ in Figure 7, where $R_2^*(T^2, 2)$ is depicted as a rectangle in the $\alpha\beta$ plane with edges identified, and in Figure 8, where $R_2^*(T^2, 2)$ is depicted as a plane with four punctures, together with the point at infinity.

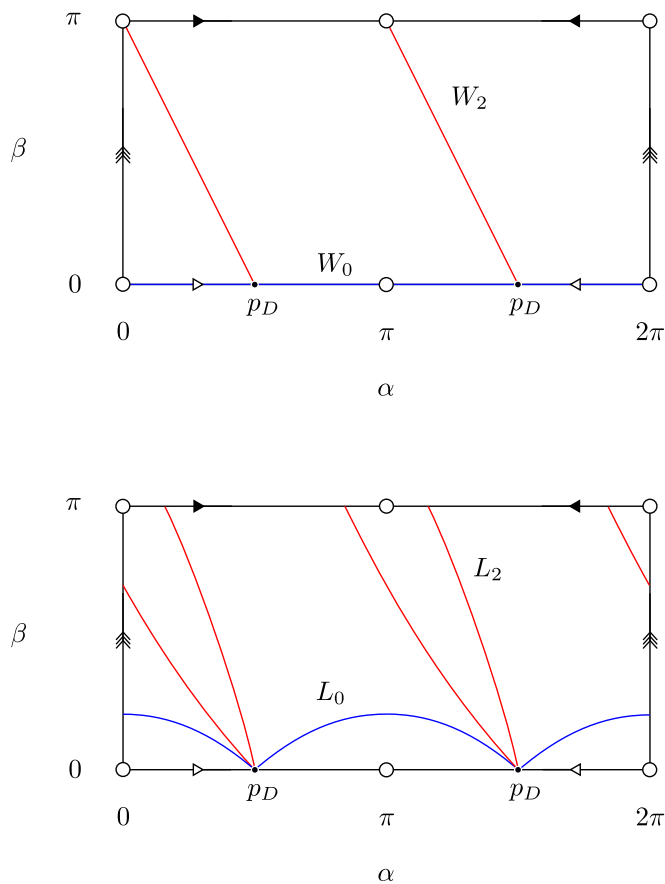


FIGURE 7. Unperturbed Lagrangians W_0 and W_2 , perturbed Lagrangians L_0 and L_2 , and double-point p_D in $R_2^*(T^2, 2)$. The edges of the rectangle in the $\alpha\beta$ plane are identified as indicated to give $R_2^*(T^2, 2)$. The circles indicate the four puncture points of $R_2^*(T^2, 2)$.

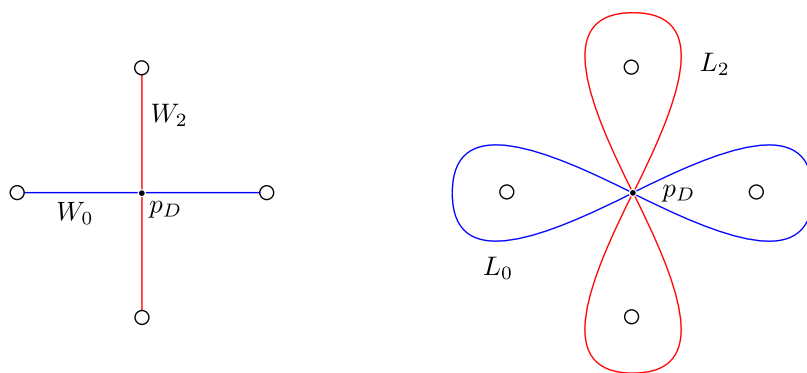


FIGURE 8. Unperturbed Lagrangians W_0 and W_2 , perturbed Lagrangians L_0 and L_2 , and double-point p_D in $R_2^*(T^2, 2)$. The four circles indicate the four puncture points of $R_2^*(T^2, 2)$.

3.7. The Fukaya category \mathcal{L} . We define a subcategory \mathcal{L} of the Fukaya category of $R^*(T^2, 2)$ whose objects are the perturbed Lagrangians L_n in $R^*(T^2, 2)$. To complete the description of \mathcal{L} , we need to describe the morphism spaces and the A_∞ operations.

We first consider the morphism spaces. Given a Lagrangian M of $R^*(T^2, 2)$, let $M^{(1)}, M^{(2)}, M^{(3)}, \dots$ denote successive Hamiltonian pushoffs of M using the Hamiltonian described in Section 3.4. Given transverse Lagrangians M and N , we define (M, N) to be the \mathbb{F} -vector space freely generated by the intersection points of $M^{(1)}$ and $N^{(0)}$:

$$(M, N) = \langle M^{(1)} \cap N^{(0)} \rangle.$$

The space of morphisms from L_n to L_m is given by

$$\text{hom}_{\mathcal{L}}(L_n, L_m) = (L_n, L_m) = \langle L_n^{(1)} \cap L_m^{(0)} \rangle.$$

Next we consider the A_∞ operations. Given $m+1$ immersed Lagrangian submanifolds M_0, \dots, M_m , we define

$$\mu_{\mathcal{L}}^m : (M_{m-1}, M_m) \otimes (M_{m-2}, M_{m-1}) \otimes \dots \otimes (M_0, M_1) \rightarrow (M_0, M_m)$$

as follows. Given generators $p_k \in M_{k-1} \cap M_k$ for $k = 1, \dots, m$, we define

$$\mu_{\mathcal{L}}^m(p_m, \dots, p_1) = q,$$

where the coefficient of the point $q \in M_0^{(m)} \cap M_m^{(0)}$ is given by a count of pseudo-holomorphic disks in $R^*(T, 2)$ with boundary on $M_0^{(m)} \cup M_1^{(m-1)} \cup \dots \cup M_m^{(0)}$ and corners at p_1, \dots, p_m, q .

We also need to define integer gradings on the morphism spaces. We will return to this issue in Section 3.10; for now, we will settle for defining a \mathbb{Z}_2 grading, known as an *orientation grading*, as described in [4] Section 1.3. Given a pair of oriented Lagrangians M and N , consider a generator p of (M, N) , which is a point in $M^{(1)} \cap N^{(0)}$. The tangent spaces $T_p M^{(1)}$ and $T_p N^{(0)}$ define Lagrangian 2-planes in the tangent space $T_p R^*(T^2, 2)$. One can define the notion of a *canonical short path* from $T_p M^{(1)}$ to $T_p N^{(0)}$ in the space of Lagrangian 2-planes of $T_p R^*(T^2, 2)$. We assign the point p grading plus or minus depending on whether the canonical short path from $T_p M^{(1)}$ to $T_p N^{(0)}$ does or does not map the given orientation of $T_p M^{(1)}$ to $T_p N^{(0)}$. We will use the notation $p^{(+)}$ or $p^{(-)}$ to indicate that p has orientation grading plus or minus. The orientation grading of $\mu_{\mathcal{L}}^m$ is plus for m even and minus for m odd.

3.8. Lagrangian intersections. Our goal in this section is to describe the morphism spaces (M, N) for various pairs of Lagrangians M and N in $R^*(T^2, 2)$. We will focus our attention on the Lagrangians W_0, L_0, W_2 , and L_2 . For these Lagrangians, the intersection points that generate (M, N) all lie in the two-dimensional submanifold $R_2^*(T^2, 2)$ of $R^*(T^2, 2)$. We can thus find the generators of (M, N) by plotting the Lagrangians $M^{(1)}$ and $N^{(0)}$ in $R_2^*(T^2, 2)$ and identifying the intersection points of the resulting curves.

To check that pairs of Lagrangians intersect transversely and to compute the orientation gradings of the intersection points, we will want to calculate tangent vectors to the Lagrangians. We will express the tangent vectors in terms the following basis of vector fields on $R_3^*(T^2, 2) \cap \{\sin \alpha \neq 0\}$:

$$v_1 = \sin \alpha_1 \partial_{\alpha_1}, \quad v_2 = \sin \alpha_1 \partial_{\beta_1}, \quad v_3 = \sin \alpha_1 \cos s_1 \partial_{s_1}, \quad v_4 = \cos s_1 \partial_{t_1}.$$

These vector fields are invariant under the coordinate identifications given in equation (3) and are thus well-defined. A computation using the symplectic form given in Theorem 3.3 shows that these vector fields do in fact form a basis.

The Lagrangians W_0, L_0, W_2 , and L_2 all contain the double-point p_D , and for our purposes it will suffice to compute tangent vectors at this point. For $n \in \{0, 2\}$, the point p_D has a unique preimage under $R^*(U_1, T_1) \rightarrow W_n$ whose coordinates are $(\chi, \psi) = (\pi/2, 0)$. For $n \in \{0, 2\}$, the point p_D has two preimages under $R_\pi^{\natural}(U_1, T_1) \rightarrow L_n$, namely the north pole ($\phi = 0$) and the south pole ($\phi = \pi$). We will orient W_n so that $(\partial_\chi, \partial_\psi)$ is a positively oriented basis. We will orient L_n so that $(\partial_\phi, \partial_\theta)$ is a positively oriented basis. For points along the great circle $y = 0$ of $R_\pi^{\natural}(U_1, T_1) = S^2$, it follows that $(\partial_\phi, \partial_y)$ is an oriented basis, where

$$\partial_\phi = \cos \phi \partial_x - \sin \phi \partial_z, \quad \partial_y = \csc \phi \partial_\theta.$$

Lemma 3.15. *The tangent vectors to W_0 at the point p_D are*

$$\partial_\chi = v_1, \quad \partial_\psi = v_3.$$

The tangent vectors to W_2 at the point p_D are

$$\partial_\chi = v_1 - 2v_2, \quad \partial_\psi = v_3 + 2v_4.$$

The tangent vectors to L_0 at the point p_D corresponding to the north pole ($p_D = L_0(0, 0)$) and south pole ($p_D = L_0(\pi, 0)$) are

$$\begin{aligned} L_0(0, 0) : \quad & \partial_\phi = v_1 + \epsilon v_2, & \partial_y = (1 + \epsilon)v_3 + \epsilon v_4, \\ L_0(\pi, 0) : \quad & \partial_\phi = -v_1 + \epsilon v_2, & \partial_y = (1 - \epsilon)v_3 - \epsilon v_4. \end{aligned}$$

The tangent vectors to L_2 at the point p_D corresponding to the north pole ($p_D = L_2(0, 0)$) and south pole ($p_D = L_2(\pi, 0)$) are

$$\begin{aligned} L_2(0, 0) : \quad & \partial_\phi = v_1 - (2 - \epsilon)v_2, & \partial_y = (1 + \epsilon)v_3 + (2 + 3\epsilon)v_4, \\ L_2(\pi, 0) : \quad & \partial_\phi = -v_1 + (2 + \epsilon)v_2, & \partial_y = (1 - \epsilon)v_3 + (2 - 3\epsilon)v_4. \end{aligned}$$

Proof. We define functions $f^\mu : R(T^2, 2) \rightarrow \mathbb{R}$ by

$$f^1 = -\frac{1}{2}(\text{tr } A), \quad f^2 = -\frac{1}{2}(\text{tr } AB - \text{tr } A), \quad f^3 = -\frac{1}{2}(\text{tr } Aa), \quad f^4 = -\frac{1}{4}(\text{tr } Aa + \text{tr } Ab).$$

We define derivatives ∂_μ :

$$\partial_1 = \partial_{\alpha_1}, \quad \partial_2 = \partial_{\beta_1}, \quad \partial_3 = \partial_{s_1}, \quad \partial_4 = \partial_{t_1}.$$

A calculation shows that the derivatives of f^μ at the point p_D are given by

$$(\partial_\nu f^\mu)(p_D) = \delta_\nu^\mu,$$

so f^μ define coordinates on a neighborhood of p_D . The tangent vector to a curve $\gamma : \mathbb{R} \rightarrow R^*(T^2, 2)$, $t \mapsto \gamma(t)$ passing through the point p_D at $t = 0$ is thus given by

$$(f^1 \circ \gamma)'(0) v_1 + (f^2 \circ \gamma)'(0) v_2 + (f^3 \circ \gamma)'(0) v_3 + (f^4 \circ \gamma)'(0) v_4.$$

The expressions for the tangent vectors are obtained via straightforward calculations using Theorems 3.9 and 3.11 for W_0 and L_0 and the action of α_1 . \square

Theorem 3.16. *We have*

$$(W_0, L_0) = \langle \alpha_0^{(-)}, \beta_0^{(+)} \rangle, \quad (W_0, L_2) = \langle \sigma_{2,0}^{(-)}, \tau_{2,0}^{(+)} \rangle, \quad (W_2, L_0) = \langle \sigma_{0,2}^{(-)}, \tau_{0,2}^{(+)} \rangle,$$

where the points $\alpha_0, \beta_0, \sigma_{2,0}, \tau_{2,0}, \sigma_{0,2}, \tau_{0,2} \in R_2^*(T^2, 2)$ are as shown in Figure 9.

Proof. First consider (W_0, L_0) . To show that α_0 and β_0 are the only points at which $W_0^{(1)}$ and $L_0^{(0)}$ intersect, we consider the limit in which the Hamiltonian perturbation goes to zero. In this limit we have $W_0^{(1)} = W_0$ and $L_0^{(0)} = L_0$. Recall from Theorem 3.9 that $W_0 = R_3^*(U_1, T_1) \cap \{\beta = 0\}$. From Theorem 3.11 for L_0 it follows that W_0 and L_0 intersect in the unique point p_D . Theorems 3.9 and 3.11 show that p_D has a unique preimage point under $R(U_1, T_1) \rightarrow W_0$ and two preimage points under $R_\pi^*(U_1, T_1) \rightarrow L_0$:

$$p_D = W_0(\pi/2, 0) = L_0(0, 0) = L_0(\pi, 0).$$

So in the limit in which the Hamiltonian perturbation goes to zero we have a 2-fold intersection $W_0^{(1)} \cap L_0^{(0)} = W_0 \cap L_0 = \{p_D\}$. In this limit the intersection of $W_0^{(1)}$ and $L_0^{(0)}$ is transversal, as can be verified using the tangent vectors given in Lemma 3.15. If we turn on the Hamiltonian perturbation, the point p_D splits into two points α_0 and β_0 , and the transversality of the intersection shows that for a sufficiently small perturbation there are no additional intersection points. The argument for (W_0, L_2) and (W_2, L_0) is similar.

To compute the orientation gradings, we note that

$$\begin{aligned} \alpha_0 &= W_0^{(1)}(\pi/2, 0) = L_0^{(0)}(\pi, 0) = p_D, & \beta_0 &= W_0^{(1)}(\pi/2, 0) = L_0^{(0)}(0, 0) = p_D, \\ \sigma_{2,0} &= W_0^{(1)}(\pi/2, 0) = L_2^{(0)}(0, 0) = p_D, & \tau_{2,0} &= W_0^{(1)}(\pi/2, 0) = L_2^{(0)}(\pi, 0) = p_D, \\ \sigma_{0,2} &= W_2^{(1)}(\pi/2, 0) = L_0^{(0)}(0, 0) = p_D, & \tau_{0,2} &= W_2^{(1)}(\pi/2, 0) = L_0^{(0)}(\pi, 0) = p_D. \end{aligned}$$

The orientation gradings now follow from a computation using the tangent vectors given in Lemma 3.15. \square

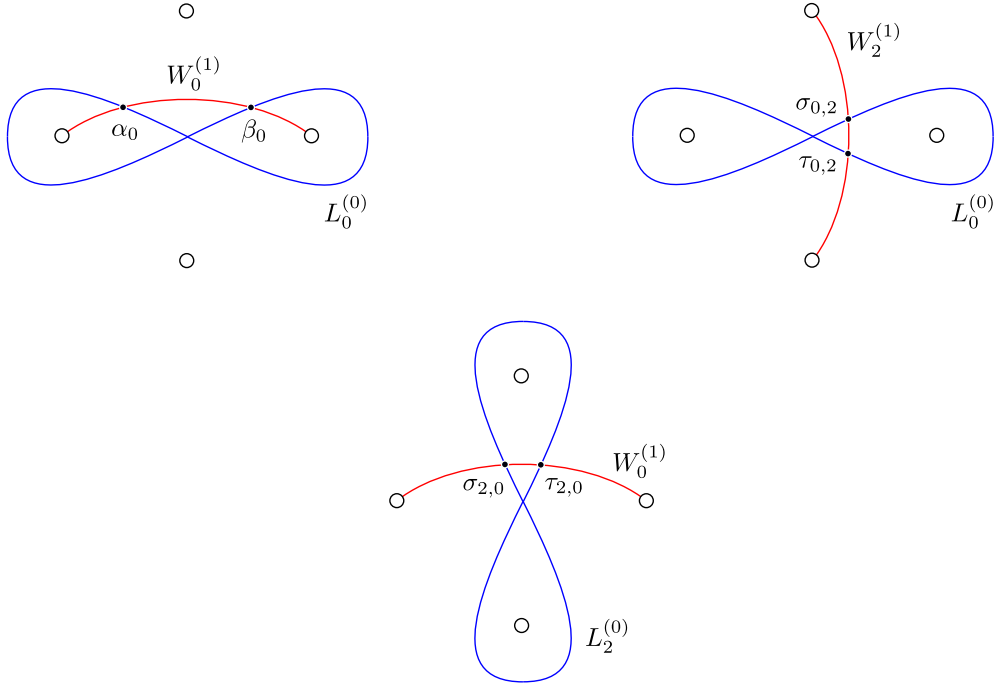


FIGURE 9. Generators α_0 and β_0 of (W_0, L_0) , generators $\sigma_{0,2}$ and $\tau_{0,2}$ of (W_2, L_0) , and generators $\sigma_{2,0}$ and $\tau_{2,0}$ of (W_0, L_2) in $R_2^*(T^2, 2)$. The four circles indicate the four puncture points of $R_2^*(T^2, 2)$.

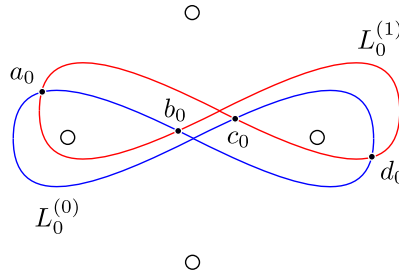


FIGURE 10. Generators $a_0, b_0, c_0,$ and d_0 of (W_0, L_0) in $R_2^*(T^2, 2)$. The four circles indicate the four puncture points of $R_2^*(T^2, 2)$.

Theorem 3.17. *We have*

$$(L_0, L_0) = \langle a_0^{(+)}, b_0^{(-)}, c_0^{(-)}, d_0^{(+)} \rangle,$$

where the points $a_0, b_0, c_0, d_0 \in R_2^*(T^2, 2)$ are as shown in Figure 10.

Proof. To show that $a_0, b_0, c_0,$ and d_0 are the only points at which $L_0^{(1)}$ and $L_0^{(0)}$ intersect, we first take the limit in which the Hamiltonian perturbation goes to zero. In this limit $L_0^{(1)} = L_0^{(0)} = L_0$. We next take the limit in which the holonomy perturbation of $L_0^{(1)}$ goes to zero but the holonomy perturbation of $L_0^{(0)}$ remains nonzero. In this limit $L_0^{(1)} = W_0$ and $L_0^{(0)} = L_0$. Recall from Theorem 3.9 that $W_0 = R_3^*(U_1, T_1) \cap \{\beta = 0\}$. From Theorem 3.11 it follows that W_0 and L_0 intersect in the unique point p_D . From Theorems 3.9 and

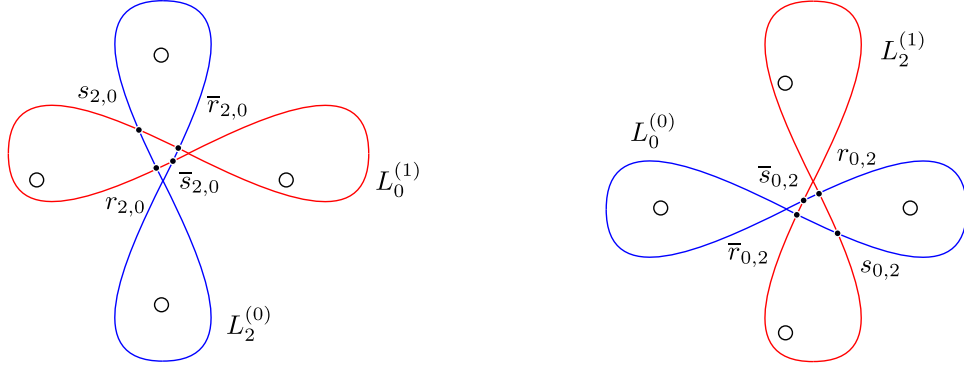


FIGURE 11. Generators $r_{2,0}$, $\bar{r}_{2,0}$, $s_{2,0}$, and $\bar{s}_{2,0}$ of (L_0, L_2) and generators $r_{0,2}$, $\bar{r}_{0,2}$, $s_{0,2}$, and $\bar{s}_{0,2}$ of (L_2, L_0) in $R_2^*(T^2, 2)$. The four circles indicate the four puncture points of $R_2^*(T^2, 2)$.

3.11 it follows that p_D has two preimage points under $R_\pi^h(U_1, T_1) \rightarrow R(U_1, T_1) \rightarrow W_0$:

$$p_D = W_0(\pi/2, 0) = L_0^{(1)}(0, 0) = L_0^{(1)}(\pi, 0)$$

and two preimage points under $R_\pi^h(U_1, T_1) \rightarrow L_0$:

$$p_D = L_0^{(0)}(0, 0) = L_0^{(0)}(\pi, 0).$$

So in the combined limit in which the Hamiltonian perturbation goes to zero and the holonomy perturbation of $L_0^{(1)}$ goes to zero, we have a four-fold intersection $L_0^{(1)} \cap L_0^{(0)} = W_0 \cap L_0 = \{p_D\}$. In the combined limit the intersection of $L_0^{(1)}$ and $L_0^{(0)}$ is transversal, as can be verified using the tangent vectors given in Lemma 3.15. If we now turn on the Hamiltonian and holonomy perturbations, the point p_D splits into the four points a_0 , b_0 , c_0 , d_0 indicated in Figure 10, and there are no additional intersection points.

To compute the orientation gradings, we note that in the combined limit we have

$$b_0 = L_0^{(1)}(0, 0) = L_0^{(0)}(\pi, 0) = p_D, \quad c_0 = L_0^{(1)}(\pi, 0) = L_0^{(0)}(0, 0) = p_D.$$

The orientation gradings now follow from a computation using the tangent vectors given in Lemma 3.15. The orientation gradings of a_0 and d_0 follow from the fact that L_0 has self-intersection number 0, as can be seen by noting that L_0 is homotopic to the closure of W_0 in $R(T^2, 2)$, which is a closed disk, and hence contractible in $R(T^2, 2)$ \square

Theorem 3.18. *We have*

$$(L_0, L_2) = \langle r_{2,0}^{(-)}, \bar{r}_{2,0}^{(-)}, s_{2,0}^{(+)}, \bar{s}_{2,0}^{(+)} \rangle, \quad (L_2, L_0) = \langle r_{0,2}^{(-)}, \bar{r}_{0,2}^{(-)}, s_{0,2}^{(+)}, \bar{s}_{0,2}^{(+)} \rangle,$$

where $r_{2,0}, \bar{r}_{2,0}, s_{2,0}, \bar{s}_{2,0}, r_{0,2}, \bar{r}_{0,2}, s_{0,2}, \bar{s}_{0,2} \in R_2^*(T^2, 2)$ are as shown in Figure 11.

Proof. Similar arguments as those used in Theorems 3.16 and 3.17 show that $L_2^{(1)}$ and $L_0^{(0)}$ intersect transversely in the four points $r_{0,2}, \bar{r}_{0,2}, s_{0,2}, \bar{s}_{0,2}$ shown in Figure 11. In the limit that the Hamiltonian perturbation goes to zero, each of these points approaches p_D and we have

$$\begin{aligned} r_{0,2} &= L_2^{(1)}(0, 0) = L_0^{(0)}(0, 0) = p_D, & \bar{r}_{0,2} &= L_2^{(1)}(\pi, 0) = L_0^{(0)}(\pi, 0) = p_D, \\ s_{0,2} &= L_2^{(1)}(0, 0) = L_0^{(0)}(\pi, 0) = p_D, & \bar{s}_{0,2} &= L_2^{(1)}(\pi, 0) = L_0^{(0)}(0, 0) = p_D. \end{aligned}$$

The orientation gradings now follow from a computation using the tangent vectors given in Lemma 3.15. \square

By acting with suitable powers of α_1 , we can generalize Theorems 3.16, 3.17, and 3.18 as follows:

Corollary 3.19. *We have*

$$(W_0, L_0) = \langle \alpha_0^{(-)}, \beta_0^{(+)} \rangle, \quad (W_0, L_{\pm 2}) = \langle \sigma_{\pm 2, 0}^{(-)}, \tau_{\pm 2, 0}^{(+)} \rangle,$$

where

$$\sigma_{-2, 0} = \alpha_1^{-2} \cdot \sigma_{0, 2}, \quad \tau_{-2, 0} = \alpha_1^{-2} \cdot \tau_{0, 2}.$$

Corollary 3.20. *We have*

$$(L_n, L_n) = \langle a_n^{(+)}, b_n^{(-)}, c_n^{(-)}, d_n^{(+)} \rangle, \quad (L_n, L_{n\pm 2}) = \langle r_{n\pm 2, n}^{(-)}, \bar{r}_{n\pm 2, n}^{(-)}, s_{n\pm 2, n}^{(+)}, \bar{s}_{n\pm 2, n}^{(+)} \rangle,$$

where

$$\begin{aligned} a_n &= \alpha_1^n \cdot a_0, & b_n &= \alpha_1^n \cdot b_0, & c_n &= \alpha_1^n \cdot c_0, & d_n &= \alpha_1^n \cdot d_0, \\ r_{n+2, n} &= \alpha_1^n \cdot r_{2, 0}, & \bar{r}_{n+2, n} &= \alpha_1^n \cdot \bar{r}_{2, 0}, & s_{n+2, n} &= \alpha_1^n \cdot s_{2, 0}, & \bar{s}_{n+2, n} &= \alpha_1^n \cdot \bar{s}_{2, 0}, \\ r_{n-2, n} &= \alpha_1^{n-2} \cdot r_{0, 2}, & \bar{r}_{n-2, n} &= \alpha_1^{n-2} \cdot \bar{r}_{0, 2}, & s_{n-2, n} &= \alpha_1^{n-2} \cdot s_{0, 2}, & \bar{s}_{n-2, n} &= \alpha_1^{n-2} \cdot \bar{s}_{0, 2}. \end{aligned}$$

3.9. Lagrangians and Lagrangian intersections for links in S^3 . Given a link L in S^3 , we can split S^3 into two solid tori, each containing a 1-tangle, that are glued together using the mapping class group element s defined in Section 3.5. As we describe in Section 6, we will choose the splitting in such a way that one of the 1-tangles is trivial. The other 1-tangle is projected onto an annulus to yield a tangle diagram, which is closed with the trivial tangle to yield a description of the original link L . We thus define unperturbed Lagrangians that can be used for describing links in S^3 :

$$\bar{W}_n = s \cdot W_n.$$

We can also use the relation $s\alpha_1 = \beta_1 s$ to express \bar{W}_n as

$$\bar{W}_n = s \cdot \bar{W}_n = s\alpha_1^n \cdot W_0 = \beta_1^n s \cdot W_0 = \beta_1^n \cdot \bar{W}_n.$$

The following result describes the action of s^2 on the Lagrangians W_n and \bar{W}_n :

Lemma 3.21. *We have*

$$s^2 \cdot W_n = W_{1-n}, \quad s^2 \cdot \bar{W}_n = \bar{W}_{1-n}.$$

Proof. First we show that $s^2 \cdot W_0 = W_1$. Recall from Theorem 3.9 that $W_0 = \{B = \mathbb{1}\}$. A computation gives $(\text{tr } B)(\alpha_1^{-1} s^2 \cdot W_0) = 2$, so $\alpha_1^{-1} s^2 \cdot W_0 = W_0$ and thus $s^2 \cdot W_0 = \alpha_1 \cdot W_0 = W_1$. We then have

$$s^2 \cdot W_n = s^2 \alpha_1^n \cdot W_0 = \alpha_1^{-n} s^2 \cdot W_0 = \alpha_1^{-n} \cdot W_1 = W_{1-n}, \quad s^2 \cdot \bar{W}_n = s^3 \cdot W_n = s \cdot W_{1-n} = \bar{W}_{1-n}. \quad \square$$

We can depict the action of s on the unperturbed Lagrangians W_n and \bar{W}_n as

$$\begin{array}{ccc} W_n & \xrightarrow{s} & \bar{W}_n \\ \uparrow s & & \downarrow s \\ \bar{W}_{1-n} & \xleftarrow{s} & W_{1-n} \end{array}$$

We can explicitly describe the Lagrangian \bar{W}_0 :

Lemma 3.22. *We have*

$$\bar{W}_0 = \{A = \mathbb{1}\} = R_3^*(T^2, 2) \cap \{\alpha = 0\}.$$

Proof. The result follows from Theorem 3.9, the definition $\bar{W}_0 = s \cdot W_0$, and the known action of s . \square

The Lagrangians W_0 and W_1 correspond to the 1-tangles shown in Figure 6(a) and 6(b), so the Lagrangians \bar{W}_0 and \bar{W}_1 correspond to an overpass arc A_+ and an underpass arc A_- for a link in S^3 . Recall that the braid group elements α_1 and β_1 drag the point p_1 around fundamental cycles of T^2 . For W_0 and W_1 , the element β_1 drags p_1 around a meridian. For \bar{W}_0 and \bar{W}_1 , the element α_1 drags p_1 around a meridian. As we would expect, the braid group element β_1 acts trivially on W_0 and W_1 and the braid group element α_1 acts trivially on \bar{W}_0 and \bar{W}_1 :

Lemma 3.23. *We have*

$$\beta_1 \cdot W_0 = W_0, \quad \beta_1 \cdot W_1 = W_1, \quad \alpha_1 \cdot \overline{W}_0 = \overline{W}_0, \quad \alpha_1 \cdot \overline{W}_1 = \overline{W}_1.$$

Proof. Recall from Theorem 3.9 that $W_0 = \{B = \mathbb{1}\}$. A computation gives $(\text{tr } B)(\beta_1^{-1} \cdot W_0) = 2$, so $\beta_1 \cdot W_0 = W_0$. We have

$$\beta_1 \cdot W_1 = \beta_1 s^2 \cdot W_0 = s^2 \beta_1^{-1} \cdot W_0 = s^2 \cdot W_0 = W_1, \quad \alpha_1 \cdot \overline{W}_n = \alpha_1 s \cdot W_n = s \beta_1^{-1} \cdot W_n = s \cdot W_n = \overline{W}_n$$

for $n = 0, 1$. \square

Theorem 3.24. *We have*

$$(\overline{W}_0, L_n) = \langle \overline{w}_{n,0}^{(+)} \rangle,$$

where the point $\overline{w}_{n,0}$ lies in $R_3^*(T^2, 2)$ and has coordinates

$$(\alpha, \beta, s)(\overline{w}_{n,0}) = \begin{cases} (0, \epsilon, 0) & \text{for } n \equiv 0 \pmod{4}, \\ (0, \pi/2, \pi/2 - \epsilon) & \text{for } n \equiv 1 \pmod{4}, \\ (0, \pi - \epsilon, 0) & \text{for } n \equiv 2 \pmod{4}, \\ (0, \pi/2, -\pi/2 + \epsilon) & \text{for } n \equiv 3 \pmod{4}. \end{cases}$$

Proof. Recall from Lemma 3.22 that $\overline{W}_0 = R_3^*(T^2, 2) \cap \{\alpha = 0\}$. From Lemma 3.11 for L_0 it follows that \overline{W}_0 and L_0 intersect in a unique point $\overline{w}_{0,0}$ in $R_3^*(T^2, 2)$ with coordinates

$$(\alpha, \beta, s)(\overline{w}_{0,0}) = (0, \epsilon, 0).$$

We apply α_1^n to both sides of the equation $\overline{W}_0 \cap L_0 = w_0$ to obtain

$$(\alpha_1^n \cdot \overline{W}_0) \cap (\alpha_1^n \cdot L_0) = \overline{W}_0 \cap L_n = \alpha_1^n \cdot \overline{w}_{0,0},$$

where we substituted $L_n = \alpha_1^n \cdot L_0$ and used the fact that $\overline{W}_0 = \alpha_1^n \cdot \overline{W}_0$. So \overline{W}_0 and L_n intersect in a single point $\overline{w}_{n,0} := \alpha_1^n \cdot \overline{w}_{0,0}$. Using the coordinates of $\overline{w}_{0,0}$ and the known action of α_1 , we find that

$$\begin{aligned} \overline{w}_{4r,0} &= \overline{W}_0(\pi/2, -\pi/2 + \epsilon) = L_0(3\pi/2, 0), & \overline{w}_{4r+1,0} &= \overline{W}_0(\epsilon, 0), \\ \overline{w}_{4r+2,0} &= \overline{W}_0(\pi/2, \pi/2 - \epsilon), & \overline{w}_{4r+3,0} &= \overline{W}_0(\pi - \epsilon, 0), \end{aligned}$$

so in particular $\overline{w}_{n,0}$ lies in $R_3^*(T^2, 2)$, and $\overline{w}_{n,0}$ has the coordinates stated in the theorem.

To check that \overline{W}_0 and L_n intersect transversely and to compute the orientation grading of $\overline{w}_{n,0}$, we compute the tangent vectors to \overline{W}_0 and L_n at $\overline{w}_{n,0}$. We define the following basis of vector fields on $R_3^*(T^2, 2) \cap \{\sin \beta \neq 0\}$:

$$u_1 = \sin \beta \partial_{\alpha_2}, \quad u_2 = \sin \beta \partial_{\beta_2}, \quad u_3 = \sin \beta \partial_{s_2}, \quad u_4 = \cos s \partial_{t_2}.$$

These vector fields are invariant under the coordinate identifications given in equation (3) and are thus well-defined. A computation using the symplectic form given in Theorem 3.3 shows that these vector fields do in fact form a basis. We define functions $h^\mu : R(T^2, 2) \rightarrow \mathbb{R}$:

$$h^1 = -\frac{1}{2}(\text{tr } AB - \text{tr } B), \quad h^2 = -\frac{1}{2}(\text{tr } B), \quad h^3 = -\frac{1}{2}(\text{tr } Ba), \quad h^4 = \frac{1}{4}(\text{tr } Ba + \text{tr } Bb).$$

We define derivatives $\overline{\partial}_\mu$:

$$\overline{\partial}_1 = \partial_{\alpha_2}, \quad \overline{\partial}_2 = \partial_{\beta_2}, \quad \overline{\partial}_3 = \partial_{s_2}, \quad \overline{\partial}_4 = \partial_{t_2}.$$

A calculation shows that $\overline{\partial}_\nu h^\mu$ is diagonal at each intersection point $\overline{w}_{n,0}$, so the functions h^μ serve as convenient coordinates these points. A calculation using the coordinates h^μ , the vector fields u_μ , and the tangent vectors for W_0 given in Lemma 3.15 shows that \overline{W}_0 and L_n intersect transversely at $\overline{w}_{n,0}$ and $\overline{w}_{n,0}$ has positive intersection grading. \square

A similar argument proves:

Theorem 3.25. *We have*

$$(\overline{W}_1, L_n) = \langle \overline{w}_{n,1}^{(+)} \rangle,$$

where the point $\beta_1^{-1} \cdot \overline{w}_{n,1}$ lies in $R_3^*(T^2, 2)$ and has coordinates

$$(\alpha, \beta, \gamma)(\beta_1^{-1} \cdot \overline{w}_{n,1}) = \begin{cases} (0, \nu_0, 0) & \text{for } n \equiv 0 \pmod{4}, \\ (0, \pi/2, \pi/2 - \nu_0) & \text{for } n \equiv 1 \pmod{4}, \\ (0, \pi - \nu_0, 0) & \text{for } n \equiv 2 \pmod{4}, \\ (0, \pi/2, -\pi/2 + \nu_0) & \text{for } n \equiv 3 \pmod{4}, \end{cases}$$

where $\nu_0 = \epsilon \sin \phi_0$ and ϕ_0 is defined such that

$$\phi_0 + \epsilon \sin \phi_0 = \pi/2.$$

3.10. A_∞ operations for \mathcal{L} . We would like to determine the A_∞ operations involving the Lagrangians L_0 and L_2 , but a direct calculation of these operations does not appear feasible. Instead, we conjecture the operations we will need based on certain considerations.

Let $E \rightarrow R_2^*(T^2, 2)$ denote the restriction of the tangent bundle of $R^*(T^2, 2)$ to the 2-dimensional submanifold $R_2^*(T^2, 2)$. The bundle E has the structure of a symplectic vector bundle with symplectic form given by Theorem 3.3. We can split (E, ω) as $(E_1, \omega_1) \oplus (E_2, \omega_2)$, where

$$\omega_1 = d\alpha_1 \wedge d\beta_1 = d\alpha_1 \wedge d\beta_1, \quad \omega_2 = \sin \alpha_1 ds_1 \wedge dt_1 = -\sin \beta_2 ds_2 \wedge dt_2,$$

and E_1 and E_2 are the kernel of $v \mapsto \omega_2(v, -)$ and $v \mapsto \omega_1(v, -)$, respectively. We can choose compatible almost complex structures J_k on (E_k, ω_k) and define an almost complex structure $J = J_1 \oplus J_2$ on E . We can extend J to an almost-complex structure on $R^*(T^2, 2)$, and with this choice of complex structure pseudo-holomorphic disks in $R_2^*(T^2, 2)$ are also pseudo-holomorphic disks in $R^*(T^2, 2)$.

To conjecture the A_∞ operations, we plot the intersections of the relevant Lagrangians with $R_2^*(T^2, 2)$ and look for topological disks within that 2-dimensional submanifold of $R^*(T^2, 2)$. For example, to conjecture $\mu_{\mathcal{L}}^1$ operations for generators of (L_0, L_0) , we look for topological disks in Figure 10. The only bigons we find are two canceling pairs of bigons $a_0 \rightarrow d_0$, so we conjecture that $\mu_{\mathcal{L}}^1 = 0$ for (L_0, L_0) . Based on Figure 11, we conjecture that $\mu_{\mathcal{L}}^1 = 0$ for (L_0, L_2) and (L_2, L_0) .

Next we consider product operations. Based on counts of topological disks in $R_2^*(T^2, 2)$, we conjecture the following product operations:

- (1) We have the following operations $\mu_{\mathcal{L}}^2 : (L_0, L_0) \otimes (L_0, L_0) \rightarrow (L_0, L_0)$:

$$\begin{aligned} \mu_{\mathcal{L}}^2(b_0, c_0) &= \mu_{\mathcal{L}}^2(c_0, b_0) = d_0, \\ \mu_{\mathcal{L}}^2(a_0, a_0) &= a_0, & \mu_{\mathcal{L}}^2(a_0, b_0) &= \mu_{\mathcal{L}}^2(b_0, a_0) = b_0, \\ \mu_{\mathcal{L}}^2(a_0, c_0) &= \mu_{\mathcal{L}}^2(c_0, a_0) = c_0, & \mu_{\mathcal{L}}^2(a_0, d_0) &= \mu_{\mathcal{L}}^2(d_0, a_0) = d_0. \end{aligned}$$

- (2) We have the following operations $\mu_{\mathcal{L}}^2 : (L_2, L_0) \otimes (L_0, L_2) \rightarrow (L_0, L_0)$:

$$\begin{aligned} \mu_{\mathcal{L}}^2(\overline{s}_{0,2} \cdot \overline{r}_{2,0}) &= \mu_{\mathcal{L}}^2(r_{0,2}, s_{2,0}) = c_0, \\ \mu_{\mathcal{L}}^2(r_{0,2}, r_{2,0}) &= \mu_{\mathcal{L}}^2(\overline{r}_{0,2}, \overline{r}_{2,0}) = \mu_{\mathcal{L}}^2(s_{0,2}, s_{2,0}) = \mu_{\mathcal{L}}^2(\overline{s}_{0,2}, \overline{s}_{2,0}) = d_0. \end{aligned}$$

- (3) We have the following operations $\mu_{\mathcal{L}}^2 : (L_0, L_2) \otimes (L_2, L_0) \rightarrow (L_2, L_2)$:

$$\begin{aligned} \mu_{\mathcal{L}}^2(r_{2,0}, \overline{s}_{0,2}) &= \mu_{\mathcal{L}}^2(s_{2,0}, \overline{r}_{0,2}) = c_2, \\ \mu_{\mathcal{L}}^2(r_{2,0}, r_{0,2}) &= \mu_{\mathcal{L}}^2(\overline{r}_{2,0}, \overline{r}_{0,2}) = \mu_{\mathcal{L}}^2(s_{2,0}, s_{0,2}) = \mu_{\mathcal{L}}^2(\overline{s}_{2,0}, \overline{s}_{0,2}) = d_2. \end{aligned}$$

- (4) We have the following operations $\mu_{\mathcal{L}}^2 : (L_0, L_2) \otimes (L_0, L_0) \rightarrow (L_0, L_2)$:

$$\begin{aligned} \mu_{\mathcal{L}}^2(\overline{r}_{2,0}, b_0) &= \overline{s}_{2,0}, & \mu_{\mathcal{L}}^2(s_{2,0}, b_0) &= r_{2,0}, \\ \mu_{\mathcal{L}}^2(r_{2,0}, a_0) &= r_{2,0}, & \mu_{\mathcal{L}}^2(\overline{r}_{2,0}, a_0) &= \overline{r}_{2,0}, & \mu_{\mathcal{L}}^2(s_{2,0}, a_0) &= s_{2,0}, & \mu_{\mathcal{L}}^2(\overline{s}_{2,0}, a_0) &= \overline{s}_{2,0}. \end{aligned}$$

- (5) We have the following operations $\mu_{\mathcal{L}}^2 : (L_2, L_0) \otimes (L_2, L_2) \rightarrow (L_2, L_0)$:

$$\begin{aligned} \mu_{\mathcal{L}}^2(\overline{s}_{0,2}, b_2) &= r_{0,2}, & \mu_{\mathcal{L}}^2(\overline{r}_{0,2}, b_2) &= s_{0,2}, \\ \mu_{\mathcal{L}}^2(r_{0,2}, a_2) &= r_{0,2}, & \mu_{\mathcal{L}}^2(\overline{r}_{0,2}, a_2) &= \overline{r}_{0,2}, & \mu_{\mathcal{L}}^2(s_{0,2}, a_2) &= s_{0,2}, & \mu_{\mathcal{L}}^2(\overline{s}_{0,2}, a_2) &= \overline{s}_{0,2}. \end{aligned}$$

(6) We have the following operations $\mu_{\mathcal{L}}^2 : (L_2, L_2) \otimes (L_0, L_2) \rightarrow (L_0, L_2)$:

$$\begin{aligned} \mu_{\mathcal{L}}^2(b_2, r_{2,0}) &= \bar{s}_{2,0}, & \mu_{\mathcal{L}}^2(b_2, s_{2,0}) &= \bar{r}_{2,0}, \\ \mu_{\mathcal{L}}^2(a_2, r_{2,0}) &= r_{2,0}, & \mu_{\mathcal{L}}^2(a_2, \bar{r}_{2,0}) &= \bar{r}_{2,0}, & \mu_{\mathcal{L}}^2(a_2, s_{2,0}) &= s_{2,0}, & \mu_{\mathcal{L}}^2(a_2, \bar{s}_{2,0}) &= \bar{s}_{2,0}. \end{aligned}$$

(7) We have the following operations $\mu_{\mathcal{L}}^2 : (L_0, L_0) \otimes (L_2, L_0) \rightarrow (L_2, L_0)$:

$$\begin{aligned} \mu_{\mathcal{L}}^2(b_0, \bar{s}_{0,2}) &= \bar{r}_{0,2}, & \mu_{\mathcal{L}}^2(b_0, r_{0,2}) &= s_{0,2}, \\ \mu_{\mathcal{L}}^2(a_0, r_{0,2}) &= r_{0,2}, & \mu_{\mathcal{L}}^2(a_0, \bar{r}_{0,2}) &= \bar{r}_{0,2}, & \mu_{\mathcal{L}}^2(a_0, s_{0,2}) &= s_{0,2}, & \mu_{\mathcal{L}}^2(a_0, \bar{s}_{0,2}) &= \bar{s}_{0,2}. \end{aligned}$$

There are several consistency checks we can perform on our conjectured operations. First, the product operations must respect orientation gradings: the orientation grading of a product of generators must be the product of their orientation gradings. Second, if $\mu_{\mathcal{L}}^1 = 0$, then the relations for the A_∞ operations imply that the product operations must be associative. Third, the product operations must satisfy the following invariance result:

Theorem 3.26. *The product operations $(L_{n_1}, L_{n_2}) \otimes (L_{n_0}, L_{n_1}) \rightarrow (L_{n_0}, L_{n_2})$ for $n_1, n_2, n_3 \in \{0, 2\}$ are invariant under the substitutions*

$$\begin{aligned} a_0 &\leftrightarrow a_2, & b_0 &\leftrightarrow b_2, & c_0 &\leftrightarrow c_2, & d_0 &\leftrightarrow d_2, \\ r_{2,0} &\leftrightarrow r_{0,2}, & \bar{r}_{2,0} &\leftrightarrow \bar{r}_{0,2}, & s_{2,0} &\leftrightarrow s_{0,2}, & \bar{s}_{2,0} &\leftrightarrow s_{0,2}. \end{aligned}$$

Proof. A symplectic automorphism of $R^*(T^2, 2)$ must preserve the product structure. Invariance under the stated substitutions follows from considering the action of the symplectic automorphism $\alpha_1 s^2$ of $R^*(T^2, 2)$ on the generators. To understand this action, it is helpful to consider the limit in which both the Hamiltonian and holonomy perturbations of the Lagrangians go to zero. Consider, for example, the generators of (L_0, L_2) . In the limit that both perturbations go to zero we have $L_0^{(1)} \rightarrow W_0$ and $L_2^{(0)} \rightarrow W_2$. The automorphism $\alpha_1 s^2$ maps W_n to W_{2-n} . Recall from the proof of Theorem 3.18 that in the limit in which the Hamiltonian perturbation goes to zero we have

$$\begin{aligned} r_{0,2} &= L_2^{(1)}(0, 0) = L_0^{(0)}(0, 0) = p_D, & \bar{r}_{0,2} &= L_2^{(1)}(\pi, 0) = L_0^{(0)}(\pi, 0) = p_D, \\ s_{0,2} &= L_2^{(1)}(0, 0) = L_0^{(0)}(\pi, 0) = p_D, & \bar{s}_{0,2} &= L_2^{(1)}(\pi, 0) = L_0^{(0)}(0, 0) = p_D, \end{aligned}$$

so the action of $\alpha_1 s^2$ on the generators of (L_0, L_2) is as stated. The argument for the generators of (L_0, L_0) is similar. \square

It is straightforward to check that the conjectured product operations do in fact satisfy all three conditions. By acting with suitable powers of α_1 , we obtain the following generalized conjecture:

Conjecture 3.27. *The following are the only nonzero product operations $(L_{n_1}, L_{n_2}) \otimes (L_{n_0}, L_{n_1}) \rightarrow (L_{n_0}, L_{n_2})$ for $n_i - n_j \in \{0, \pm 2\}$. We have*

$$\mu_{\mathcal{L}}^2(a_n, x) = x, \quad \mu_{\mathcal{L}}^2(y, a_n) = y$$

whenever these operations are defined. We have

$$\mu_{\mathcal{L}}^2(b_n, c_n) = \mu_{\mathcal{L}}^2(c_n, b_n) = d_n.$$

$$\begin{aligned} \mu_{\mathcal{L}}^2(r_{n,n+2}, s_{n+2,n}) &= \mu_{\mathcal{L}}^2(\bar{r}_{n,n+2}, \bar{s}_{n+2,n}) = \mu_{\mathcal{L}}^2(s_{n,n-2}, \bar{r}_{n-2,n}) = \mu_{\mathcal{L}}^2(\bar{s}_{n,n-2}, r_{n-2,n}) = c_n, \\ \mu_{\mathcal{L}}^2(r_{n,n\pm 2}, r_{n\pm 2,n}) &= \mu_{\mathcal{L}}^2(\bar{r}_{n,n\pm 2}, \bar{r}_{n\pm 2,n}) = \mu_{\mathcal{L}}^2(s_{n,n\pm 2}, s_{n\pm 2,n}) = \mu_{\mathcal{L}}^2(\bar{s}_{n,n\pm 2}, \bar{s}_{n\pm 2,n}) = d_n. \end{aligned}$$

$$\begin{aligned} \mu_{\mathcal{L}}^2(b_{n+2}, r_{n+2,n}) &= \mu_{\mathcal{L}}^2(\bar{r}_{n+2,n}, b_n) = \bar{s}_{n+2,n}, & \mu_{\mathcal{L}}^2(b_{n-2}, r_{n-2,n}) &= \mu_{\mathcal{L}}^2(\bar{r}_{n-2,n}, b_n) = s_{n-2,n}, \\ \mu_{\mathcal{L}}^2(s_{n+2,n}, b_n) &= r_{n+2,n}, & \mu_{\mathcal{L}}^2(b_{n+2}, s_{n+2,n}) &= \bar{r}_{n+2,n}, \\ \mu_{\mathcal{L}}^2(\bar{s}_{n-2,n}, b_n) &= r_{n-2,n}, & \mu_{\mathcal{L}}^2(b_{n-2}, \bar{s}_{n-2,n}) &= \bar{r}_{n-2,n}. \end{aligned}$$

As described in Section 2.2, part of the data of an A_∞ category is an integer grading on the morphism spaces. In the case of the Fukaya category of a symplectic manifold M , one would like this integer grading to be given by the Maslov grading of the Lagrangian intersection points that generate these spaces, but this is possible only if two conditions are met. First, the first Chern class of M must be 2-torsion. Second, the Maslov classes of the Lagrangians must vanish. If these conditions are met, then the integer grading depends

on the additional data of a choice of *graded lifts* of the Lagrangians. We do not know if these conditions are met for our category \mathcal{L} , so rather than use Maslov gradings we simply assign integer gradings to the generators of (L_n, L_n) and $(L_n, L_{n\pm 2})$ as follows:

$$(L_n, L_n) = \langle a_n^{(0)}, b_n^{(0)}, c_n^{(-2)}, d_n^{(-2)} \rangle, \quad (L_n, L_{n\pm 2}) = \langle r_{n\pm 2, n}^{(-1)}, \bar{r}_{n\pm 2, 0}^{(-1)}, s_{n\pm 2, n}^{(-1)}, \bar{s}_{n\pm 2, 0}^{(-1)} \rangle.$$

Given a pair of Lagrangians N_1 and N_2 , one defines the *Floer cohomology* $HF(N_1, N_2)$ to be the cohomology of the vector space (N_1, N_2) with respect to the differential $\mu^1 : (N_1, N_2) \rightarrow (N_1, N_2)$. If conditions described above for (N_1, N_2) to carry an integer grading are met, then $HF(N_1, N_2)$ is integer-graded and we have a *Poincaré duality* isomorphism

$$HF^*(N_1, N_2) \rightarrow HF^{n-*}(N_2, N_1),$$

where $2n$ is the real dimension of the symplectic manifold M . We note that integer gradings we have defined on (L_n, L_n) and $(L_n, L_{n\pm 2})$ are not consistent with Poincaré duality, though they are consistent with gradings collapsed to \mathbb{Z}_4 .

3.11. A_∞ operations for unperturbed Lagrangians. We would also like to know certain product operations involving the unperturbed Lagrangians W_n . Strictly speaking, these Lagrangians are not objects of the category \mathcal{L} ; rather, they will be used to define A_∞ functors $\mathcal{G}_{W_n} : \mathcal{L} \rightarrow \text{Ch}$ as described in Section 2.2. We proceed as in Section 3.10 and count topological disks in $R_2^*(T^2, 2)$. Based on these counts, we conjecture that $\mu_1 = 0$ for (W_0, L_0) , (W_0, L_2) , (W_2, L_0) , and (W_2, L_2) . We also conjecture the following product operations:

(1) We have the following operations $\mu^2 : (L_0, L_0) \otimes (W_0, L_0) \rightarrow (W_0, L_0)$:

$$\mu^2(a_0, \alpha_0) = \alpha_0, \quad \mu^2(a_0, \beta_0) = \beta_0, \quad \mu^2(c_0, \alpha_0) = \beta_0.$$

(2) We have the following operations $\mu^2 : (L_2, L_0) \otimes (W_0, L_2) \rightarrow (W_0, L_0)$:

$$\mu^2(\bar{s}_{0,2}, \tau_{2,0}) = \mu^2(r_{0,2}, \sigma_{2,0}) = \beta_0.$$

(3) We have the following operations $\mu^2 : (L_0, L_2) \otimes (W_2, L_0) \rightarrow (W_2, L_2)$:

$$\mu^2(r_{2,0}, \sigma_{0,2}) = \beta_2, \quad \mu^2(s_{2,0}, \tau_{0,2}) = \beta_2.$$

(4) We have the following operations $\mu^2 : (L_0, L_2) \otimes (W_0, L_0) \rightarrow (W_0, L_2)$:

$$\mu^2(\bar{r}_{2,0}, \alpha_0) = \tau_{2,0}, \quad \mu^2(s_{2,0}, \alpha_0) = \sigma_{2,0}.$$

(5) We have the following operations $\mu^2 : (L_2, L_0) \otimes (W_2, L_2) \rightarrow (W_2, L_0)$:

$$\mu^2(\bar{s}_{0,2}, \alpha_2) = \sigma_{0,2}, \quad \mu^2(\bar{r}_{0,2}, \alpha_2) = \tau_{0,2}.$$

(6) We have the following operations $\mu^2 : (L_2, L_2) \otimes (W_0, L_2) \rightarrow (W_0, L_2)$:

$$\mu^2(a_2, \sigma_{2,0}) = \sigma_{2,0}, \quad \mu^2(a_2, \tau_{2,0}) = \tau_{2,0}, \quad \mu^2(b_2, \sigma_{2,0}) = \tau_{2,0}.$$

(7) We have the following operations $\mu^2 : (L_0, L_0) \otimes (W_2, L_0) \rightarrow (W_2, L_0)$:

$$\mu^2(a_0, \sigma_{0,2}) = \sigma_{0,2}, \quad \mu^2(a_0, \tau_{0,2}) = \tau_{0,2}, \quad \mu^2(b_0, \sigma_{0,2}) = \tau_{0,2}.$$

It is straightforward to check that the conjectured product operations are consistent with orientation gradings and are associative when combined with the product operations for unperturbed Lagrangians conjectured in Section 3.10. By acting with suitable powers of α_1 , we obtain the following generalized conjecture:

Conjecture 3.28. *The following are the only nonzero product operations $(L_{n_1}, L_{n_2}) \otimes (W_0, L_{n_1}) \rightarrow (W_0, L_{n_2})$ for $n_1, n_2, n_1 - n_2 \in \{0, \pm 2\}$. We have*

$$\mu^2(a_n, x) = x, \quad \mu^2(y, a_n) = y$$

whenever these operations are defined. We have

$$\mu^2(c_0, \alpha_0) = \mu^2(\bar{s}_{0,2}, \tau_{2,0}) = \mu^2(s_{-2,0}, \tau_{-2,0}) = \mu^2(r_{0,2}, \sigma_{2,0}) = \mu^2(r_{-2,0}, \sigma_{-2,0}) = \beta_0.$$

$$\begin{aligned} \mu^2(s_{2,0}, \alpha_0) &= \sigma_{2,0}, & \mu^2(\bar{r}_{2,0}, \alpha_0) &= \mu^2(b_2, \sigma_{2,0}) = \tau_{2,0}, \\ \mu^2(\bar{s}_{-2,0}, \alpha_0) &= \sigma_{-2,0}, & \mu^2(\bar{r}_{-2,0}, \alpha_0) &= \mu^2(b_{-2}, \sigma_{-2,0}) = \tau_{-2,0}. \end{aligned}$$

We can depict the conjectured product operations as follows:

$$\begin{array}{ccc}
 \sigma_{-2,0} & \xleftarrow{\bar{s}_{-2,0}} & \alpha_0 \\
 \downarrow b_{-2} & \searrow r_{0,-2} & \downarrow c_0 \\
 \tau_{-2,0} & & \beta_0
 \end{array}
 \quad
 \begin{array}{ccc}
 \sigma_{-2,0} & & \sigma_{2,0} \\
 \downarrow b_{-2} & \nearrow \bar{r}_{2,0} & \downarrow b_2 \\
 \tau_{-2,0} & & \tau_{2,0}
 \end{array}
 \quad
 \begin{array}{ccc}
 \sigma_{-2,0} & & \alpha_0 & \xrightarrow{s_{2,0}} & \sigma_{2,0} \\
 \downarrow b_{-2} & \nearrow \bar{r}_{-2,0} & \downarrow c_0 & \searrow r_{0,2} & \downarrow b_2 \\
 \tau_{-2,0} & & \beta_0 & & \tau_{2,0}
 \end{array}$$

We assign integer quantum gradings to the generators of (W_0, L_0) and $(W_0, L_{\pm 2})$ as follows:

$$(W_0, L_0) = \langle \alpha_0^{(0)}, \beta_0^{(-2)} \rangle, \quad (W_0, L_{\pm 2}) = \langle \sigma_{\pm 2,0}^{(-1)}, \tau_{\pm 2,0}^{(-1)} \rangle.$$

It is straightforward to check that these gradings are consistent with the product operations in Conjecture 3.28.

4. TWISTED COMPLEXES CORRESPONDING TO TANGLE DIAGRAMS

In Section 3.7 we defined a Fukaya category \mathcal{L} for $R^*(T^2, 2)$ whose objects are the perturbed Lagrangians L_n and whose A_∞ operations are given by counting pseudo-holomorphic disks. As described in Section 2.2, we can define an A_∞ category $\text{Tw } \mathcal{L}$ of twisted complexes over \mathcal{L} . Our goal in this section is to construct a twisted complex (X, δ) in $\text{Tw } \mathcal{L}$ from a 1-tangle diagram T in the annulus.

4.1. Conjectures regarding \mathcal{L} . To construct the twisted object (X, δ) , we need certain A_∞ operations of \mathcal{L} that we are currently unable to compute. We make the following conjecture regarding the operations we will need:

Conjecture 4.1. *We have identity elements $a_n \in (L_n, L_n)$ that satisfy*

$$\mu_{\mathcal{L}}^2(a_n, x) = x, \quad \mu_{\mathcal{L}}^2(y, a_n) = y$$

whenever these operations are defined. We have elements $c_n \in (L_n, L_n)$, $p_{n+2,n} \in (L_n, L_{n+2})$, and $q_{n-2,n} \in (L_n, L_{n-2})$ that satisfy

$$\begin{aligned}
 \mu_{\mathcal{L}}^2(q_{n,n+2}, p_{n+2,n}) &= \mu_{\mathcal{L}}^2(p_{n,n-2}, q_{n-2,n}) = c_n, & \mu_{\mathcal{L}}^2(c_n, c_n) &= 0, \\
 \mu_{\mathcal{L}}^2(c_{n+2}, p_{n+2,n}) &= \mu_{\mathcal{L}}^2(p_{n+2,n}, c_n) = 0, & \mu_{\mathcal{L}}^2(c_{n-2}, q_{n-2,n}) &= \mu_{\mathcal{L}}^2(q_{n-2,n}, c_n) = 0.
 \end{aligned}$$

All operations of the form $\mu_{\mathcal{L}}^m(x_m, \dots, x_1)$ for $m \neq 2$ and $x_m, \dots, x_1 \in \{a_n, c_n, p_{n+2,n}, q_{n-2,n} \mid n \in \mathbb{Z}\}$ are zero.

We do not conjecture values for the products $\mu_{\mathcal{L}}^2(p_{n+4,n+2}, p_{n+2,n})$ and $\mu_{\mathcal{L}}^2(q_{n-4,n-2}, q_{n-2,n})$.

Conjecture 4.1 is motivated by several considerations. First, it is consistent with the conjectured A_∞ relations described in Section 3.10. The elements a_n and c_n are the generators described in Corollary 3.20. The elements $p_{n+2,n}$ and $q_{n-2,n}$ are defined in terms of the generators described in Corollary 3.20 in one of two ways. We could either define

$$p_{n+2,n}^{(-)} = r_{n+2,n}^{(-)} + \bar{r}_{n+2,n}^{(-)}, \quad q_{n-2,n}^{(+)} = s_{n-2,n}^{(+)} + \bar{s}_{n-2,n}^{(+)}$$

or

$$p_{n+2,n}^{(+)} = s_{n+2,n}^{(+)} + \bar{s}_{n+2,n}^{(+)}, \quad q_{n-2,n}^{(-)} = r_{n-2,n}^{(-)} + \bar{r}_{n-2,n}^{(-)}$$

where we have indicated orientation gradings using superscripts. For some purposes it does not matter which of the two definitions is used, but when it does matter we will indicate the definition we have in mind by specifying the orientation gradings, which are opposite for the two definitions. It is straightforward to check that for both definitions Conjecture 4.1 is consistent with the product operations in Conjecture 3.27.

A second motivation for Conjecture 4.1 is that it is a natural generalization of a corresponding statement regarding the A_∞ operations for the Fukaya category of $R^*(S^2, 4)$, which as we discuss in Appendix A appears to be closely related to the Fukaya category of $R^*(T^2, 2)$. Indeed, Conjecture 4.1 is in fact true if we restrict n to $n \in \{\pm 1\}$ and reinterpret it as a statement about $R^*(S^2, 4)$.

Recall that part of the data of an A_∞ category is an integer grading on the morphism spaces. We will refer to this grading as a *quantum grading* q . We will also take the morphism spaces to carry a second integer

grading that we refer to as a *homological grading* h . We assign bigradings (h, q) to a_n , c_n , $p_{n+2, n}$, and $q_{n-2, n}$ as follows, as indicated by superscripts:

$$(6) \quad a_n^{(0,0)} \quad c_n^{(0,-2)}, \quad p_{n+2,n}^{(0,-1)}, \quad q_{n-2,n}^{(0,-1)}.$$

The quantum gradings of these generators are consistent with the grading assignments described at the end of Section 3.10. We say that A_∞ operations *respect bigradings* if whenever

$$\mu_{\mathcal{L}}^m(x_m^{(h_m, q_m)}, \dots, x_1^{(h_1, q_1)}) = y$$

is nonzero for homogeneous vectors $x_m^{(h_m, q_m)}, \dots, x_1^{(h_1, q_1)}$, the bigrading (h, q) of y is given by

$$h = h_m + \dots + h_1 + 2 - m, \quad q = q_m + \dots + q_1 + 2 - m.$$

As discussed in Section 2.2, the operations of an A_∞ category are required to respect quantum gradings. Given the bigrading assignments in equation (6), the A_∞ operations described in Conjecture 4.1 respect bigradings.

4.2. Vector spaces and linear maps. As described in Section 2.2, given an A_∞ category \mathcal{A} one can construct a corresponding A_∞ category $\Sigma\mathcal{A}$ called the additive enlargement of \mathcal{A} . The objects of $\Sigma\mathcal{A}$ are constructed from objects of \mathcal{A} and vector spaces, and the morphisms of $\Sigma\mathcal{A}$ are constructed from morphisms of \mathcal{A} and linear maps. We define here the vector spaces and linear maps that we will use to construct objects and morphisms of $\Sigma\mathcal{L}$.

The vector spaces that are used to construct objects of $\Sigma\mathcal{L}$ are required to carry an integer grading. We will refer to this grading as a *quantum grading* q . We will take these vector spaces to carry a second integer grading that we refer to as a *homological grading* h . Given a bigraded vector space V , we use the notation $v^{(h, q)}$ to indicate that a homogeneous vector $v \in V$ has bigrading (h, q) . We define the vector space $V[h, q]$ to be V with gradings shifted upwards by (h, q) , so if $v \in V$ is homogeneous with bigrading (h_v, q_v) then the corresponding vector $v \in V[h, q]$ is homogeneous with bigrading $(h_v + h, q_v + q)$. We define \mathbb{F} to be the field of two elements, where $1 \in \mathbb{F}$ is assigned bigrading $(0, 0)$. We define a bigraded \mathbb{F} -vector space

$$A = \langle e^{(0,1)}, x^{(0,-1)} \rangle.$$

We define the following \mathbb{F} -linear maps. We define *unit maps* $\eta^{(0,1)}$ and $\dot{\eta}^{(0,-1)}$:

$$\begin{aligned} \eta : \mathbb{F} &\rightarrow A, & \eta(1) &= e, \\ \dot{\eta} : \mathbb{F} &\rightarrow A, & \dot{\eta}(1) &= x. \end{aligned}$$

We define *counit maps* $\epsilon^{(0,1)}$ and $\dot{\epsilon}^{(0,-1)}$:

$$\begin{aligned} \epsilon : A &\rightarrow \mathbb{F}, & \epsilon(e) &= 0, & \epsilon(x) &= 1, \\ \dot{\epsilon} : A &\rightarrow \mathbb{F}, & \dot{\epsilon}(e) &= 1, & \dot{\epsilon}(x) &= 0. \end{aligned}$$

We define a *raising map* $\mathbb{1}_{ex}^{(0,2)}$ and a *lowering map* $\mathbb{1}_{xe}^{(0,-2)}$:

$$\begin{aligned} \mathbb{1}_{ex} : A &\rightarrow A, & \mathbb{1}_{ex}(e) &= 0, & \mathbb{1}_{ex}(x) &= e, \\ \mathbb{1}_{xe} : A &\rightarrow A, & \mathbb{1}_{xe}(e) &= x, & \mathbb{1}_{xe}(x) &= 0. \end{aligned}$$

We define a *multiplication map* $m^{(0,-1)}$:

$$m : A \otimes A \rightarrow A, \quad m(e \otimes e) = e, \quad m(e \otimes x) = m(x \otimes e) = x, \quad m(x \otimes x) = 0.$$

We define a *comultiplication map* $\Delta^{(0,-1)}$:

$$\Delta : A \rightarrow A \otimes A, \quad \Delta(e) = e \otimes x + x \otimes e, \quad \Delta(x) = x \otimes x.$$

We define an *identity map* $I_r^{(0,0)}$:

$$I_r : A^{\otimes r} \rightarrow A^{\otimes r}, \quad I_r = \mathbb{1}^{\otimes r}.$$

We define a *raising map* $\Sigma_r^{(0,2)}$:

$$\Sigma_r : A^{\otimes r} \rightarrow A^{\otimes r}, \quad \Sigma_r = \sum_{s=0}^{r-1} \mathbb{1}^{\otimes s} \otimes \mathbb{1}_{ex} \otimes \mathbb{1}^{\otimes (r-1-s)}.$$

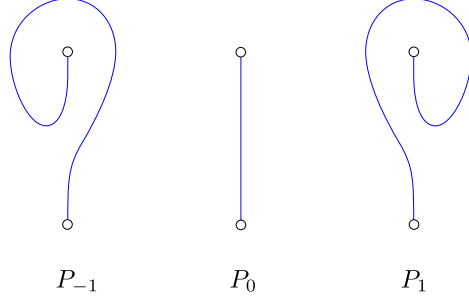


FIGURE 12. Planar 1-tangles in the annulus.

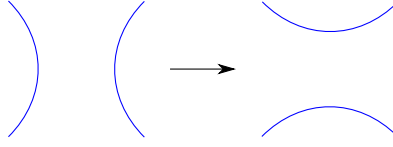


FIGURE 13. Local replacement for a saddle.

Note that for $r = 0$ we have $A^{\otimes r} = \mathbb{F}$, so $I_0 = \mathbb{1}_{\mathbb{F}}$ and $\Sigma_0 = 0$. For simplicity we will often omit tensor product symbols; for example we write $\eta \otimes I_r$ as ηI_r . We record here several useful identities involving Σ_r :

$$(7) \quad \Sigma_{a+b} = \Sigma_a I_b + I_a \Sigma_b, \quad \Sigma_2 \circ \Delta = \Delta \circ \Sigma_1, \quad \Sigma_1 \circ m = m \circ \Sigma_2.$$

4.3. Planar tangles and saddles. We will assign objects of $\Sigma\mathcal{L}$ to planar 1-tangles in the annulus and morphisms of $\Sigma\mathcal{L}$ to saddles between pairs of such tangles. Here we describe these assignments.

Fix points p_1 and p_2 on the outer and inner bounding circle of the annulus $S^1 \times [0, 1]$. A *planar 1-tangle* is a compact 1-dimensional submanifold of the annulus with boundary $\{p_1, p_2\}$. A planar 1-tangle consists of an *arc component* connecting p_1 to p_2 , together with a finite number of *circle components*. We orient the arc component in the direction from the outer boundary point p_1 to the inner boundary point p_2 .

For each integer n we define a planar tangle P_n for which the arc component winds n times clockwise around the annulus, as shown in Figure 12. We define $P_n(r)$ to be the set of planar tangles whose arc component is isotopic to P_n and which contains r circle components. We also let $P_n(r)$ denote any specific tangle in the set $P_n(r)$. We say that n is the *winding number* and r is the *circle number* of the tangle $P_n(r)$. To the planar tangle $P_n(r)$ we assign the following object of $\Sigma\mathcal{L}$:

$$L_n \otimes A^{\otimes r},$$

where A is the 2-dimensional bigraded vector space defined in Section 4.2.

Given a planar tangle $P_{n_1}(r_1)$, we can make a local replacement of the form shown in Figure 13 to obtain a new planar tangle $P_{n_2}(r_2)$. We say that the local replacement defines a *saddle* $P_{n_1}(r_1) \rightarrow P_{n_2}(r_2)$. The possible types of saddles are shown in Figure 14. For saddles $P_n(r) \rightarrow P_n(r+1)$ or $P_n(r+1) \rightarrow P_n(r)$ that split or merge a circle component C from the arc component, we say that circle components of $P_n(r+1)$ that lie inside (outside) C , and circle components of $P_n(r)$ whose counterparts in $P_n(r+1)$ lie inside (outside) C , are *enclosed (non-enclosed) circles*. To each saddle $P_{n_1}(r_1) \rightarrow P_{n_2}(r_2)$ we assign a corresponding *differential*, which is a morphism

$$L_{n_1} \otimes A^{\otimes r_1} \rightarrow L_{n_2} \otimes A^{\otimes r_2}$$

in $\Sigma\mathcal{L}$ with bigrading $(h, q) = (0, -1)$. The assignments are as follows:

- (1) For a saddle $S_{C^+} : P_n(r+1) \rightarrow P_n(r+2)$ that splits one circle into two circles:

$$d_{C^+} : L_n \otimes A^{\otimes(r+1)} \rightarrow L_n \otimes A^{\otimes(r+2)}, \quad d_{C^+} = a_n \Delta I_r.$$

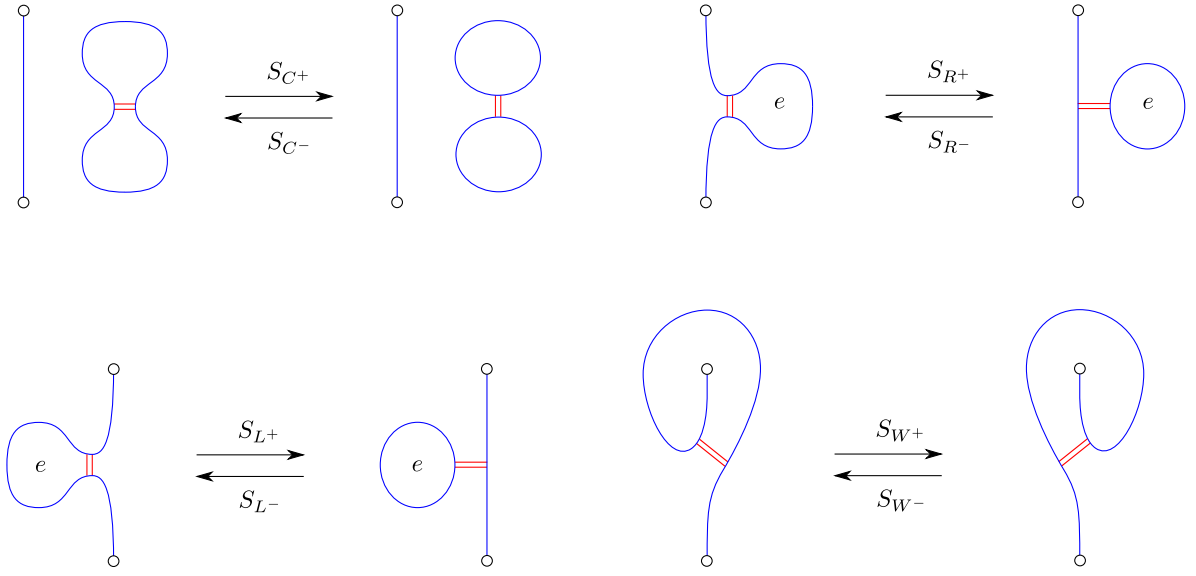


FIGURE 14. Types of saddles for planar 1-tangles in the annulus. Circle components in regions marked e are said to be *enclosed circles*.

For a saddle $S_{C-} : P_n(r+2) \rightarrow P_n(r+1)$ that merges two circles into one circle:

$$d_{C-} : L_n \otimes A^{\otimes(r+2)} \rightarrow L_n \otimes A^{\otimes(r+1)}, \quad d_{C-} = a_n m I_r.$$

(2) For a saddle $S_{R+} : P_n(r) \rightarrow P_n(r+1)$ that splits a circle from the right side of the arc component:

$$d_{R+} : L_n \otimes A^{\otimes r} \rightarrow L_n \otimes A^{\otimes(r+1)}, \quad d_{R+} = (a_n \dot{\eta} + c_n \eta) I_r + c_n \dot{\eta} I_{r_n} \Sigma_{r_e}.$$

For a saddle $S_{R-} : P_n(r+1) \rightarrow P_n(r)$ that merges a circle with the right side of the arc component:

$$d_{R-} : L_n \otimes A^{\otimes(r+1)} \rightarrow L_n \otimes A^{\otimes r}, \quad d_{R-} = (a_n \dot{\epsilon} + c_n \epsilon) I_r + c_n \dot{\epsilon} I_{r_n} \Sigma_{r_e}.$$

Here $r = r_e + r_n$, where r_e is the number of enclosed circles and r_n is the number of non-enclosed circles.

(3) For a saddle $S_{L+} : P_n(r) \rightarrow P_n(r+1)$ that splits a circle from the left side of the arc component:

$$d_{L+} : L_n \otimes A^{\otimes r} \rightarrow L_n \otimes A^{\otimes(r+1)}, \quad d_{L+} = a_n \dot{\eta} I_r + c_n \dot{\eta} I_{r_n} \Sigma_{r_e}.$$

For a saddle $S_{L-} : P_n(r+1) \rightarrow P_n(r)$ that merges a circle with the left side of the arc component:

$$d_{L-} : L_n \otimes A^{\otimes(r+1)} \rightarrow L_n \otimes A^{\otimes r}, \quad d_{L-} = a_n \dot{\epsilon} I_r + c_n \dot{\epsilon} I_{r_n} \Sigma_{r_e}.$$

Here $r = r_e + r_n$, where r_e is the number of enclosed circles and r_n is the number of non-enclosed circles.

(4) For a saddle $S_{W+} : P_n(r) \rightarrow P_{n+2}(r)$ that increases winding number of the arc component by two:

$$d_{W+} : L_n \otimes A^{\otimes r} \rightarrow L_{n+2} \otimes A^{\otimes r}, \quad d_{W+} = p_{n+2,n} I_r.$$

For a saddle $S_{W-} : P_n(r) \rightarrow P_{n-2}(r)$ that decreases the winding number of the arc component by two:

$$d_{W-} : L_n \otimes A^{\otimes r} \rightarrow L_{n-2} \otimes A^{\otimes r}, \quad d_{W-} = q_{n-2,n} I_r.$$

The linear maps in the expressions for the differentials are as defined in Section 4.2. The expressions for the differentials depend on a specific choice of ordering of the factors of A corresponding to the circle components of the planar tangles. For a different ordering of the circle factors, we would need to modify the expressions accordingly. The differentials $d_{R\pm}$ and $d_{L\pm}$ corresponding to saddles that split or merge a circle from the arc component contain terms involving Σ_{r_e} and are thus *nonlocal*, in the sense that they act

nontrivially on the factors of A corresponding to enclosed circles. As we will show in Section 4.4, these terms are needed to ensure that differentials corresponding to distinct saddles commute.

Given a planar tangle $P_n(r+1)$ and a choice of a circle component C , we define $P_n(r)$ to be the planar tangle obtained by removing C from $P_n(r+1)$. We say that adding C to $P_n(r)$ defines a *cup* $P_n(r) \rightarrow P_n(r+1)$ and removing C from $P_n(r+1)$ defines a *cap* $P_n(r+1) \rightarrow P_n(r)$. To a cup $P_n(r) \rightarrow P_n(r+1)$ we assign a corresponding *cup map* with bigrading $(h, q) = (0, 1)$:

$$\cup : L_n \otimes A^{\otimes r} \rightarrow L_n \otimes A^{\otimes(r+1)}, \quad \cup = a_n \eta I_r.$$

To a cap $P_n(r+1) \rightarrow P_n(r)$ we assign a corresponding *cap map* with bigrading $(h, q) = (0, 1)$:

$$\cap : L_n \otimes A^{\otimes(r+1)} \rightarrow L_n \otimes A^{\otimes r}, \quad \cap = a_n \epsilon I_r.$$

We will use the same notation for cups and caps as for their corresponding maps.

For simplicity, in what follows we will often denote $\mu_{\Sigma \mathcal{L}}^2(x, y)$ as $x \circ y$.

4.4. Differentials, cup maps, and cap maps commute. Consider a planar tangle $P_{n_1}(r_1)$ and distinct saddles $S_1 : P_{n_1}(r_1) \rightarrow P_{n_2}(r_2)$ and $S_2 : P_{n_1}(r_1) \rightarrow P_{n_3}(r_3)$. We can apply the local replacements for both S_1 and S_2 to $P_{n_1}(r_1)$ to obtain a planar tangle $P_{n_4}(r_4)$. We have induced saddles $S'_2 : P_{n_2}(r_2) \rightarrow P_{n_4}(r_4)$ and $S'_1 : P_{n_3}(r_3) \rightarrow P_{n_4}(r_4)$ obtained by applying the local replacement for S_2 to $P_{n_2}(r_2)$ and the local replacement for S_1 to $P_{n_3}(r_3)$:

$$(8) \quad \begin{array}{ccc} P_{n_1}(r_1) & \xrightarrow{S_1} & P_{n_2}(r_2) \\ \downarrow S_2 & & \downarrow S'_2 \\ P_{n_3}(r_3) & \xrightarrow{S'_1} & P_{n_4}(r_4). \end{array}$$

Theorem 4.2. *Assuming the A_∞ operations of \mathcal{L} are as described in Conjecture 4.1, the differentials corresponding to the saddles in diagram (8) commute.*

Proof. We prove this result by explicit computation for all possible pairs of saddles. The computations are straightforward, though somewhat tedious, so we describe only a few representative examples.

Consider the pair of interleaved saddles shown in Figure 15. We let a , b , and c denote the number of circle components in the regions labeled a , b , and c in Figure 15. The diagram corresponding to Figure 15 is

$$(9) \quad \begin{array}{ccc} L_n \otimes A^{\otimes(a+b+c)} & \xrightarrow{d_1} & L_n \otimes A^{\otimes(a+b+c+1)} \\ \downarrow d_2 & & \downarrow d'_2 \\ L_n \otimes A^{\otimes(a+b+c+1)} & \xrightarrow{d'_1} & L_n \otimes A^{\otimes(a+b+c)}, \end{array}$$

where

$$\begin{aligned} d_1 &= d_{L^+} = a_n \dot{\eta} I_{a+b+c} + c_n \dot{\eta} I_a \Sigma_b I_c, & d'_2 &= d_{L^-} = a_n \dot{\epsilon} I_{a+b+c} + c_n \dot{\epsilon} I_a \Sigma_b I_c, \\ d_2 &= d_{R^+} = (a_n \dot{\eta} + c_n \eta) I_{a+b+c} + c_n \dot{\eta} \Sigma_a I_{b+c}, & d'_1 &= d_{R^-} = (a_n \dot{\epsilon} + c_n \epsilon) I_{a+b+c} + c_n \dot{\eta} \Sigma_a I_{b+c}. \end{aligned}$$

A calculation shows that

$$d'_2 \circ d_1 = d'_1 \circ d_2 = 0,$$

so diagram (9) commutes.

Consider the pair of nested saddles shown in Figure 16. We let a , b , and c denote the number of circle components in the regions labeled a , b , and c in Figure 16. The diagram corresponding to Figure 16 is

$$(10) \quad \begin{array}{ccc} L_n \otimes A^{\otimes(a+b+c)} & \xrightarrow{d_1} & L_n \otimes A^{\otimes(a+b+c+1)} \\ \downarrow d_2 & & \downarrow d'_2 \\ L_n \otimes A^{\otimes(a+b+c+1)} & \xrightarrow{d'_1} & L_n \otimes A^{\otimes(a+b+c+2)}, \end{array}$$

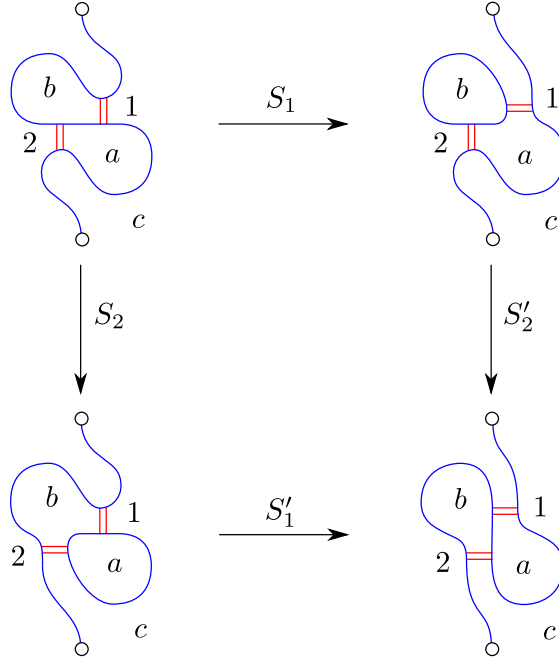


FIGURE 15. Interleaved saddles.

where

$$\begin{aligned} d_1 &= d_{L^+} = a_n \dot{\eta} I_{a+b+c} + c_n \dot{\eta} I_a \Sigma_b I_c, & d'_2 &= d_{R^+} = (a_n \dot{\eta} + c_n \eta) I_{a+b+c+1} + c_n \dot{\eta} \Sigma_{a+b+1} I_c, \\ d_2 &= d_{R^+} = (a_n \dot{\eta} + c_n \eta) I_{a+b+c} + c_n \dot{\eta} \Sigma_a I_b, & d'_1 &= d_{C^+} = a_n \Delta I_{a+b+c}. \end{aligned}$$

A calculation shows that

$$d'_2 \circ d_1 = d'_1 \circ d_2 = (a_n \dot{\eta} \dot{\eta} + c_n (\dot{\eta} \eta + \eta \dot{\eta})) I_{a+b+c} + c_n \dot{\eta} \dot{\eta} \Sigma_a I_{b+c},$$

where we have used the identity

$$\Sigma_{a+b+1} \circ \dot{\eta} I_{a+b} = (\Sigma_1 I_{a+b} + I_1 \Sigma_{a+b}) \circ \dot{\eta} I_{a+b} = \eta I_{a+b} + \dot{\eta} \Sigma_{a+b}.$$

So diagram (10) commutes. We note that without the nonlocal terms involving Σ_r , diagram (10) would not commute.

The fact that differentials of the form d_{C^\pm} commute with differentials of the form d_{R^\pm} and d_{L^\pm} is due to the identities in equation (7).

Similar calculations for the remaining pairs of saddles prove the result. \square

Consider a saddle $S_{21} : P_{n_1}(r_1+1) \rightarrow P_{n_2}(r_2+1)$. Choose a circle component C_1 in $P_{n_1}(r_1+1)$ that is unchanged under S_{21} , so there is a corresponding circle component C_2 in $P_{n_2}(r_2+1)$. Remove the circle components C_1 and C_2 from $P_{n_1}(r_1+1)$ and $P_{n_2}(r_2+1)$ to obtain planar tangles $P_{n_1}(r_1)$ and $P_{n_2}(r_2)$, and apply the local replacement for S_{21} to $P_{n_1}(r_1)$ to obtain an induced saddle $S'_{21} : P_{n_1}(r_1) \rightarrow P_{n_2}(r_2)$. We have cups $\cup_k : P_{n_k}(r_k) \rightarrow P_{n_k}(r_k+1)$ and caps $\cap_k : P_{n_k}(r_k+1) \rightarrow P_{n_k}(r_k)$ that add and remove the circle components C_k . We have the following diagram:

$$(11) \quad \begin{array}{ccc} P_{n_1}(r_1+1) & \xrightarrow{S_{21}} & P_{n_2}(r_2+1) \\ \cup_1 \updownarrow \cap_1 & & \cup_2 \updownarrow \cap_2 \\ P_{n_1}(r_1) & \xrightarrow{S'_{21}} & P_{n_2}(r_2). \end{array}$$

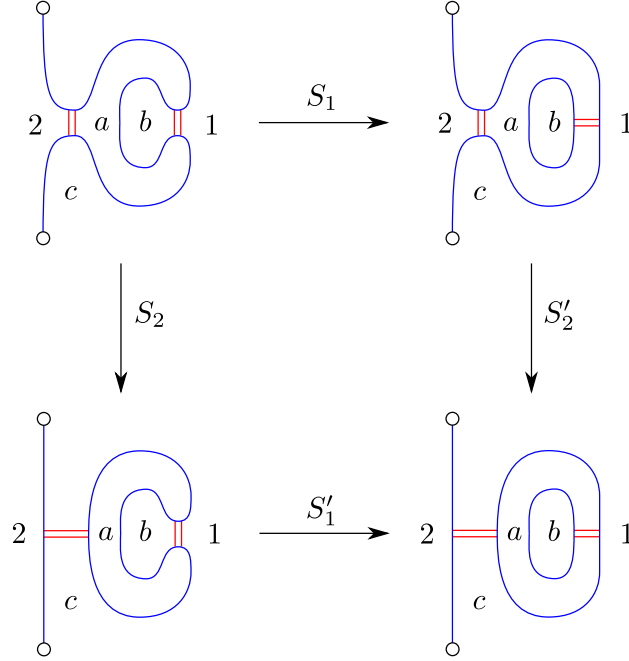


FIGURE 16. Nested saddles.

Theorem 4.3. *Assuming the A_∞ operations for \mathcal{L} are as described in Conjecture 4.1, the differentials corresponding to the saddles in diagram (11) commute with the maps corresponding to the cups and caps.*

Proof. If the circles C_1 and C_2 are not enclosed circles, then the differentials corresponding to S_{21} and S'_{21} act as the identity on the factor of A corresponding to C_1 , so the result is clear. If C_1 and C_2 are enclosed circles, the result follows from the identities

$$\begin{aligned}\Sigma_{r+1} \circ \eta I_r &= (\Sigma_1 I_r + I_1 \Sigma_r) \circ \eta I_r = \eta \Sigma_r = \eta I_r \circ \Sigma_r, \\ \epsilon I_r \circ \Sigma_{r+1} &= \epsilon I_r \circ (\Sigma_1 I_r + I_1 \Sigma_r) = \epsilon \Sigma_r = \Sigma_r \circ \epsilon I_r,\end{aligned}$$

where we have used the fact that $\Sigma_1 \circ \eta = \epsilon \circ \Sigma_1 = 0$. \square

4.5. Construction of the twisted complex. Given an oriented 1-tangle diagram T , we will construct a corresponding object (X, δ) of $\text{Tw } \mathcal{L}$. Recall that (X, δ) consists of an object X of $\Sigma \mathcal{L}$ and a differential $\delta : X \rightarrow X$ with bigrading $(h, q) = (1, 1)$.

We construct the object X of $\Sigma \mathcal{L}$ from a cube of resolutions of the tangle diagram T . Let m_+ and m_- denote the number of positive and negative crossings of T , and let $m = m_+ + m_-$ denote the total number of crossings. Fix an arbitrary ordering of the crossings. Define the 0-resolution, respectively 1-resolution, of a crossing such that the overpass turns left, respectively right. We can specify a planar resolution of T in terms of a binary string i of length m , where the k -th bit of i tells us how to resolve the k -th crossing of T . Define $I = \{0, 1\}^m$ to be the set of binary strings of length m . For each binary string $i \in I$, define T_i to be the planar resolution of T specified by i . We have $T_i = P_{n_i}(c_i)$, where n_i is the winding number of T_i and c_i is the number of circle components of T_i . Define the *resolution degree* $r(i) \in \{0, 1, \dots, m\}$ to be the number of 1's in the binary string $i \in I$. We define

$$(12) \quad X = \bigoplus_{i \in I} (L_{n_i} \otimes A^{\otimes c_i}[r(i) + h_T, 2r(i) + q_T]),$$

where $[h_T, q_T]$ is a bigrading shift due to the oriented crossings of T that is given by

$$[h_T, q_T] = [-m_-, m_+ - 3m_-].$$

The quantum grading shift $q_T = m_+ - 3m_-$ differs from the usual shift of $m_+ - 2m_-$ for Khovanov homology, since the quantum grading of δ is 1 in our convention but 0 in the usual convention.

We construct the differential $\delta : X \rightarrow X$ by summing over maps corresponding to saddles that relate different resolutions of the tangle diagram T . Consider two binary strings $i, j \in I$ that are identical except for a single bit that is 0 for i and 1 for j , so $r(j) = r(i) + 1$. The corresponding planar tangles T_i and T_j are related by a saddle $S_{ji} : T_i \rightarrow T_j$ that changes a 0-resolution in T_i to a 1-resolution in T_j . We define

$$d_{ji} : L_{n_i} \otimes A^{\otimes c_i} [r(i) + h_T, 2r(i) + q_T] \rightarrow L_{n_j} \otimes A^{\otimes c_j} [r(j) + h_T, 2r(j) + q_T]$$

to be the differential corresponding to the saddle S_{ji} shifted in bigrading by $[1, 2]$, so d_{ji} has bigrading $(h, q) = (1, 1)$. We define δ to be the sum of the differentials d_{ji} over all pairs of binary strings $i, j \in I$ that are identical except for a single bit that is 0 for i and 1 for j .

Recall from Section 4.1 that we considered two different ways of defining the elements $p_{n+2, n}$ and $q_{n-2, n}$ that appear in the differentials d_{W+} and d_{W-} . The two possible definitions of $p_{n+2, n}$ and $q_{n-2, n}$ correspond to two possible definitions of δ , which we denote δ_+ and δ_- . For δ_+ , we define $p_{n+2, n}$ and $q_{n-2, n}$ as

$$p_{n+2, n}^{(-)} = r_{n+2, n}^{(-)} + \bar{r}_{n+2, n}^{(-)}, \quad q_{n-2, n}^{(+)} = s_{n-2, n}^{(+)} + \bar{s}_{n-2, n}^{(+)}.$$

For δ_- , we define $p_{n+2, n}$ and $q_{n-2, n}$ as

$$p_{n+2, n}^{(+)} = s_{n+2, n}^{(+)} + \bar{s}_{n+2, n}^{(+)}, \quad q_{n-2, n}^{(-)} = r_{n-2, n}^{(-)} + \bar{r}_{n-2, n}^{(-)}.$$

For some purposes it does not matter which definition is used, in which case we use the notation δ with no subscript.

Theorem 4.4. *Assuming the A_∞ operations for \mathcal{L} are as described in Conjecture 4.1, the pair (X, δ) is a twisted complex.*

Proof. We need to show that

$$(13) \quad \sum_{m=1}^{\infty} \mu_{\Sigma \mathcal{L}}^m(\delta, \dots, \delta) = 0$$

and that X admits a filtration with respect to which δ is strictly lower triangular. Conjecture 4.1 states that the $m \neq 2$ terms of equation (13) are zero. Assuming Conjecture 4.1, Theorem 4.2 states that the $m = 2$ term of equation (13) is zero. We will take the filtration to be the one given by the resolution degree. By construction, the differential δ increases the resolution degree by 1, so it is lower triangular with respect to this filtration. \square

4.6. Example twisted complex. Consider the tangle diagram T shown in Figure 17. There are $m_+ = 2$ positive crossings and $m_- = 0$ negative crossings, corresponding to a bigrading shift

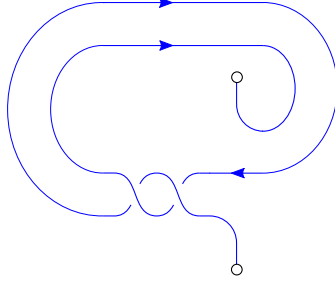
$$[h_T, q_T] = [-m_-, m_+ - 3m_-] = [0, 2].$$

The tangle diagram T thus corresponds to the following object of the twisted Fukaya category:

$$\begin{array}{ccc}
 & L_0 \otimes \mathbb{F}[1, 4] & \\
 d_{W-}[1, 2] \nearrow & & \searrow d_{L+}[1, 2] \\
 L_2 \otimes \mathbb{F}[0, 2] & & L_0 \otimes A[2, 6], \\
 d_{W-}[1, 2] \searrow & & \nearrow d_{R+}[1, 2] \\
 & L_0 \otimes \mathbb{F}[1, 4] &
 \end{array}$$

where the differentials are given by

$$d_{W-} = q_{0, 2} \otimes \mathbb{1}_{\mathbb{F}}, \quad d_{L+} = a_0 \otimes \dot{\eta}, \quad d_{R+} = a_0 \otimes \dot{\eta} + c_0 \otimes \eta.$$

FIGURE 17. Example tangle diagram T .

5. INVARIANCE UNDER REIDEMEISTER MOVES

Consider an A_∞ category \mathcal{A} . Let $\text{Tw } \mathcal{A}$ denote the category of twisted complexes over \mathcal{A} . We say that two twisted complexes (X, δ_X) and (Y, δ_Y) are *homotopy equivalent* if there are morphisms $F : (X, \delta_X) \rightarrow (Y, \delta_Y)$, $G : (Y, \delta_Y) \rightarrow (X, \delta_X)$, $K : (X, \delta_X) \rightarrow (X, \delta_X)$, and $H : (Y, \delta_Y) \rightarrow (Y, \delta_Y)$ such that

$$\begin{aligned} \mu_{\text{Tw } \mathcal{A}}^1(F) &= 0, & \mu_{\text{Tw } \mathcal{A}}^1(G) &= 0, \\ \mu_{\text{Tw } \mathcal{A}}^2(G, F) &= \mathbb{1}_{(X, \delta_X)} + \mu_{\text{Tw } \mathcal{A}}^1(K), & \mu_{\text{Tw } \mathcal{A}}^2(F, G) &= \mathbb{1}_{(Y, \delta_Y)} + \mu_{\text{Tw } \mathcal{A}}^1(H). \end{aligned}$$

In this case we say that F and G are *homotopy equivalences* and H and K are *homotopies*. Our goal in this section is to prove:

Theorem 5.1. *Assuming the A_∞ operations of \mathcal{L} are as described in Conjecture 4.1, if two oriented 1-tangle diagrams T_1 and T_2 are isotopic rel boundary, then the corresponding twisted complexes (X_1, δ_1) and (X_2, δ_2) are homotopy equivalent.*

According to Conjecture 4.1, the A_∞ operations $\mu_{\Sigma \mathcal{L}}^m$ are zero for $m \neq 2$. In this situation the conditions for morphisms F and G to be homotopy equivalences reduce to

$$\begin{aligned} \delta_Y \circ F &= F \circ \delta_X, & \delta_X \circ G &= G \circ \delta_Y, \\ G \circ F &= \mathbb{1}_{(X, \delta_X)} + \delta_X \circ K + K \circ \delta_X, & F \circ G &= \mathbb{1}_{(Y, \delta_Y)} + \delta_Y \circ H + H \circ \delta_Y, \end{aligned}$$

where \circ denotes the product operation $\mu_{\Sigma \mathcal{L}}^2$ in $\Sigma \mathcal{L}$. So if Conjecture 4.1 is correct, the notion of homotopy equivalence in $\text{Tw } \mathcal{L}$ is formally identical to the notion of homotopy equivalence in the category of cochain complexes, only we interpret \circ as the product operation in $\Sigma \mathcal{L}$ rather than as the composition of linear maps.

Using this observation, we can prove Theorem 5.1 by adapting Bar-Natan's proof of the isotopy invariance of Khovanov homology in [5]. Proving the isotopy invariance of Khovanov homology amounts to showing that the cochain complexes of link diagrams related by Reidemeister moves are homotopy equivalent. Bar-Natan defines the relevant homotopy equivalences in terms of certain elementary cobordisms in a cobordism category for planar tangles. The invariance proof then reduces to showing that these elementary cobordisms satisfy a small number of relations. We will show that analogous relations hold for the differentials, cup maps, and cap maps that we defined in Section 4.3. Using these relations, we will define homotopy equivalences for Reidemeister moves that are formally identical to those defined by Bar-Natan.

5.1. Bar-Natan relations. We prove here the relations we will need involving differentials, cup maps, and cap maps. We name the relations by analogy with corresponding relations in Bar-Natan's cobordism category.

Suppose we create a circle component C with a cup $\cup : P_n(r) \rightarrow P_n(r+1)$ and then remove C with a cap $\cap : P_n(r+1) \rightarrow P_n(r)$. Let \cup and \cap also denote the corresponding cup and cap maps. We have:

Theorem 5.2. *We have the following sphere relation in $\Sigma \mathcal{L}$:*

$$\cap \circ \cup = 0.$$

Proof. We have

$$\cap \circ \cup = a_n \epsilon I_r \circ a_n \eta I_r = a_n (\epsilon \circ \eta) I_r = 0,$$

since $\epsilon \circ \eta = 0$. □

Take the left diagram in in Figure 19 to describe a portion of a planar tangle $P_n(r)$, where the arc A could either belong to the arc component of $P_n(r)$ or a circle component of $P_n(r)$. Define saddles $S_{A^+} : P_n(r) \rightarrow P_n(r+1)$ and $S_{A^-} : P_n(r+1) \rightarrow P_n(r)$ that split the indicated circle component C from and merge C with the arc A . Let d_{A^\pm} denote the differential corresponding to the saddle S_{A^\pm} . Define a cup $\cup : P_n(r) \rightarrow P_n(r+1)$ that creates C and a cap $\cap : P_n(r+1) \rightarrow P_n(r)$ that removes C . We will also use \cup and \cap to denote the corresponding cup and cap maps. We have:

Theorem 5.3. *We have the following isotopy invariance relations in $\Sigma\mathcal{L}$:*

$$d_{A^-} \circ \cup = \cap \circ d_{A^+} = a_n I_r.$$

We have the following neck cutting relations in $\Sigma\mathcal{L}$:

$$d_{A^+} \circ \cap + \cup \circ d_{A^-} = a_n I_{r+1}, \quad d_{A^-} \circ d_{A^+} = 0.$$

Proof. The cup and cap maps are

$$\cup = a_n \eta I_r, \quad \cap = a_n \epsilon I_r.$$

We have the following cases:

- (1) The arc A belongs to a circle component of $P_n(r)$. Then

$$d_{A^+} = d_{C^+} = a_n \Delta I_{r-1}, \quad d_{A^-} = d_{C^-} = a_n m I_{r-1}.$$

- (2) The arc A belongs to the arc component of $P_n(r)$ and the saddles S_{A^+} and S_{A^-} split C from and merge C with the right side of the arc component. Then

$$d_{A^+} = d_{R^+} = (a_n \dot{\eta} + c_n \eta) I_r, \quad d_{A^-} = d_{R^-} = (a_n \dot{\epsilon} + c_n \epsilon) I_r.$$

- (3) The arc A belongs to the arc component of $P_n(r)$ and the saddles S_{A^+} and S_{A^-} split C from and merge C with the left side of the arc component. Then

$$d_{A^+} = d_{L^+} = a_n \dot{\eta} I_r, \quad d_{A^-} = d_{L^-} = a_n \dot{\epsilon} I_r.$$

The result now follows from straightforward calculations. □

Take the leftmost diagram in Figure 20 to describe a portion of a planar tangle $P_n(r)$, where the arcs A and B could belong to either the arc component of $P_n(r)$ or to circle components of $P_n(r)$. Define saddles $S_{A^+} : P_n(r) \rightarrow P_n(r+1)$ and $S_{B^-} : P_n(r+1) \rightarrow P_n(r)$ that spit the indicated circle component C from arc A and merge C with arc B . Define saddles $S_{\parallel} : P_n(r) \rightarrow P_m(s)$ and $S_{\parallel=} : P_m(s) \rightarrow P_n(r)$ as shown in Figure 20. Let d_{A^+} , d_{B^-} , d_{\parallel} , and $d_{\parallel=}$ denote the differentials corresponding to the saddles S_{A^+} , S_{B^-} , S_{\parallel} , and $S_{\parallel=}$. Define a cup $\cup : P_n(r) \rightarrow P_n(r+1)$ that creates C and a cap $\cap : P_n(r+1) \rightarrow P_n(r)$ that removes C . We will also use \cup and \cap to denote the corresponding maps. We have:

Theorem 5.4. *We have the following isotopy invariance relation in $\Sigma\mathcal{L}$:*

$$d_{B^-} \circ d_{A^+} = d_{\parallel=} \circ d_{\parallel}.$$

We have the following 4-tube relation in $\Sigma\mathcal{L}$:

$$d_{A^+} \circ \cap + \cup \circ (d_{\parallel=} \circ d_{\parallel}) \circ \cap + \cup \circ d_{B^-} = a_n I_{r+1}.$$

Proof. We have the following cases:

- (1) Arcs A and B both belong to the arc component of $P_n(r)$, saddle S_{A^+} splits C from the right side of the arc, and saddle S_{B^-} merges C with the right side of the arc. We have

$$\begin{aligned} \cup &= a_0 \eta I_r, & \cap &= a_0 \epsilon I_r, \\ d_{A^+} &= d_{L^+} = a_n \dot{\eta} I_r, & d_{B^-} &= d_{L^-} = a_n \dot{\epsilon} I_r, \\ d_{\parallel} &= d_{R^+} = (a_n \dot{\eta} + c_n \eta) I_r + c_n \dot{\eta} I_{r_n} \Sigma_{r_e}, & d_{\parallel=} &= d_{R^-} = (a_n \dot{\epsilon} + c_n \epsilon) I_r + c_n \dot{\epsilon} I_{r_n} \Sigma_{r_e}. \end{aligned}$$

- (2) Arcs A and B both belong to the arc component of $P_n(r)$, saddle S_{A^+} splits C from the left side of the arc, and saddle S_{B^-} merges C with the left side of the arc. We have

$$\begin{aligned} \cup &= a_0\eta I_r, & \cap &= a_0\epsilon I_r, \\ d_{A^+} &= d_{R^+} = (a_n\dot{\eta} + c_n\eta)I_r, & d_{B^-} &= d_{R^-} = (a_n\dot{\epsilon} + c_n\epsilon)I_r, \\ d_{=||} &= d_{L^+} = a_n\dot{\eta}I_r + c_n\dot{\eta}I_{r_n}\Sigma_{r_e}, & d_{=||} &= d_{L^-} = a_n\dot{\epsilon}I_r + c_n\dot{\epsilon}I_{r_n}\Sigma_{r_e}. \end{aligned}$$

- (3) Arcs A and B both belong to the arc component of $P_n(r)$, saddle S_{A^+} splits C from the right side of the arc, and saddle S_{B^-} merges C with the left side of the arc. We have

$$\begin{aligned} \cup &= a_0\eta I_r, & \cap &= a_0\epsilon I_r, \\ d_{A^+} &= d_{R^+} = (a_n\dot{\eta} + c_n\eta)I_r, & d_{B^-} &= d_{L^-} = a_n\dot{\epsilon}I_r, \\ d_{=||} &= d_{W^+} = p_{n,n+2}I_r, & d_{=||} &= d_{W^-} = q_{n,n+2}I_r. \end{aligned}$$

- (4) Arcs A and B both belong to the arc component of $P_n(r)$, saddle S_{A^+} splits C from the left side of the arc, and saddle S_{B^-} merges C with the right side of the arc.

$$\begin{aligned} \cup &= a_0\eta I_r, & \cap &= a_0\epsilon I_r, \\ d_{A^+} &= d_{L^+} = a_n\dot{\eta}I_r, & d_{B^-} &= d_{R^-} = (a_n\dot{\epsilon} + c_n\epsilon)I_r, \\ d_{=||} &= d_{W^-} = q_{n,n-2}I_r, & d_{=||} &= d_{W^+} = p_{n,n-2}I_r. \end{aligned}$$

- (5) Arc A belongs to a circle component of $P_n(r)$, arc B belongs to the arc component, and saddle S_{B^-} merges C with the right side of the arc component. We have

$$\begin{aligned} \cup &= a_0\mathbb{1}\eta I_r, & \cap &= a_0\mathbb{1}\epsilon I_r, \\ d_{A^+} &= d_{C^+} = a_n\Delta I_r, & d_{B^-} &= d_{R^-} = (a_n\mathbb{1}\dot{\epsilon} + c_n\mathbb{1}\epsilon)I_r, \\ d_{=||} &= d_{R^-} = (a_n\dot{\epsilon} + c_n\epsilon)I_r + c_n\dot{\epsilon}I_{r_n}\Sigma_{r_e}, & d_{=||} &= d_{R^+} = (a_n\dot{\eta} + c_n\eta)I_r + c_n\dot{\eta}I_{r_n}\Sigma_{r_e}. \end{aligned}$$

- (6) Arc A belongs to a circle component of $P_n(r)$, arc B belongs to the arc component, and saddle S_{B^-} merges C with the left side of the arc component. We have

$$\begin{aligned} \cup &= a_0\mathbb{1}\eta I_r, & \cap &= a_0\mathbb{1}\epsilon I_r, \\ d_{A^+} &= d_{C^+} = a_n\Delta I_r, & d_{B^-} &= d_{L^-} = a_n\mathbb{1}\dot{\epsilon}I_r, \\ d_{=||} &= d_{L^-} = a_n\dot{\epsilon}I_r + c_n\dot{\epsilon}I_{r_n}\Sigma_{r_e}, & d_{=||} &= d_{L^+} = a_n\dot{\eta}I_r + c_n\dot{\eta}I_{r_n}\Sigma_{r_e}. \end{aligned}$$

- (7) Arcs A and B belong to distinct circle components of $P_n(r)$. We have

$$\begin{aligned} \cup &= a_n\mathbb{1}\eta\mathbb{1}I_{r-2}, & \cap &= a_n\mathbb{1}\epsilon\mathbb{1}I_{r-2}, \\ d_{A^+} &= d_{C^+} = a_n\Delta\mathbb{1}I_{r-2}, & d_{B^-} &= d_{C^-} = a_n\mathbb{1}mI_{r-2}, \\ d_{=||} &= d_{C^-} = a_nmI_{r-2}, & d_{=||} &= d_{C^+} = a_n\Delta I_{r-2}. \end{aligned}$$

- (8) Arcs A and B belong to the same circle component of $P_n(r)$. We have

$$\begin{aligned} \cup &= \mathbb{1}\eta I_{r-1}, & \cap &= \mathbb{1}\epsilon I_{r-1}, \\ d_{A^+} &= d_{C^+} = a_n\Delta I_{r-1}, & d_{B^-} &= d_{C^-} = a_nmI_{r-1}, \\ d_{=||} &= d_{C^-} = mI_{r-1}, & d_{=||} &= d_{C^+} = \Delta I_{r-1}. \end{aligned}$$

The now result follows from straightforward calculations. \square

In [15], twisted complexes over the Fukaya category of the pillowcase are constructed from 2-tangle diagrams in the disk via an A_∞ functor whose source is the A_∞ category of twisted complexes over Bar-Natan's cobordism category. The relations described in Theorems 5.2, 5.3, and 5.4 suggest that it may be possible to construct an analogous cobordism category and A_∞ functor that would yield the twisted complex (X, δ) described in Section 4.5. It would be interesting to attempt to construct such a cobordism category.

We will now show invariance under the Reidemeister moves shown in Figure 18, under the assumption that the A_∞ relations for \mathcal{L} are as described in Conjecture 4.1.

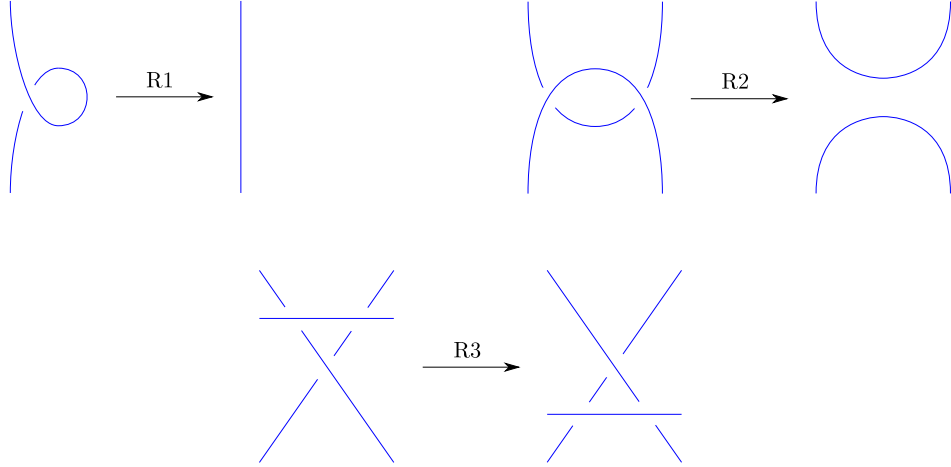


FIGURE 18. Reidemeister moves R1, R2, and R3.

5.2. Reidemeister move R1. Suppose we apply the Reidemeister move R1 shown in Figure 18 to a tangle diagram T_A , resulting in a tangle diagram T_B . Let (X_A, δ_A) and (X_B, δ_B) denote the twisted objects corresponding to T_A and T_B . The objects X_A and X_B are formal direct sums of terms, as described by equation (12). Each term of X_B corresponds to a planar tangle $P_n(r)$ obtained by resolving T_B , and can be viewed as a subobject $(x_B, 0)$ of (X_B, δ_B) with zero differential:

$$(x_B, 0) = L_n \otimes A^{\otimes r}[h_B, q_B],$$

where the bigrading shift $[h_B, q_B]$ depends on the crossing numbers of T_B and on the location of $P_n(r)$ within the cube of resolutions.

If we apply the move R1 in reverse to the planar tangle $P_n(r)$ and then resolve the resulting crossing, we obtain a saddle $S_{A^+} : P_n(r) \rightarrow P_n(r+1)$ that splits a circle component C from the arc A , as shown in Figure 19. Let $d_{A^+} : L_n \otimes A^{\otimes r} \rightarrow L_n \otimes A^{\otimes(r+1)}$ denote the corresponding differential. We conclude that for each subobject $(x_B, 0)$ of (X_B, δ_B) , there is a corresponding subobject (x_A, d^0) of (X_A, δ_A) given by

$$(x_A, d^0) = L_n \otimes A^{\otimes r}[h_A, q_A] \xrightarrow{d^0} L_n \otimes A^{\otimes(r+1)}[h_A + 1, q_A + 2],$$

where

$$(d^0)^{(1,1)} = d_{A^+}[1, 2].$$

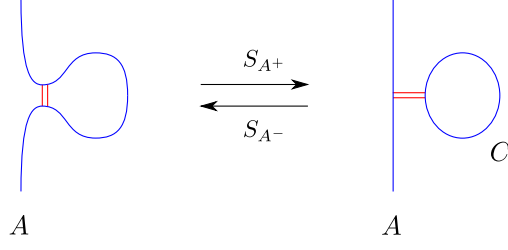
The tangle diagram T_A contains one more negative crossing than T_B , so the relative crossing numbers of T_A and T_B are $\delta m_+ = 0$ and $\delta m_- = 1$, corresponding to a bigrading shift

$$[h_A, q_A] = [h_B, q_B] + [-\delta m_-, \delta m_+ - 3\delta m_-] = [h_B, q_B] + [-1, -3].$$

We will show that (X_A, δ_A) and (X_B, δ_B) are homotopy equivalent by constructing homotopy equivalences between each pair of corresponding subobjects $(x_A, 0)$ and (x_B, d^0) . The homotopy equivalences will commute with the differentials δ_A and δ_B , and will thus combine to give homotopy equivalences of (X_A, δ_A) and (X_B, δ_B) .

We define homotopy equivalences $F : (x_B, 0) \rightarrow (x_A, d^0)$ and $G : (x_A, d^0) \rightarrow (x_B, 0)$ and a homotopy $H : (x_A^0, d^0) \rightarrow (x_A^0, d^0)$:

$$\begin{array}{ccc} L_n \otimes A^{\otimes r} & \begin{array}{c} \xrightarrow{d^0} \\ \xleftarrow{H^1} \end{array} & L_n \otimes A^{\otimes(r+1)} \\ & \begin{array}{c} \uparrow F^1 \\ \downarrow G^1 \end{array} & \\ & & L_n \otimes A^{\otimes r}. \end{array}$$

FIGURE 19. Saddles S_{A+} and S_{A-} for Reidemeister move R1.

For simplicity we have omitted bigrading shifts in the diagram. The homotopy equivalences are given by

$$(F^1)^{(0,0)} = \cup[0, -1], \quad (G^1)^{(0,0)} = d_{A-}[0, 1],$$

where \cup is the cup map for creating C and d_{A-} is the differential for the saddle $S_{A-} : P_n(r+1) \rightarrow P_n(r)$ that merges C with the arc A . The homotopy is given by

$$(H^1)^{(-1,-1)} = \cap[-1, -2],$$

where \cap is the cap map for removing C . Using the Bar-Natan relations described in Theorem 5.3, we find

$$\begin{aligned} G^1 \circ d^0 &= (d_{A-} \circ d_{A+})[1, 3] = 0, \\ G^1 \circ F^1 &= d_{A-} \circ \cup = a_n I_r, \\ H^1 \circ d^0 &= \cap \circ d_{A+} = a_n I_r, \\ d^0 \circ H^1 + F^1 \circ G^1 &= d_{A+} \circ \cap + \cup \circ d_{A-} = a_n I_{r+1}, \end{aligned}$$

so F and G are indeed homotopy equivalences.

The homotopy equivalences we have defined for subobjects are constructed from differentials and cup maps, which by Theorems 4.2 and 4.3 commute with the differentials δ_A and δ_B . It follows that the homotopy equivalences for subobjects combine to yield homotopy equivalences of the objects (X_A, δ_A) and (X_B, δ_B) .

A similar argument shows invariance under R1 with a positive crossing.

5.3. Reidemeister move R2. Suppose we apply the Reidemeister move R2 shown in Figure 18 to a tangle diagram T_A , resulting in a tangle diagram T_B . Let (X_A, δ_A) and (X_B, δ_B) denote the twisted objects corresponding to T_A and T_B . The objects X_A and X_B are formal direct sums of terms, as described by equation (12). Each term of X_B corresponds to a planar tangle $P_n(r)$ obtained by resolving T_B , and can be viewed as a subobject $(x_B, 0)$ of (X_B, δ_B) with zero differential:

$$(x_B, 0) = L_n \otimes A^{\otimes r}[h_B, q_B],$$

where the bigrading shift $[h_B, q_B]$ depends on the crossing numbers of T_B and on the location of $P_n(r)$ within the cube of resolutions.

If we apply the move R2 in reverse to the planar tangle $P_n(r)$ and then resolve the two resulting crossings, we obtain a cube of resolutions

$$\begin{array}{ccccc} & & P_m(s+1) & & \\ & S_{A+} \nearrow & & \searrow S_{B-} & \\ P_m(s) & & & & P_m(s) \\ & S_{=||} \searrow & & \nearrow S_{=||} & \\ & & P_n(r) & & \end{array}$$

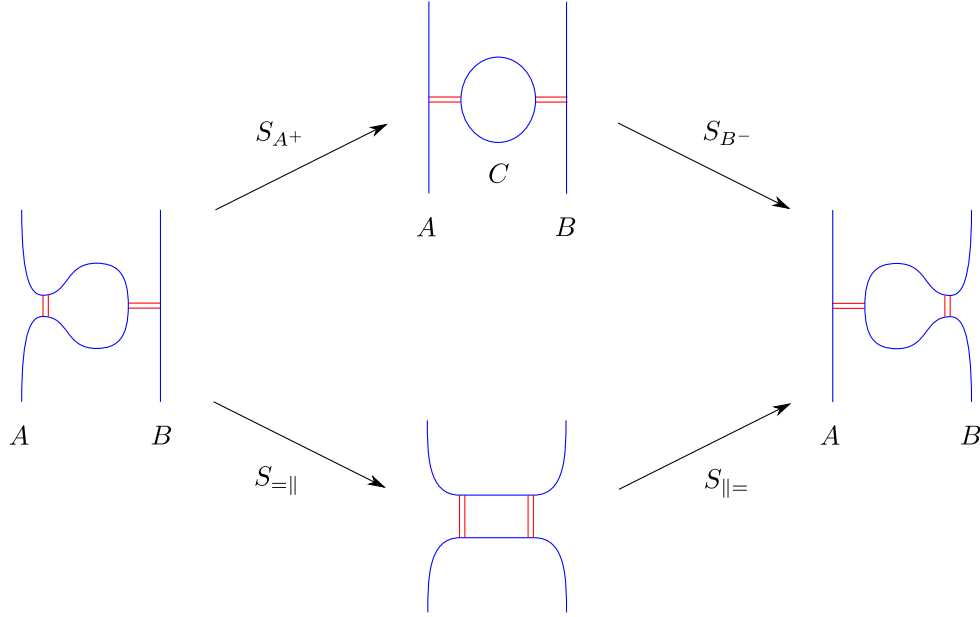


FIGURE 20. Cube of resolutions for Reidemeister move R2.

as shown in Figure 20. The winding number m and circle number s of the planar tangle $P_m(s)$ depend on how the move is applied. As shown in Figure 20, the saddle S_{A+} splits the circle component C from arc A and the saddle S_{B-} merges the circle component C with arc B . Let d_{A+} , d_{B-} , $d_{=||}$, and $d_{||=}$ denote the differentials corresponding to the saddles S_{A+} , S_{B-} , $S_{=||}$, and $S_{||=}$. We conclude that for each subobject $(x_B, 0)$ of (X_B, δ_B) , there is a corresponding subobject (x_A, d) of (X_A, δ_A) given by

$$\begin{array}{ccc}
 & L_m \otimes A^{\otimes(s+1)}[h_B + 1, q_B + 2] & \\
 d_{A+}[1,2] \nearrow & & \searrow d_{B-}[1,2] \\
 (x_A, d) = L_m \otimes A^{\otimes s}[h_B, q_B] & & L_m \otimes A^{\otimes s}[h_B + 2, q_B + 4]. \\
 d_{=||}[1,2] \searrow & & \nearrow d_{||=}[1,2] \\
 & L_n \otimes A^{\otimes r}[h_B + 1, q_B + 2] &
 \end{array}$$

The differentials for (x_A, d) are

$$(d^0)^{(1,1)} = \begin{pmatrix} d_{A+}[1,2] \\ d_{=||}[1,2] \end{pmatrix}, \quad (d^1)^{(1,1)} = \begin{pmatrix} d_{B-}[1,2] & d_{||=}[1,2] \end{pmatrix}.$$

The tangle diagram T_A contains one more negative crossing and one more positive crossing than T_B , so the relative crossing numbers of T_A and T_B are $\delta m_+ = 1$ and $\delta m_- = 1$, corresponding to a bigrading shift

$$[h_A, q_A] = [h_B, q_B] + [-\delta m_-, \delta m_+ - 3\delta m_-] = [h_B, q_B] + [-1, -2].$$

We define homotopy equivalences $F : (x_B, 0) \rightarrow (x_A, d^0)$ and $G : (x_A, d) \rightarrow (x_B, 0)$ and a homotopy $H : (x_A^0, d) \rightarrow (x_A^0, d)$:

$$\begin{array}{ccccc}
 & & L_m \otimes A^{\otimes(s+1)} & \xleftarrow{G^1} & \\
 & & \swarrow d_{B^-} & \xleftarrow{F^1} & \\
 & & L_m \otimes A^{\otimes s} & & L_n \otimes A^{\otimes r} \\
 & \swarrow d_{A^+} & \cap & \searrow d_{B^-} & \\
 L_m \otimes A^{\otimes s} & & & & \\
 & \searrow d_{=} & & \swarrow d_{=} & \\
 & & L_n \otimes A^{\otimes r} & \xleftarrow{G^1} & \\
 & & & \xleftarrow{F^1} &
 \end{array}$$

For simplicity we have omitted bigrading shifts in the diagram. Here \cup and \cap the cup and cap maps for creating and removing the circle component C . The homotopy equivalences are given by

$$(F^1)^{(0,0)} = \begin{pmatrix} \cup \circ d_{=} \\ a_n I_r \end{pmatrix}, \quad (G^1)^{(0,0)} = (d_{=} \circ \cap \quad a_n I_r).$$

The homotopy H is given by

$$(H^1)^{(-1,-1)} = (\cap[-1, -2] \quad 0), \quad (H^2)^{(-1,-1)} = \begin{pmatrix} \cup[-1, -2] \\ 0 \end{pmatrix}.$$

Using the isotopy invariance relations described in Theorem 5.3, we find

$$d^1 \circ F^1 = ((d_{B^-} \circ \cup) \circ d_{=} + d_{=})[1, 2] = 0, \quad G^1 \circ d^0 = (d_{=} \circ (\cap \circ d_{A^+}) + d_{=})[1, 2] = 0.$$

Using the sphere relation described in Theorem 5.2 and the isotopy invariance relations described in Theorem 5.3, we find

$$\begin{aligned}
 H^1 \circ d^0 &= \cap \circ d_{A^+} = a_m I_s, \\
 d^1 \circ H^2 &= d_{B^-} \circ \cup = a_m I_s, \\
 G^1 \circ F^1 &= d_{=} \circ (\cap \circ \cup) \circ d_{=} + a_n I_r = a_n I_r,
 \end{aligned}$$

and using the 4-tube relation described in Theorem 5.4 we find

$$\begin{aligned}
 & d^0 \circ H^1 + F^1 \circ G^1 + H^2 \circ d^1 \\
 &= \begin{pmatrix} d_{A^+} \circ \cap & 0 \\ d_{=} \circ \cap & 0 \end{pmatrix} + \begin{pmatrix} \cup \circ (d_{=} \circ d_{=}) \circ \cap & \cup \circ d_{=} \\ d_{=} \circ \cap & a_n I_r \end{pmatrix} + \begin{pmatrix} \cup \circ d_{B^-} & \cup \circ d_{=} \\ 0 & 0 \end{pmatrix} \\
 &= \begin{pmatrix} a_m I_{s+1} & 0 \\ 0 & a_n I_r \end{pmatrix}.
 \end{aligned}$$

So F and G are indeed homotopy equivalences. We note also that using the sphere relation from Theorem 5.2, we have

$$H^1 \circ F^1 = 0.$$

The homotopy equivalences we have defined for subobjects are constructed from differentials, cup maps, and cap maps, which by Theorems 4.2 and 4.3 commute with the differentials δ_A and δ_B . It follows that the homotopy equivalences for subobjects combine to yield homotopy equivalences of the objects (X_A, δ_A) and (X_B, δ_B) .

The homotopy equivalence $(X_A, \delta_A) \rightarrow (X_B, \delta_B)$ that we have constructed has a special property that will be useful in proving invariance under move R3. In the category of cochain complexes, a cochain map $G : (C_A, d_A) \rightarrow (C_B, d_B)$ is said to be a *strong deformation retraction* if there is a cochain map $F : (C_B, d_B) \rightarrow (C_A, d_A)$ and a homotopy $H : (C_A, d_A) \rightarrow (C_A, d_A)$ such that

$$G \circ F = I_{(C_B, d_B)}, \quad F \circ G = I_{(C_A, d_A)} + d_A \circ H + H \circ d_A, \quad H \circ F = 0.$$

We can extend this notion to the category of twisted complexes over an arbitrary A_∞ category \mathcal{A} . We say that a homotopy equivalence $G : (X, \delta_X) \rightarrow (Y, \delta_Y)$ of twisted complexes is a *strong deformation retraction*

if there is a homotopy equivalence $F : (Y, \delta_Y) \rightarrow (X, \delta_X)$ and a homotopy $H : (X, \delta_X) \rightarrow (X_X, \delta_X)$ such that

$$\mu_{\text{Tw } \mathcal{A}}^2(G, F) = \mathbb{1}_{(X_Y, \delta_Y)}, \quad \mu_{\text{Tw } \mathcal{A}}^2(F, G) = \mathbb{1}_{(X, \delta_X)} + \mu_{\text{Tw } \mathcal{A}}^1(H), \quad \mu_{\text{Tw } \mathcal{A}}^2(H, F) = 0.$$

According to Conjecture 4.1, the A_∞ operations $\mu_{\mathcal{L}}^m$ are zero for $m \neq 0$, so these conditions reduce to conditions that are formally identical to those used to define the notion of a strong deformation retraction in the category of cochain complexes:

$$G \circ F = \mathbb{1}_{(X_Y, \delta_Y)}, \quad F \circ G = \mathbb{1}_{(X, \delta_X)} + \delta_Y \circ H + H \circ \delta_X, \quad H \circ F = 0,$$

where \circ denotes the product operation $\mu_{\Sigma \mathcal{L}}^2$ in $\Sigma \mathcal{L}$. So the homotopy equivalence $(X_A, \delta_A) \rightarrow (X_B, \delta_B)$ we have constructed is a strong deformation retraction.

5.4. Reidemeister move R3. An argument presented by Bar-Natan in Section 4.3 of [5] now proves invariance under move R3 using invariance under move R2 and the fact that the homotopy equivalence for R2 is a strong deformation retraction. Bar-Natan's argument is formulated in terms of the category of twisted complexes over a cobordism category modulo local relations, but given Conjecture 4.1, which states that only product operations of \mathcal{L} are nonzero, it carries over directly to $\text{Tw } \mathcal{L}$. This completes the proof of Theorem 3.26

6. LINKS IN S^3

In Section 4, we showed that given an oriented 1-tangle diagram T we can construct corresponding twisted complexes (X, δ_+) and (X, δ_-) . We can close T with an overpass arc A_+ or underpass arc A_- , as shown in Figure 2, to obtain diagrams of oriented links L_{T+} and L_{T-} in S^3 . Our goal in this section is to use the twisted complexes (X, δ_+) and (X, δ_-) to recover the reduced Khovanov homology for these links.

Recall from Section 3.9 that for links in S^3 an overpass arc A_+ and an underpass arc A_- correspond to Lagrangians \overline{W}_0 and \overline{W}_1 in $R^*(T^2, 2)$. For convenience, we will denote these Lagrangians as W_+ and W_- :

$$W_+ = \overline{W}_0, \quad W_- = \overline{W}_1.$$

Recall from Section 2.2 that given a Lagrangian M in $R^*(T^2, 2)$ we can define an A_∞ functor $\text{Tw } \mathcal{G}_M : \text{Tw } \mathcal{L} \rightarrow \text{Ch}$. We define cochain complex (C_\pm, ∂_\pm) for the link $L_{T\pm}$ by applying the functor $\text{Tw } \mathcal{G}_{W_\pm}$ to the twisted object (X, δ_\pm) and shifting the bigrading:

$$(C_\pm, \partial_\pm) = (\text{Tw } \mathcal{G}_{W_\pm}((X, \delta_\pm)))[h_A, q_A].$$

The bigrading shift $[h_A, q_A]$ accounts for crossings between the arc A_\pm and the tangle diagram T , and is computed as follows. Assume that the arc intersects the tangle diagram T transversely. Let a_+ and a_- denote the number of positive and negative intersection points between the arc and T . Note that a_+ and a_- depend on the position of the arc in relation to T , but the difference $a_+ - a_-$ does not. The bigrading shift $[h_A, q_A]$ is then given by

$$[h_A, q_A] = \begin{cases} [r, 4r] & \text{for } a_+ - a_- = 2r \text{ even,} \\ [r, 4r + 2] & \text{for } a_+ - a_- = 2r + 1 \text{ odd.} \end{cases}$$

Recall that (X, δ_\pm) already includes a bigrading shift $[h_T, q_T]$ that accounts for crossings of T with itself.

Given certain assumptions regarding the A_∞ operations of \mathcal{L} and the gradings of the generators of the vector spaces (W_\pm, L_n) , we can explicitly construct the cochain complex (C_\pm, ∂_\pm) from the tangle diagram T . We first describe the assumptions that we will need.

6.1. A_∞ operations and gradings of generators. Recall from Theorems 3.24 and 3.25 that the vector spaces (W_\pm, L_n) are 1-dimensional and are each generated by a vector with positive orientation grading:

$$(W_+, L_n) = (\overline{W}_0, L_n) = \langle w_{n,+}^{(+)} \rangle, \quad (W_-, L_n) = (\overline{W}_1, L_n) = \langle w_{n,-}^{(+)} \rangle,$$

where for convenience we have defined

$$w_{n,+} = \overline{w}_{n,0}, \quad w_{n,-} = \overline{w}_{n,1}.$$

We assign an integer homological grading h and an integer quantum grading q to each generator, as indicated by the superscripts (h, q) :

$$(W_{\pm}, L_n) = \begin{cases} \langle w_{n,\pm}^{(\pm\frac{1}{2}n, \pm 2n)} \rangle & \text{for } n \text{ even,} \\ \langle w_{n,\pm}^{(\frac{1}{2}(1\pm n), \pm 2n)} \rangle & \text{for } n \text{ odd,} \end{cases}$$

To construct the cochain complex $(C_{\pm}, \partial_{\pm})$, we need to know A_{∞} operations involving the generators $w_{n,\pm}$ of (W_{\pm}, L_n) as well as the generators a_n , c_n , $p_{n+2,n}^{(\mp)}$, and $q_{n-2,n}^{(\pm)}$ that appear in δ_{\pm} . We make the following conjecture regarding these operations:

Conjecture 6.1. *We have the following product operations:*

$$\mu^2(a_n, w_{n,\pm}) = w_{n,\pm}.$$

We have the following μ^3 operations:

$$\begin{aligned} \mu^3(c_{n-2}, q_{n-2,n}^{(+)}, w_{n,+}) &= \mu^3(q_{n-2,n}^{(+)}, c_n, w_{n,+}) = w_{n-2,+}, \\ \mu^3(c_{n+2}, p_{n+2,n}^{(+)}, w_{n,-}) &= \mu^3(p_{n+2,n}^{(+)}, c_n, w_{n,-}) = w_{n+2,-}. \end{aligned}$$

All other operations of the form

$$\mu^m(x_{m-1}, \dots, x_1, w_{n,+}), \quad \mu^m(x_{m-1}, \dots, x_1, w_{n,-})$$

for $x_{m-1}, \dots, x_1 \in \{a_n, c_n, p_{n+2,n}^{(\mp)}, q_{n-2,n}^{(\pm)} \mid n \in \mathbb{Z}\}$ are zero.

It is straightforward to check that Conjecture 6.1 is consistent with the orientation gradings of the generators. As described in Appendix A, Conjecture 6.1 is a natural generalization of a corresponding statement regarding the Fukaya category of $R^*(S^2, 4)$. One motivation for Conjecture 6.1 is the following result:

Theorem 6.2. *If the A_{∞} operations respect bigradings, then all operations of the form*

$$\mu^m(x_{m-1}, \dots, x_1, w_{n,+}), \quad \mu^m(x_{m-1}, \dots, x_1, w_{n,-}),$$

for $x_{m-1}, \dots, x_1 \in \{a_n, c_n, p_{n+2,n}^{(\mp)}, q_{n-2,n}^{(\pm)} \mid n \in \mathbb{Z}\}$ must be zero, with the exception of

$$\begin{aligned} \mu^2(a_n, w_{n,+}), & \quad \mu^3(c_{n-2}, q_{n-2,n}^{(+)}, w_{n,+}), & \quad \mu^3(q_{n-2,n}^{(+)}, c_n, w_{n,+}), \\ \mu^2(a_n, w_{n,-}), & \quad \mu^3(c_{n+2}, p_{n+2,n}^{(+)}, w_{n,-}), & \quad \mu^3(p_{n+2,n}^{(+)}, c_n, w_{n,-}). \end{aligned}$$

Proof. Let n_a , n_c , n_p , and n_q denote the number of x_k 's that belong to the sets

$$\{a_n \mid n \in \mathbb{Z}\}, \quad \{c_n \mid n \in \mathbb{Z}\}, \quad \{p_{n+2,n}^{(\pm)} \mid n \in \mathbb{Z}\}, \quad \{q_{n-2,n}^{(\pm)} \mid n \in \mathbb{Z}\}.$$

We have

$$(14) \quad n_a + n_c + n_p + n_q = m - 1.$$

If the A_{∞} operation involving $w_{n,+}$ is nonzero, then we must have

$$(15) \quad \mu^m(x_{m-1}, \dots, x_1, w_{n,+}^{(h,q)}) = w_{n-2r,+}^{(h-r,q-4r)}$$

for some integer r . We must balance the winding numbers on both sides of equation (15), so:

$$(16) \quad n_q - n_p = r.$$

Given our assumption that the A_{∞} relations respect bigradings, we have

$$(17) \quad 2n_c + n_p + n_q + m - 2 = 4r, \quad m - 2 = r.$$

From equations (14), (16), and (17), it follows that

$$n_a + n_c + 2n_p = 1.$$

So $n_p = 0$ and either $(n_a, n_c) = (1, 0)$, in which case

$$n_a = 1, \quad n_c = 0, \quad n_p = 0, \quad n_q = 0, \quad m = 2, \quad r = 0,$$

or $(n_a, n_c) = (0, 1)$, in which case

$$n_a = 0, \quad n_c = 1, \quad n_p = 0, \quad n_q = 1, \quad m = 3, \quad r = 1.$$

The operations

$$\mu^3(c_{n-2}, q_{n-2,n}^{(-)}, w_{n,+}), \quad \mu^3(q_{n-2,n}^{(-)}, c_n, w_{n,+}),$$

must be zero, since otherwise they would have to be $w_{n-2,+}$, which is inconsistent with orientation gradings. The proof for the A_∞ operations involving $w_{n,-}$ is similar. \square

6.2. Chain complex. Using Conjecture 6.1, the description of the functor $\text{Tw } \mathcal{G}_{W_\pm}$ from Section 2.2, and the description of the twisted complex (X, δ_\pm) from Section 4.5, we can explicitly construct the cochain complex (C_\pm, ∂_\pm) for the link L_{T^\pm} . The vector space C_\pm is given by

$$C_\pm = \bigoplus_{i \in I} ((W_\pm, L_{n_i}) \otimes A^{\otimes c_i} [r(i) + h_T + h_A, 2r(i) + q_T + q_A]).$$

There are no μ^1 operations, so the differentials ∂_\pm are due entirely to δ_\pm . The μ^2 operations give *short differentials* corresponding to single saddles, and the μ^3 operations give *long differentials* corresponding to pairs of successive saddles.

For both L_{T^+} and L_{T^-} , the μ^2 operations involving $w_{n,\pm}$ give the following short differentials:

- (1) For a saddle $P_n(r+1) \rightarrow P_n(r+2)$ that splits one circle into two circles:

$$\partial_{C^+} : (W_\pm, L_n) \otimes A^{\otimes(r+1)} \rightarrow (W_\pm, L_n) \otimes A^{\otimes(r+2)}[1, 2], \quad \partial_{C^+} = ((w_{n,\pm} \mapsto w_{n,\pm}) \otimes \Delta I_r)[1, 2].$$

For a saddle $P_n(r+2) \rightarrow P_n(r+1)$ that merges two circles into one circle:

$$\partial_{C^-} : (W_\pm, L_n) \otimes A^{\otimes(r+2)} \rightarrow (W_\pm, L_n) \otimes A^{\otimes(r+1)}[1, 2], \quad \partial_{C^-} = ((w_{n,\pm} \mapsto w_{n,\pm}) \otimes m I_r)[1, 2].$$

- (2) For a saddle $P_n(r) \rightarrow P_n(r+1)$ that splits a circle from either side of the arc component:

$$\partial_{A^+} : (W_\pm, L_n) \otimes A^{\otimes r} \rightarrow (W_\pm, L_n) \otimes A^{\otimes(r+1)}[1, 2], \quad \partial_{A^+} = ((w_{n,\pm} \mapsto w_{n,\pm}) \otimes \dot{\eta} I_r)[1, 2].$$

For a saddle $P_n(r+1) \rightarrow P_n(r)$ that merges a circle with either side of the arc component:

$$\partial_{A^-} : (W_\pm, L_n) \otimes A^{\otimes(r+1)} \rightarrow (W_\pm, L_n) \otimes A^{\otimes r}[1, 2], \quad \partial_{A^-} = ((w_{n,\pm} \mapsto w_{n,\pm}) \otimes \dot{\epsilon} I_r)[1, 2].$$

For L_{T^+} , the μ^3 operations involving $w_{n,+}$ give the following long differentials:

- (1) For a saddle $P_n(r) \rightarrow P_{n-2}(r)$ that decreases the winding number by two followed by a saddle $P_{n-2}(r) \rightarrow P_{n-2}(r+1)$ that splits a circle from the right side of the arc component, or for a saddle $P_n(r) \rightarrow P_n(r+1)$ that splits a circle from the right side of the arc component followed by a saddle $P_n(r+1) \rightarrow P_{n-2}(r+1)$ that decreases the winding number by two:

$$\partial_{R^+W^-} : (W_+, L_n) \otimes A^{\otimes r} \rightarrow (W_+, L_{n-2}) \otimes A^{\otimes(r+1)}[2, 4], \quad \partial_{R^+W^-} = ((w_{n,+} \mapsto w_{n-2,+}) \otimes \eta I_r)[2, 4].$$

- (2) For a saddle $P_n(r+1) \rightarrow P_{n-2}(r+1)$ that decreases the winding number by two followed by a saddle $P_{n-2}(r+1) \rightarrow P_{n-2}(r)$ that merges a circle with the right side of the arc component, or for a saddle $P_n(r+1) \rightarrow P_n(r)$ that merges a circle with the right side of the arc component followed by a saddle $P_n(r) \rightarrow P_{n-2}(r)$ that decreases the winding number by two:

$$\partial_{R^-W^-} : (W_+, L_n) \otimes A^{\otimes(r+1)} \rightarrow (W_+, L_{n-2}) \otimes A^{\otimes r}[2, 4], \quad \partial_{R^-W^-} = ((w_{n,+} \mapsto w_{n-2,+}) \otimes \epsilon I_r)[2, 4].$$

For L_{T^-} , the μ^3 operations involving $w_{n,-}$ give the following long differentials:

- (1) For a saddle $P_n(r) \rightarrow P_{n+2}(r)$ that increases the winding number by two followed by a saddle $P_{n+2}(r) \rightarrow P_{n+2}(r+1)$ that splits a circle from the right side of the arc component, or for a saddle $P_n(r) \rightarrow P_n(r+1)$ that splits a circle from the right side of the arc component followed by a saddle $P_n(r+1) \rightarrow P_{n+2}(r+1)$ that increases the winding number by two:

$$\partial_{R^+W^+} : (W_-, L_n) \otimes A^{\otimes r} \rightarrow (W_-, L_{n+2}) \otimes A^{\otimes(r+1)}[2, 4], \quad \partial_{R^+W^+} = ((w_{n,-} \mapsto w_{n+2,-}) \otimes \eta I_r)[2, 4].$$

- (2) For a saddle $P_n(r+1) \rightarrow P_{n+2}(r+1)$ that increases the winding number by two followed by a saddle $P_{n+2}(r+1) \rightarrow P_{n+2}(r)$ that merges a circle with the right side of the arc component, or for a saddle $P_n(r+1) \rightarrow P_n(r)$ that merges a circle with the right side of the arc component followed by a saddle $P_n(r) \rightarrow P_{n+2}(r)$ that increases the winding number by two:

$$\partial_{R^-W^+} : (W_-, L_n) \otimes A^{\otimes r} \rightarrow (W_-, L_{n+2}) \otimes A^{\otimes(r+1)}[2, 4], \quad \partial_{R^-W^+} = ((w_{n,-} \mapsto w_{n+2,-}) \otimes \epsilon I_r)[2, 4].$$

In fact, the long differentials due to the μ^3 operations contain additional terms involving the nonlocal operator Σ_r . However, in a cube of resolutions for a tangle diagram these terms always occur in canceling pairs corresponding to saddles on opposite sides of the arc component, so we can omit them from the expressions for the differentials. We note that for tangle diagrams with loop number 0, there are no long differentials and the cochain complex is the usual cochain complex for reduced Khovanov homology, where the marked component is the one containing the arc component T , and with the convention that the differential has quantum grading 1, rather than the usual quantum grading of 0.

Theorem 6.3. *We have*

$$\text{Khr}^{(h,q)}(L_{T^\pm}) = H^{(h,h+q)}((C_\pm, \partial_\pm)).$$

Proof. This is shown in [8], although we need to translate conventions. Here we define generators $w_{n,+}$ and $w_{n,-}$ for an overpass and underpass arc, and we shift bigradings by $[h_A, q_A]$ to account for crossings of the arc with the tangle. In [8], the corresponding cochain complex is defined in terms of generators $P_{\ell,n}^+$ or $P_{\ell,n}^-$ for an overpass or underpass arc, where $\ell = a_+ + a_-$, and we shift bigradings by $[h_A^P, q_A^P]$ to account for crossings of the arc with the tangle diagram. The bigrading (h, q) of $P_{\ell,n}^\pm$ is

$$((1/2)(\ell \pm n), (1/2)(\ell \pm 3n)).$$

The bigrading shift $[h_A^P, q_A^P]$ is given by

$$[h_A^P, q_A^P] = [-a_-, a_+ - 2a_-].$$

The generators of the two complexes are thus related by

$$\begin{array}{ccc} P_{\ell,n}^+[h_A^P, q_A^P] & \longleftrightarrow & w_{n,+}[h_A, q_A], \\ P_{\ell,n}^-[h_A^P, q_A^P] & \longleftrightarrow & w_{n,-}[h_A, q_A]. \end{array}$$

The convention for the bigrading of the differential is $(1, 0)$ in [8] and $(1, 1)$ here, so we want to show that the bigradings of the generators are related by

$$(h, q) \longleftrightarrow (h, h + q).$$

This is a straightforward calculation. □

6.3. Example: unknot in S^3 . We can close the tangle diagram T shown in Figure 17 with an overpass arc A_+ as shown in Figure 2 to obtain the link L_{T^+} , which is the unknot. The number of positive and negative crossings between T and A_+ is $a_+ = 0$ and $a_- = 2$, so $a_+ - a_- = -2 = 2r$ for $r = -1$, corresponding to a bigrading shift

$$[h_A, q_A] = [r, 4r] = [-1, -4].$$

We obtain the following cochain complex (C_+, ∂_+) :

$$\begin{array}{ccc} \langle w_{0,+}^{(0,0)} \rangle \otimes \mathbb{F}[0, 0] & & \\ & \searrow^{((w_{0,+} \mapsto w_{0,+}) \otimes \dot{\eta})[1,2]} & \\ \langle w_{2,+}^{(1,4)} \rangle \otimes \mathbb{F}[-1, -2] & \xrightarrow{((w_{2,+} \mapsto w_{0,+}) \otimes \eta)[2,4]} & \langle w_{0,+}^{(0,0)} \rangle \otimes A[1, 2]. \\ & \nearrow_{((w_{0,+} \mapsto w_{0,+}) \otimes \dot{\eta})[1,2]} & \\ \langle w_{0,+}^{(0,0)} \rangle \otimes \mathbb{F}[0, 0] & & \end{array}$$

So we obtain the reduced Khovanov homology $\mathbb{F}[0, 0]$ for the unknot.

6.4. Example: right trefoil in S^3 . We can close the tangle diagram T shown in Figure 17 with an underpass arc A_- as shown in Figure 2 to obtain the link L_{T^-} , which is the right trefoil. The number of positive and negative crossings between T and A_- is $a_+ = 2$ and $a_- = 0$, so $a_+ - a_- = 2 = 2r$ for $r = 1$, corresponding to a bigrading shift

$$[h_A, q_A] = [r, 4r] = [1, 4].$$

We obtain the following cochain complex (C_-, ∂_-) :

$$\begin{array}{ccc}
 & \langle w_{0,-}^{(0,0)} \rangle \otimes \mathbb{F}[2, 8] & \\
 & \searrow^{((w_{0,-} \mapsto w_{0,-}) \otimes \dot{\eta})[1,2]} & \\
 \langle w_{2,-}^{(-1,-4)} \rangle \otimes \mathbb{F}[1, 6] & & \langle w_{0,-}^{(0,0)} \rangle \otimes A[3, 10]. \\
 & \nearrow_{((w_{0,-} \mapsto w_{0,-}) \otimes \dot{\eta})[1,2]} & \\
 & \langle w_{0,-}^{(0,0)} \rangle \otimes \mathbb{F}[2, 8] &
 \end{array}$$

So we obtain the reduced Khovanov homology $\mathbb{F}[0, 2] \oplus \mathbb{F}[2, 6] \oplus \mathbb{F}[3, 8]$ for the right trefoil.

7. LINKS IN $S^2 \times S^1$

In Section 4, we showed that given an oriented 1-tangle diagram T we can construct corresponding twisted complexes (X, δ_+) and (X, δ_-) . We can construct links L'_{T+} and L'_{T-} in $S^2 \times S^1$ by closing the tangle diagram T with an overpass arc A_+ or underpass arc A_- as shown in Figure 2. The links L'_{T+} and L'_{T-} are isotopic, since one can isotope A_+ to A_- by moving A_+ around the S^2 factor, and we will let L_{T^0} denote either of these isotopic links. For links in $S^2 \times S^1$, an overpass arc A_+ and an underpass A_- correspond to the same unperturbed Lagrangian W_0 in $R^*(T^2, 2)$. Recall from Section 2.2 that given a Lagrangian M in $R^*(T^2, 2)$ we can define an A_∞ functor $\text{Tw } \mathcal{G}_M : \text{Tw } \mathcal{L} \rightarrow \text{Ch}$. We define a cochain complex (C_0, ∂_0) by applying the functor $\text{Tw } \mathcal{G}_{W_0}$ to the twisted complex (X, δ_-) :

$$(C_0, \partial_0) = (\text{Tw } \mathcal{G}_{W_0})((X, \delta_-)).$$

Our goal in this section is to explicitly describe this cochain complex and to investigate its cohomology. Given a tangle diagram T , we define a bigraded vector space that we call the *generalized reduced Khovanov homology of T* :

$$\text{Khr}^{(h,q)}(S^2 \times S^1, T) = H^{(h,h+q)}((C_0, \partial_0)).$$

One might hope that the generalized reduced Khovanov homology depends only on the isotopy class of the link L_{T^0} and not on its description as the closure of the particular tangle diagram T . From Theorem 5.1, it follows that the generalized reduced Khovanov homology is an isotopy invariant of the tangle diagram T . But it is possible for nonisotopic tangle diagrams T_1 and T_2 to yield isotopic links $L_{T_1^0}$ and $L_{T_2^0}$ in $S^2 \times S^1$, and example calculations show that in this situation the generalized reduced Khovanov homology for T_1 and T_2 need not be the same. In all the examples we have checked, however, the dependence on the tangle diagram is reflected only in the bigradings of generators, and the generalized reduced Khovanov homology does agree if we collapse bigradings from \mathbb{Z} to \mathbb{Z}_2 . We thus make the following conjecture:

Conjecture 7.1. *If $L_{T_1^0}$ and $L_{T_2^0}$ are isotopic links in $S^2 \times S^1$, then with bigradings collapsed to \mathbb{Z}_2 we have*

$$\text{Khr}(S^2 \times S^1, T_1) = \text{Khr}(S^2 \times S^1, T_2).$$

We will focus on links obtained from a tangle diagram T with loop number 0 or 2. To compute the cochain complexes for such links, we need to know the bigradings of the generators of the vector spaces (W_0, L_n) for $n \in \{0, \pm 2\}$ and the A_∞ operations involving these generators.

7.1. A_∞ **operations and gradings of generators.** Recall from Corollary 3.19 that the vector spaces (W_0, L_0) and $(W_0, L_{\pm 2})$ are 2-dimensional. We assign integer bigradings to the generators as follows:

$$(W_0, L_0) = \langle \alpha_0^{(0,0)}, \beta_0^{(0,-2)} \rangle, \quad (W_0, L_{\pm 2}) = \langle \sigma_{\pm 2,0}^{(0,-1)}, \tau_{\pm 2,0}^{(0,-1)} \rangle.$$

Based on Conjecture 3.28 for the product operations of these generators, we make the following conjecture:

Conjecture 7.2. *We have the following product operations:*

$$\begin{array}{lll} \mu^2(a_0, -) : (W_0, L_0) \rightarrow (W_0, L_0), & x \mapsto x, & \\ \mu^2(a_{\pm 2}, -) : (W_0, L_{\pm 2}) \rightarrow (W_0, L_{\pm 2}), & x \mapsto x, & \\ \mu^2(c_0, -) : (W_0, L_0) \rightarrow (W_0, L_0), & \alpha_0 \mapsto \beta_0, & \beta_0 \mapsto 0, \\ \mu^2(c_{\pm 2}, -) : (W_0, L_{\pm 2}) \rightarrow (W_0, L_{\pm 2}), & x \mapsto 0, & \\ \mu^2(p_{2,0}^{(-)}, -) : (W_0, L_0) \rightarrow (W_0, L_2), & \alpha_0 \mapsto \tau_{2,0}, & \beta_0 \mapsto 0, \\ \mu^2(p_{2,0}^{(+)}, -) : (W_0, L_0) \rightarrow (W_0, L_2), & \alpha_0 \mapsto 0, & \beta_0 \mapsto \sigma_{2,0}, \\ \mu^2(q_{2,0}^{(+)}, -) : (W_0, L_0) \rightarrow (W_0, L_2), & \alpha_0 \mapsto \sigma_{-2,0}, & \beta_0 \mapsto 0, \\ \mu^2(q_{2,0}^{(-)}, -) : (W_0, L_0) \rightarrow (W_0, L_2), & \alpha_0 \mapsto \tau_{-2,0}, & \beta_0 \mapsto 0, \\ \mu^2(p_{0,-2}^{(-)}, -) : (W_0, L_{-2}) \rightarrow (W_0, L_0), & \sigma_{-2,0} \mapsto \beta_0, & \tau_{-2,0} \mapsto 0, \\ \mu^2(p_{0,-2}^{(+)}, -) : (W_0, L_{-2}) \rightarrow (W_0, L_0), & \sigma_{-2,0} \mapsto 0, & \tau_{-2,0} \mapsto \beta_0, \\ \mu^2(q_{0,2}^{(+)}, -) : (W_0, L_2) \rightarrow (W_0, L_0), & \sigma_{2,0} \mapsto 0, & \tau_{2,0} \mapsto \beta_0, \\ \mu^2(q_{0,2}^{(-)}, -) : (W_0, L_2) \rightarrow (W_0, L_0), & \sigma_{2,0} \mapsto \beta_0, & \tau_{2,0} \mapsto 0. \end{array}$$

All operations $\mu^m(x_{m-1}, \dots, x_1, y)$ for $m \neq 2$, $x_{m-1}, \dots, x_1 \in \{a_n, c_n, p_{n+2,n}, q_{n-2,n} \mid n \in \mathbb{Z}\}$, and $y \in (W_0, L_0)$ or $y \in (W_0, L_{\pm 2})$ are zero.

We can depict the product operations in Conjecture 7.2 as

$$\begin{array}{ccc} \sigma_{-2,0}^{(-)} & \xleftarrow{q_{-2,0}^{(+)}} & \alpha_0^{(-)} & \xrightarrow{p_{2,0}^{(-)}} & \sigma_{2,0}^{(-)} \\ & \searrow^{p_{0,-2}^{(-)}} & \downarrow^{c_0^{(-)}} & \searrow^{q_{0,2}^{(+)}} & \\ \tau_{-2,0}^{(+)} & & \beta_0^{(+)} & \xleftarrow{q_{0,2}^{(+)}} & \tau_{2,0}^{(+)} \end{array} \quad \begin{array}{ccc} \sigma_{-2,0}^{(-)} & & \alpha_0^{(-)} & \xrightarrow{p_{2,0}^{(+)}} & \sigma_{2,0}^{(-)} \\ & \swarrow^{q_{-2,0}^{(-)}} & \downarrow^{c_0^{(-)}} & \swarrow^{q_{0,2}^{(-)}} & \\ \tau_{-2,0}^{(+)} & \xrightarrow{p_{0,-2}^{(+)}} & \beta_0^{(+)} & & \tau_{2,0}^{(+)} \end{array}$$

There is a sense in which the product operations in Conjecture 7.2 are consistent with the product operations in Conjecture 3.27 for perturbed Lagrangians. We define a bigraded vector space

$$V = \langle e^{(0,0)}, v^{(0,0)} \rangle.$$

We define an isomorphism $(W_0, L_n) \otimes V \rightarrow (L_0, L_n)$ of bigraded vector spaces:

$$\begin{array}{llll} \alpha_0 \otimes e \mapsto a_0, & \alpha_0 \otimes v \mapsto b_0, & \beta_0 \otimes e \mapsto c_0, & \beta_0 \otimes v \mapsto d_0, \\ \sigma_{2,0} \otimes e \mapsto s_{2,0} + \bar{s}_{2,0}, & \sigma_{2,0} \otimes v \mapsto r_{2,0}, & \tau_{2,0} \otimes e \mapsto r_{2,0} + \bar{r}_{2,0}, & \tau_{2,0} \otimes v \mapsto \bar{s}_{2,0}, \\ \sigma_{-2,0} \otimes e \mapsto s_{-2,0} + \bar{s}_{-2,0}, & \sigma_{-2,0} \otimes v \mapsto r_{-2,0}, & \tau_{-2,0} \otimes e \mapsto r_{-2,0} + \bar{r}_{-2,0}, & \tau_{-2,0} \otimes v \mapsto s_{-2,0}. \end{array}$$

Using the product operations described in Conjecture 3.27 and Conjecture 7.2, it is straightforward to check that we have the following commutative diagrams:

$$\begin{array}{ccc}
 (W_0, L_0) \otimes V & \xrightarrow{\mu^2(p_{2,0}^{(\pm)}, -) \otimes 1_V} & (W_0, L_2) \otimes V \\
 \downarrow \cong & & \downarrow \cong \\
 (L_0, L_0) & \xrightarrow{\mu_{\mathcal{L}}^2(p_{2,0}^{(\pm)}, -)} & (L_0, L_2),
 \end{array}
 \quad
 \begin{array}{ccc}
 (W_0, L_2) \otimes V & \xrightarrow{\mu^2(q_{0,2}^{(\pm)}, -) \otimes 1_V} & (W_0, L_0) \otimes V \\
 \downarrow \cong & & \downarrow \cong \\
 (L_0, L_2) & \xrightarrow{\mu_{\mathcal{L}}^2(q_{0,2}^{(\pm)}, -)} & (L_0, L_0),
 \end{array}$$

$$\begin{array}{ccc}
 (W_0, L_0) \otimes V & \xrightarrow{\mu^2(q_{-2,0}^{(\pm)}, -) \otimes 1_V} & (W_0, L_{-2}) \otimes V \\
 \downarrow \cong & & \downarrow \cong \\
 (L_0, L_0) & \xrightarrow{\mu_{\mathcal{L}}^2(q_{-2,0}^{(\pm)}, -)} & (L_0, L_{-2}),
 \end{array}
 \quad
 \begin{array}{ccc}
 (W_0, L_{-2}) \otimes V & \xrightarrow{\mu^2(p_{0,-2}^{(\pm)}, -) \otimes 1_V} & (W_0, L_0) \otimes V \\
 \downarrow \cong & & \downarrow \cong \\
 (L_0, L_{-2}) & \xrightarrow{\mu_{\mathcal{L}}^2(p_{0,-2}^{(\pm)}, -)} & (L_0, L_0),
 \end{array}$$

$$\begin{array}{ccc}
 (W_0, L_0) \otimes V & \xrightarrow{\mu^2(c_0, -) \otimes 1_V} & (W_0, L_0) \otimes V \\
 \downarrow \cong & & \downarrow \cong \\
 (L_0, L_0) & \xrightarrow{\mu_{\mathcal{L}}^2(c_0, -)} & (L_0, L_0),
 \end{array}
 \quad
 \begin{array}{ccc}
 (W_0, L_{\pm 2}) \otimes V & \xrightarrow{\mu^2(c_{\pm 2}, -) \otimes 1_V} & (W_0, L_{\pm 2}) \otimes V \\
 \downarrow \cong & & \downarrow \cong \\
 (L_0, L_{\pm 2}) & \xrightarrow{\mu_{\mathcal{L}}^2(c_{\pm 2}, -)} & (L_0, L_{\pm 2}).
 \end{array}$$

7.2. Cochain complex. Using Conjecture 7.2, the description of the functor \mathcal{G}_{W_0} from Section 2.2, and the description of the twisted complex (X, δ_-) from Section 4.5, we can explicitly construct the cochain complex (C_0, ∂_0) for the tangle diagram T . The vector space C_0 is given by

$$C_0 = \bigoplus_{i \in I} ((W_0, L_{n_i}) \otimes A^{\otimes c_i} [r(i) + h_T, 2r(i) + q_T]).$$

The differential ∂_0 is a sum of differentials corresponding to saddles in the cube of resolutions of T . The differential corresponding to a saddle $S : P_{n_1}(r_1) \rightarrow P_{n_2}(r_2)$ is given by

$$\partial_S : (W_0, L_{n_1}) \otimes A^{\otimes r_1} \rightarrow (W_0, L_{n_2}) \otimes A^{\otimes r_2} [1, 2], \quad \partial_S = \mu_{\Sigma_{\mathcal{L}}}^2(d_S[1, 2], -).$$

We could also define a cochain complex by applying the functor \mathcal{G}_{W_0} to the twisted object (X, δ_+) , but given the A_∞ operations in Conjecture 7.2 the resulting complex is homotopy equivalent to (C_0, ∂_0) .

We obtain a nontrivial cochain complex only when the loop number of the tangle diagram T is even, due to the following result:

Theorem 7.3. *For a tangle diagram T with odd loop number, the cochain complex (C_0, ∂_0) vanishes.*

Proof. For odd loop number, the morphism spaces that appear in C_0 have the form (W_0, L_n) for n odd. But (W_0, W_n) vanishes for odd n , since there are no traceless $SU(2)$ representations for a link that winds around the solid torus an odd number of times, hence (W_0, L_n) vanishes. \square

7.3. Example: double cycle in $S^2 \times S^1$. We can close the tangle diagram T shown in Figure 17 with an overpass or underpass arc to obtain a double cycle L_{T^0} in $S^2 \times S^1$. The cochain complex (C_0, ∂_0) is given by

$$\begin{array}{ccccc}
 & & (W_0, L_0) \otimes \mathbb{F}[1, 4] & & \\
 & \nearrow \partial_{W-} & & \searrow \partial_{L+} & \\
 (W_0, L_2) \otimes \mathbb{F}[0, 2] & & & & (W_0, L_0) \otimes A[2, 6], \\
 & \searrow \partial_{W-} & & \nearrow \partial_{R+} & \\
 & & (W_0, L_0) \otimes \mathbb{F}[1, 4] & &
 \end{array}$$

where

$$\begin{array}{lll}
 \partial_{W-} : (W_0, L_2) \otimes \mathbb{F} \rightarrow (W_0, L_0) \otimes \mathbb{F}, & \sigma_{2,0} \otimes 1 \mapsto \beta_0 \otimes 1, & \tau_{2,0} \otimes 1 \mapsto 0, \\
 \partial_{L+} : (W_0, L_0) \otimes \mathbb{F} \rightarrow (W_0, L_0) \otimes A, & \alpha_0 \otimes 1 \mapsto \alpha_0 \otimes x, & \beta_0 \otimes 1 \mapsto \beta_0 \otimes x, \\
 \partial_{R+} : (W_0, L_0) \otimes \mathbb{F} \rightarrow (W_0, L_0) \otimes A, & \alpha_0 \otimes 1 \mapsto \alpha_0 \otimes x + \beta_0 \otimes e, & \beta_0 \otimes 1 \mapsto \beta_0 \otimes x.
 \end{array}$$

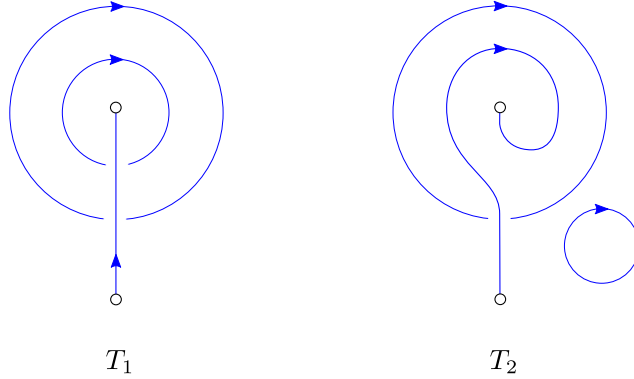


FIGURE 21. Example tangle diagrams T_1 and T_2 . The links $L_{T_1^0}$ and $L_{T_2^0}$ in $S^2 \times S^1$ are isotopic.

So the generalized reduced Khovanov homology of T is

$$\text{Khr}(S^2 \times S^1, T) = \mathbb{F}[0, 1] \oplus \mathbb{F}[2, 5].$$

The link L_{T^0} is isotopic to the link $L_{P_2^0}$ obtained by closing the planar tangle P_2 , oriented in either direction, with an overpass or underpass arc. The cochain complex for the tangle diagram P_2 is

$$(W_0, L_2) \otimes \mathbb{F}[0, 0]$$

with zero differential, so the generalized reduced Khovanov homology of P_2 is

$$\text{Khr}(S^2 \times S^1, P_2) = 2 \mathbb{F}[0, -1].$$

So if we collapse bigradings to \mathbb{Z}_2 , we have

$$\text{Khr}(S^2 \times S^1, T) = \text{Khr}(S^2 \times S^1, P_2) = 2 \mathbb{F}[0, 1],$$

as is consistent with Conjecture 7.1.

7.4. Example: two cycles and unknot in $S^2 \times S^1$. Consider the 1-tangle diagrams T_1 and T_2 shown in Figure 21. The corresponding links $L_{T_1^0}$ and $L_{T_2^0}$ in $S^2 \times S^1$ are isotopic, and describe two cycles oriented in the same direction and an unlinked unknot. We find

$$\begin{aligned} \text{Khr}(S^2 \times S^1, T_1) &= \mathbb{F}[0, 1] \oplus \mathbb{F}[1, 1] \oplus \mathbb{F}[1, 3] \oplus \mathbb{F}[2, 3], \\ \text{Khr}(S^2 \times S^1, T_2) &= \mathbb{F}[0, -1] \oplus \mathbb{F}[0, 1] \oplus \mathbb{F}[1, 1] \oplus \mathbb{F}[1, 3]. \end{aligned}$$

So if we collapse bigradings to \mathbb{Z}_2 , we have

$$\text{Khr}(S^2 \times S^1, T_1) = \text{Khr}(S^2 \times S^1, T_2) = 2 \mathbb{F}[0, 1] \oplus 2 \mathbb{F}[1, 1],$$

as is consistent with Conjecture 7.1.

We define a 1-tangle diagram T_3 by flipping the orientation of one of the two circles in T_1 that loops around the annulus. We define 1-tangle diagram T_4 by flipping the orientation of the single circle in T_2 that loops around the annulus. The corresponding links $L_{T_3^0}$ and $L_{T_4^0}$ in $S^2 \times S^1$ are isotopic, and describe two cycles oriented in the opposite direction and an unlinked unknot. We find

$$\begin{aligned} \text{Khr}(S^2 \times S^1, T_3) &= \mathbb{F}[-1, -2] \oplus \mathbb{F}[0, -2] \oplus \mathbb{F}[0, 0] \oplus \mathbb{F}[1, 0], \\ \text{Khr}(S^2 \times S^1, T_4) &= \mathbb{F}[-1, -4] \oplus \mathbb{F}[-1, -2] \oplus \mathbb{F}[0, -2] \oplus \mathbb{F}[0, 0]. \end{aligned}$$

So if we collapse bigradings to \mathbb{Z}_2 , we have

$$\text{Khr}(S^2 \times S^1, T_3) = \text{Khr}(S^2 \times S^1, T_4) = 2 \mathbb{F}[1, 0] \oplus 2 \mathbb{F}[0, 0],$$

as is consistent with Conjecture 7.1.

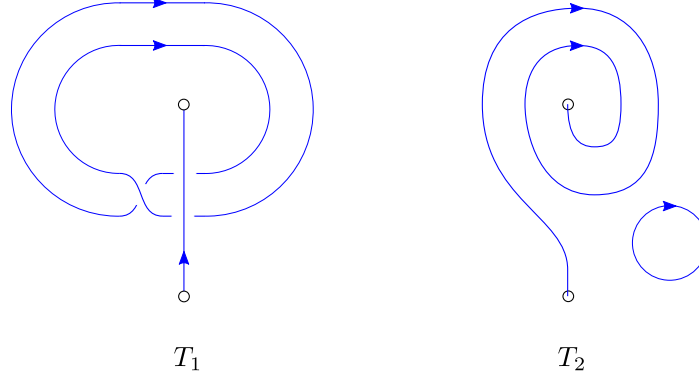


FIGURE 22. Example tangle diagrams T_1 and T_2 . The links $L_{T_1^0}$ and $L_{T_2^0}$ in $S^2 \times S^1$ are isotopic.

7.5. Example: double cycle and unknot in $S^2 \times S^1$. Consider the 1-tangle diagrams T_1 and T_2 shown in Figure 22. The corresponding links $L_{T_1^0}$ and $L_{T_2^0}$ in $S^2 \times S^1$ are isotopic, and describe a double cycle and an unlinked unknot. We find

$$\text{Khr}(S^2 \times S^1, T_1) = \mathbb{F}[0, 2] \oplus 2\mathbb{F}[2, 4] \oplus \mathbb{F}[2, 6],$$

$$\text{Khr}(S^2 \times S^1, T_2) = 2\mathbb{F}[0, -2] \oplus 2\mathbb{F}[0, 0].$$

So if we collapse gradings to \mathbb{Z}_2 we have

$$\text{Khr}(S^2 \times S^1, T_1) = \text{Khr}(S^2 \times S^1, T_2) = 4\mathbb{F}[0, 0],$$

as is consistent with Conjecture 7.1.

7.6. Tangle diagrams with loop number 0. Consider a tangle diagram T with loop number 0. The corresponding link L_{T^0} is contained inside an open 3-ball in $S^2 \times S^1$. By collapsing the complement of the open 3-ball to a point, we obtain a link L'_{T^0} in S^3 . We can also view L'_{T^0} as the link obtained by closing T with either an overpass arc A_+ or an underpass arc A_- , as shown in Figure 2, and interpreting the resulting diagram as describing a link in S^3 . In this section we relate the generalized reduced Khovanov homology of the tangle diagram T to the reduced Khovanov homology of the link L'_{T^0} in S^3 .

Let (X, δ) denote the twisted complex corresponding to the tangle diagram T . We can define a new twisted complex (X, δ') by modifying the differential δ as follows. Recall that δ is a sum of differentials d_{ji} corresponding to saddles in the cube of resolution of T . The differentials d_{ji} have the form d_{C^\pm} , d_{R^\pm} , or d_{L^\pm} , as defined in Section 4.3. Since T has loop number 0, there are no differentials of the form d_{W^\pm} . Define new differentials d'_{ji} by eliminating the terms in d_{ji} that contain c_0 . That is, we replace differentials of the form d_{C^\pm} , d_{R^\pm} , and d_{L^\pm} by d'_{C^\pm} , d'_{R^\pm} , and d'_{L^\pm} , where

$$\begin{aligned} d'_{C^+} &= d_{C^+} = a_0 \otimes \Delta I_{r-1}, & d'_{C^-} &= d_{C^-} = a_0 \otimes m I_{r-1}, \\ d'_{R^+} &= d_{L^+} = a_0 \otimes \dot{\eta} I_r, & d'_{R^-} &= d'_{L^-} = a_0 \otimes \dot{\epsilon} I_r. \end{aligned}$$

We then define δ' to be the sum of the new differentials d'_{ji} . Let (C_T, d_T) denote the cochain complex for the reduced Khovanov homology of L'_{T^0} , where the marked component is the one containing the arc component of T , and with the convention that d_T has quantum grading 1, rather than the usual quantum grading of 0. Given the construction of X and our definition δ' , we have that $X = L_0 \otimes C_T$ and $\delta' = a_0 \otimes d_T$.

Theorem 7.4. *Assuming Conjecture 4.1 for the A_∞ operations of \mathcal{L} , the pair (X, δ') is a twisted complex.*

Proof. Assuming Conjecture 4.1 for the A_∞ operations of \mathcal{L} , we have

$$\sum_{m=1}^{\infty} \mu_{\Sigma \mathcal{L}}^m(\delta', \dots, \delta') = \mu_{\Sigma \mathcal{L}}^2(\delta', \delta') = a_0 \otimes (d_T \circ d_T) = 0.$$

We can define a filtration on X using the resolution degree. The differential δ' increases the resolution degree by 1, so it is lower triangular with respect to this filtration. \square

Theorem 7.5. *Assuming Conjecture 4.1 for the A_∞ operations of \mathcal{L} , the twisted complexes (X, δ) and (X, δ') are homotopy equivalent.*

Proof. Each term of X corresponds to a planar tangle $P_0(k)$ obtained by resolving the nonplanar tangle T , and can be viewed as a subobject $(x, 0)$ of (X, δ) with zero differential:

$$(x, 0) = L_n \otimes A^{\otimes k}[h, q],$$

where the bigrading shift $[h, q]$ depends on the crossing numbers of T and on the location of $P_0(k)$ within the cube of resolutions. We have a corresponding identical subobject $(x', 0)$ of (X, δ') .

For planar tangles that are obtained by resolving a tangle diagram with loop number 0, we can distinguish between circle components to the left and to the right of the arc component. Let ℓ and r denote the number of circle components to the left and right of the arc component of $P_0(k)$, so $k = \ell + r$. Define homotopy equivalences $F : (x, 0) \rightarrow (x', 0)$ and $G : (x', 0) \rightarrow (x, 0)$:

$$F = G = a_0 I_{\ell+r} + c_0 I_\ell \Sigma_r.$$

We have

$$F \circ G = G \circ F = a_0 I_{\ell+r}.$$

Since the differentials are zero for the subobjects $(x, 0)$ and $(x', 0)$, it is clear that F and G are homotopy equivalences.

We combine the homotopy equivalences for subobjects to obtain morphisms $(X, \delta) \rightarrow (X, \delta')$ and $(X, \delta') \rightarrow (X, \delta)$. To show that these morphisms are homotopy equivalences, we must check that they commute with the differentials δ and δ' . The differential δ is the sum of differentials $d : x_1 \rightarrow x_2$ corresponding to saddles. For each such term, there is a corresponding term $d' : x'_1 \rightarrow x'_2$ of δ' . We want to show that the following diagram commutes:

$$\begin{array}{ccc} x'_1 & \xrightarrow{d'} & x'_2 \\ F_1 \uparrow \downarrow G_1 & & F_2 \uparrow \downarrow G_2 \\ x_1 & \xrightarrow{d} & x_2 \end{array}$$

For a differential d of the form d_{C^\pm} , commutativity follows from the identities in equation (7). For a differential d of the form d_{R^+} , we have

$$\begin{aligned} d &= d_{R^+} = a_0 I_{\ell+r} \dot{\eta} + c_0 I_{\ell+r} \eta + c_0 I_{\ell_n} \Sigma_{\ell_e} I_r \dot{\eta}, & d' &= d'_{R^+} = a_0 I_{\ell+r} \dot{\eta}, \\ F_1 &= G_1 = a_0 I_{\ell+r} + c_0 I_\ell \Sigma_r, & F_2 &= G_2 = a_0 I_{\ell+r+1} + c_0 I_{\ell_n} \Sigma_{\ell_e+r+1}. \end{aligned}$$

We check:

$$\begin{aligned} d' \circ F_1 &= F_2 \circ d = a_0 I_{\ell+r} \dot{\eta} + c_0 I_\ell \Sigma_r \dot{\eta}, \\ d \circ G_1 &= G_2 \circ d' = a_0 I_{\ell+r} \dot{\eta} + c_0 I_{\ell+r} \eta + c_0 I_{\ell_n} \Sigma_{\ell_e+r} \dot{\eta}. \end{aligned}$$

Similar calculations show commutativity for differentials of the form d_{R^-} and d_{L^\pm} □

The generalized reduced Khovanov homology of the tangle diagram T is related to the reduced Khovanov homology of the link L'_{T_0} in S^3 by the following result:

Theorem 7.6. *We have an isomorphism of bigraded vector spaces*

$$\text{Khr}(S^2 \times S^1, T) = (W_0, L_0) \otimes \text{Khr}(L'_0).$$

Proof. This follows from Theorem 7.5 and the fact that

$$\mathcal{G}_{W_0}((X, \delta')) = ((W_0, L_0) \otimes C_T, \mathbb{1}_{(W_0, L_0)} \otimes d_T).$$

□

Theorem 7.6 shows that if the generalized reduced Khovanov homology with bigradings collapsed to \mathbb{Z}_2 is indeed a link invariant, then it is a natural generalization of reduced Khovanov homology for links in S^3 . Since the reduced Khovanov homology of an unknot in S^3 is $\mathbb{F}[0, 0]$, we could view (W_0, L_0) as additional cohomology for $S^2 \times S^1$ that describes the topology of this space.

7.7. Tangle diagrams with loop number 2. Given a 1-tangle diagram T with loop number 2, we can define a 1-tangle diagram T_τ by adding a full twist to T as shown in Figure 3. The diagrams T and T_τ are typically not isotopic, but the corresponding links L_{T_0} and L_{T_τ} in $S^2 \times S^1$ are isotopic, since one can unwind the full twist by moving one of the strands around the S^2 factor as shown in Figure 4. Our goal in this section is to prove:

Theorem 7.7. *With bigradings collapsed from \mathbb{Z} to \mathbb{Z}_2 , there is an isomorphism of bigraded vector spaces*

$$\mathrm{Khr}(S^2 \times S^1, T) \rightarrow \mathrm{Khr}(S^2 \times S^1, T_\tau).$$

Proof. Let (C_0, ∂_0) and $(C_0^\tau, \partial_0^\tau)$ denote the cochain complexes for the tangle diagrams T and T_τ . The 1-tangle diagram T in the annulus can be viewed as a 3-tangle diagram T_D in the disk that has been closed with two arcs wrapping around the annulus. We can thus describe the planar resolution of T in terms of the planar resolution of T_D . The vector space C_0 is a direct sum of subspaces corresponding to planar tangles that occur in this resolution. Each subspace corresponds to a planar 3-tangle P_D obtained by resolving T_D , and can be viewed as a subcomplex $(c, 0)$ of (C_0, ∂_0) with zero differential. Let $P_n(r)$ denote the planar 1-tangle in the annulus obtained by closing P_D with two arcs that wrap around the annulus. The subcomplex $(c, 0)$ is then given by

$$(c, 0) = (W_0, L_n) \otimes A^{\otimes r}[h, q],$$

where the bigrading shift $[h, q]$ depends on the crossing numbers of T and on the location of P_D within the cube of resolutions. If we apply a full twist to $P_n(r)$ and then resolve the two resulting crossings, we obtain the cube of resolutions shown in Figure 23:

$$\begin{array}{ccc} & P_m(s) & \\ s_2 \nearrow & & \searrow s'_1 \\ P_n(r) & & P_m(s+1) \\ s_1 \searrow & & \nearrow s'_2 \\ & P_m(s) & \end{array}$$

where the planar tangle $P_m(s)$ depends on P_D . Thus for each such subcomplex $(c, 0)$ of (C_0, ∂_0) , there is a corresponding subcomplex (c_τ, d) of $(C_0^\tau, \partial_0^\tau)$ given by

$$(c_\tau, d) = (W_0, L_n) \otimes A^{\otimes r}[h_\tau, q_\tau] \begin{array}{ccc} & (W_0, L_m) \otimes A^{\otimes s}[h_\tau + 1, q_\tau] & \\ \partial_{s_2} \nearrow & & \searrow \partial_{s'_1} \\ & & (W_0, L_m) \otimes A^{\otimes(s+1)}[h_\tau, q_\tau] \\ \partial_{s_1} \searrow & & \nearrow \partial_{s'_2} \\ & (W_0, L_m) \otimes A^{\otimes s}[h_\tau + 1, q_\tau] & \end{array}$$

where we have collapsed bigradings to \mathbb{Z}_2 . The relative crossing numbers of the tangle diagrams T_τ and T are either $\delta m_+ = 2$ and $\delta m_- = 0$ or $\delta m_+ = 0$ and $\delta m_- = 2$. In either case, we have

$$[h_\tau, q_\tau] = [h, q] + [-\delta m_-, \delta m_+ - 3\delta m_-] = [0, 0].$$

Since we are collapsing homological gradings to \mathbb{Z}_2 , we can express the subcomplex (c_τ, d) as

$$(c_\tau, d) = \left(\begin{array}{c} (W_0, L_m) \otimes A^{\otimes(s+1)}[h, q] \\ (W_0, L_n) \otimes A^{\otimes r}[h, q] \end{array} \right) \begin{array}{c} \xrightarrow{d^0} \\ \xleftarrow{d^1} \end{array} \left(\begin{array}{c} (W_0, L_m) \otimes A^{\otimes s}[h+1, q] \\ (W_0, L_m) \otimes A^{\otimes s}[h+1, q] \end{array} \right),$$

where

$$d^0 = \begin{pmatrix} 0 & \partial_{S_2} \\ 0 & \partial_{S_1} \end{pmatrix}, \quad d^1 = \begin{pmatrix} \partial_{S'_1} & \partial_{S'_2} \\ 0 & 0 \end{pmatrix}.$$

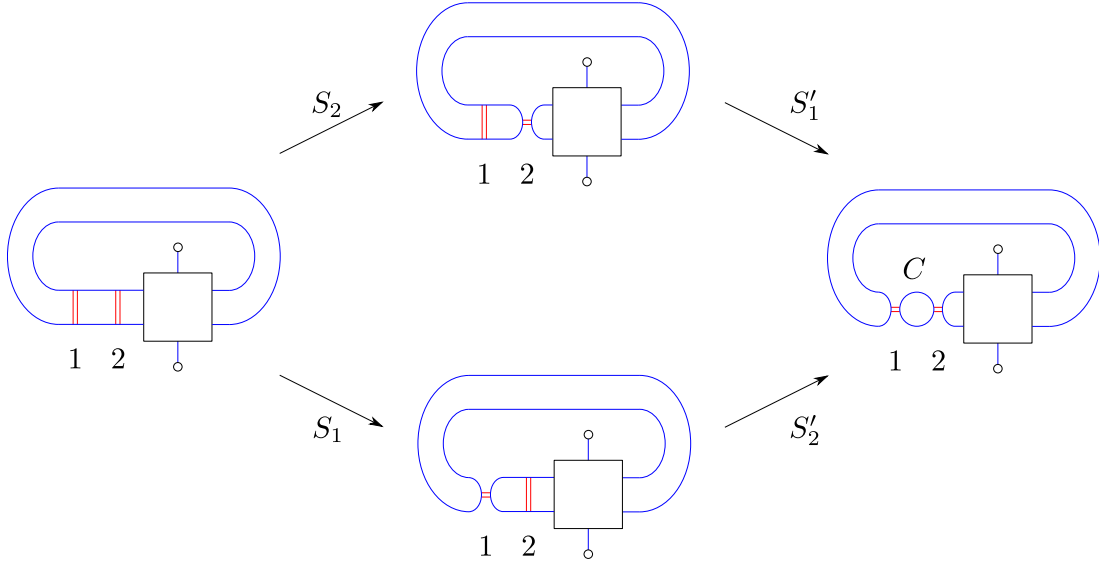


FIGURE 23. Resolution of a full twist.

For each isotopy class of planar 3-tangle P_D in the disk, we define homotopy equivalences $F : (c, 0) \rightarrow (c_\tau, d)$ and $G : (c_\tau, d) \rightarrow (c, 0)$ of the corresponding subobjects of $(c, 0)$ and (c_τ, d) :

$$(18) \quad \begin{array}{ccc} \left(\begin{array}{l} (W_0, L_m) \otimes A^{\otimes(s+1)} \\ (W_0, L_n) \otimes A^{\otimes r} \end{array} \right) & \begin{array}{c} \xleftarrow{d^0, H^0} \\ \xrightarrow{d^1, H^1} \end{array} & \left(\begin{array}{l} (W_0, L_m) \otimes A^{\otimes s} \\ (W_0, L_m) \otimes A^{\otimes s} \end{array} \right) \\ F^0 \updownarrow G^0 & & \\ (W_0, L_n) \otimes A^{\otimes r} & & \end{array}$$

The specific homotopy equivalences are rather complicated and are described in Appendix B.

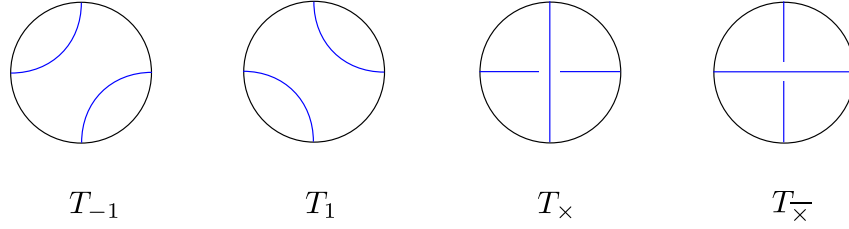
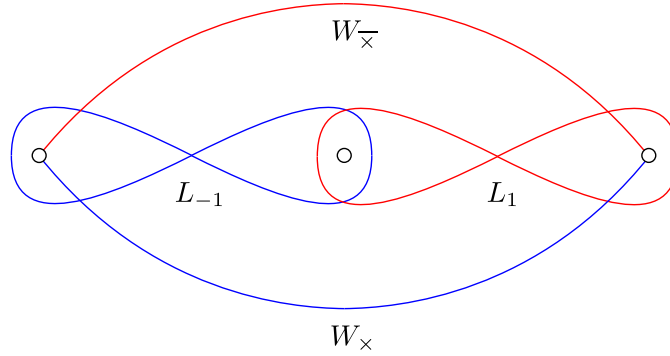
We combine the homotopy equivalences for subcomplexes to obtain linear maps $C_0 \rightarrow C_0^\tau$ and $C_0^\tau \rightarrow C_0$. We now want to show that these maps commute with the differentials ∂_0 and ∂_0^τ . The differential ∂_0 is a sum of terms corresponding to saddles that occur in the cube of resolutions of the 3-tangle T_D . Given a saddle $S : P_{D1} \rightarrow P_{D2}$, let d_S denote the corresponding term of ∂_0 . We have a corresponding term \tilde{d}_S of ∂_0^τ and a diagram

$$\begin{array}{ccc} \left(\begin{array}{l} (W_0, L_{m_1}) \otimes A^{\otimes(s_1+1)} \\ (W_0, L_{n_1}) \otimes A^{\otimes r_1} \end{array} \right) & \xrightarrow{\tilde{d}_S} & \left(\begin{array}{l} (W_0, L_{m_2}) \otimes A^{\otimes(s_2+1)} \\ (W_0, L_{m_2}) \otimes A^{\otimes r_2} \end{array} \right) \\ F^0 \updownarrow G^0 & & F^0 \updownarrow G^0 \\ (W_0, L_{n_1}) \otimes A^{\otimes r_1} & \xrightarrow{d_S} & (W_0, L_{n_2}) \otimes A^{\otimes r_2} \end{array}$$

We show that this diagram commutes for each type of saddle, as described in Appendix B. Thus the maps define homotopy equivalences $(C_0, \partial_0) \rightarrow (C_0^\tau, \partial_0^\tau)$ and $(C_0^\tau, \partial_0^\tau) \rightarrow (C_0, \partial_0)$. We have verified the necessary calculations with Mathematica, since they are rather involved. \square

APPENDIX A. THE FUKAYA CATEGORY OF $R^*(S^2, 4)$

We describe here some results regarding the Fukaya category of the pillowcase $R^*(S^2, 4)$, so they can be compared with corresponding results for $R^*(T^2, 2)$. These results are either derived in [15], or are easily obtained using the methods described there.


 FIGURE 24. Tangles T_{-1} , T_1 , T_{\times} , and $T_{\overline{\times}}$ in the disk.

 FIGURE 25. Lagrangians L_1 , L_{-1} , W_{\times} , and $W_{\overline{\times}}$ in the pillowcase $R^*(S^2, 4)$. The three circles indicate three of the puncture points of $R^*(S^2, 4)$; the fourth puncture point is the point at infinity.

As described in Section 3.2, the traceless character variety $R(S^2, 4)$ is a 2-sphere with four reducible points. One of these four reducible points is special, in that the action of the mapping class group $\text{MCG}_4(S^2)$ on $R(S^2, 4)$ fixes the special point and permutes the other three reducible points. We will depict $R^*(S^2, 4)$ as a plane with three punctures, where the point at infinity is the puncture corresponding to the special point.

We define 2-tangles in the disk T_{-1} , T_1 , T_{\times} , and $T_{\overline{\times}}$ as shown in Figure 24. The planar 2-tangles $T_{\pm 1}$ are analogous to the planar 1-tangles in the annulus P_n that we defined in Section 4.3. The nonplanar 2-tangles T_{\times} and $T_{\overline{\times}}$ are analogous to the overpass arc A_+ and underpass arc A_- that we use to define links in S^3 , since closing $T_{\pm 1}$ with T_{\times} or $T_{\overline{\times}}$ yields an unknot in S^3 just as closing P_n with A_+ or A_- yields an unknot in S^3 .

To the tangle $T_{\pm 1}$ we associate a compact Lagrangian $L_{\pm 1}$ and to the tangles T_{\times} and $T_{\overline{\times}}$ we associate noncompact Lagrangians W_{\times} and $W_{\overline{\times}}$ as shown in Figure 25, which should be compared to Figure 8 for $R_2^*(T^2, 2)$. As discussed in [15], one can define a Fukaya category \mathcal{P} whose objects are the compact Lagrangians $L_{\pm 1}$. The pillowcase has vanishing first Chern class, and the Lagrangians $L_{\pm 1}$, W_{\times} , and $W_{\overline{\times}}$ all have vanishing Maslov class, so the morphism spaces of \mathcal{P} carry an integer Maslov grading. One can choose graded lifts of the Lagrangians such that the morphism spaces for \mathcal{P} are

$$(L_{\pm 1}, L_{\pm 1}) = \langle a_{\pm 1}^{(0)}, b_{\pm 1}^{(3)}, c_{\pm 1}^{(-2)}, d_{\pm 1}^{(1)} \rangle, \quad (L_{-1}, L_1) = \langle p_{1,-1}^{(-1)}, q_{1,-1}^{(3)} \rangle, \quad (L_1, L_{-1}) = \langle p_{-1,1}^{(3)}, q_{-1,1}^{(-1)} \rangle.$$

We note that the Maslov gradings are consistent with Poincaré duality, as described at the end of Section 3.10. The morphism spaces for \mathcal{P} should be compared with the corresponding morphism spaces for \mathcal{L} described in Corollary 3.20. The morphism spaces involving the Lagrangians W_{\times} and $W_{\overline{\times}}$ are

$$(W_{\times}, L_{\pm 1}) = \langle w_{\pm 1}^{(\pm 2)} \rangle, \quad (W_{\overline{\times}}, L_{\pm 1}) = \langle \overline{w}_{\pm 1}^{(\mp 2)} \rangle.$$

These spaces should be compared to the analogous morphism spaces (W_+, L_n) and (W_-, L_n) for \mathcal{L} described in Section 6.1.

The A_∞ operations derived in [15] prove the following result for \mathcal{P} , which should be compared to Conjecture 4.1 for \mathcal{L} :

Theorem A.1. *The generators $a_{\pm 1}$ are identity elements that satisfy*

$$\mu_{\mathcal{P}}^2(a_{\pm 1}, x) = x, \quad \mu_{\mathcal{P}}^2(y, a_{\pm 1}) = y$$

whenever these operations are defined. We have the following product operations:

$$\begin{aligned} \mu_{\mathcal{P}}^2(p_{1,-1}, q_{-1,1}) &= c_1, & \mu_{\mathcal{P}}^2(q_{-1,1}, p_{1,-1}) &= c_{-1}, \\ \mu_{\mathcal{P}}^2(c_1, c_1) &= \mu_{\mathcal{P}}^2(c_1, p_{1,-1}) = \mu_{\mathcal{P}}^2(p_{1,-1}, c_{-1}) = 0, & \mu_{\mathcal{P}}^2(c_{-1}, c_{-1}) &= \mu_{\mathcal{P}}^2(c_{-1}, q_{-1,1}) = \mu_{\mathcal{P}}^2(q_{-1,1}, c_1) = 0. \end{aligned}$$

All operations of the form $\mu_{\mathcal{P}}^m(x_m, \dots, x_1)$ for $m \neq 2$ and $x_m, \dots, x_1 \in \{a_{\pm 1}, c_{\pm 1}, p_{1,-1}, q_{-1,1}\}$ are zero.

We have the following result for $R^*(S^2, 4)$, which should be compared to Conjecture 6.1 for $R^*(T^2, 2)$:

Theorem A.2. *We have the following product operations:*

$$\mu^2(a_{\pm 1}, w_{\pm 1}) = w_{\pm 1}, \quad \mu^2(a_{\pm 1}, \bar{w}_{\pm 1}) = \bar{w}_{\pm 1}.$$

We have the following μ^3 operations:

$$\mu^3(c_{-1}, q_{-1,1}, w_1) = \mu^3(q_{-1,1}, c_1, w_1) = w_{-1}, \quad \mu^3(c_1, p_{1,-1}, \bar{w}_{-1}) = \mu^3(p_{1,-1}, c_{-1}, \bar{w}_1) = \bar{w}_1.$$

All other operations of the form

$$\mu^m(x_{m-1}, \dots, x_1, w_{\pm 1}), \quad \mu^m(x_{m-1}, \dots, x_1, \bar{w}_{\pm 1})$$

for $x_{m-1}, \dots, x_1 \in \{a_{\pm 1}, c_{\pm 1}, p_{1,-1}, q_{-1,1}\}$ are zero.

Proof. This is a straightforward application of the methods described in [15]. \square

APPENDIX B. HOMOTOPY EQUIVALENCES

Here we describe the homotopy equivalences and differentials used to prove Theorem 7.7. For economy of space we do not describe differentials that merge circles, since they are straightforward modifications of corresponding differentials that split circles.

We define planar 3-tangles in the disk P_2 , P_0^L , P_0^C , P_0^R , and P_{-2} as shown in Figure 26. Any planar 3-tangle in the disk is isotopic to one of these five planar tangles, together with some number of circle components. We let ℓ , r , and c denote the number of circle components in the regions labeled ℓ , r , and c in Figure 26, and we use the notation

$$P_2(\ell, r), \quad P_0^L(c, \ell, r), \quad P_0^C(\ell, r), \quad P_0^R(\ell, r, c), \quad P_{-2}(\ell, r)$$

to describe a planar 3-tangle whose arc components are isotopic to P_2 , P_0^L , P_0^C , P_0^R , and P_{-2} , and which contains the indicated number of circle components.

We define linear maps $\mathbb{1}_{\alpha\alpha}^{(0,0)}$, $\mathbb{1}_{\beta\beta}^{(0,0)}$, $\mathbb{1}_{\beta\alpha}^{(0,-2)}$, $\mathbb{1}_{\alpha\beta}^{(0,2)}$:

$$\begin{aligned} \mathbb{1}_{\alpha\alpha} &: (W_0, L_0) \rightarrow (W_0, L_0), & \alpha_0 &\mapsto \alpha_0, & \beta_0 &\mapsto 0, \\ \mathbb{1}_{\beta\beta} &: (W_0, L_0) \rightarrow (W_0, L_0), & \alpha_0 &\mapsto 0, & \beta_0 &\mapsto \beta_0, \\ \mathbb{1}_{\beta\alpha} &: (W_0, L_0) \rightarrow (W_0, L_0), & \alpha_0 &\mapsto \beta_0, & \beta_0 &\mapsto 0, \\ \mathbb{1}_{\alpha\beta} &: (W_0, L_0) \rightarrow (W_0, L_0), & \alpha_0 &\mapsto 0, & \beta_0 &\mapsto \alpha_0. \end{aligned}$$

We define a *projection map* $\mathbb{1}_{ee}^{(0,0)}$:

$$\mathbb{1}_{ee} : A \rightarrow A, \quad \mathbb{1}_{ee}(e) = e, \quad \mathbb{1}_{ee}(x) = 0.$$

We define a *swap map* $\tau_{a,b}^{(0,0)}$:

$$\tau_{a,b} : A^{\otimes(a+b)} \rightarrow A^{\otimes(a+b)}, \quad v_1 \otimes \dots \otimes v_a \otimes w_1 \otimes \dots \otimes w_b \mapsto w_1 \otimes \dots \otimes w_b \otimes v_1 \otimes \dots \otimes v_a.$$

For simplicity, we denote the maps $\mu^2(a_n, -)$ and $\mu^2(c_n, -)$ as a_n and c_n .

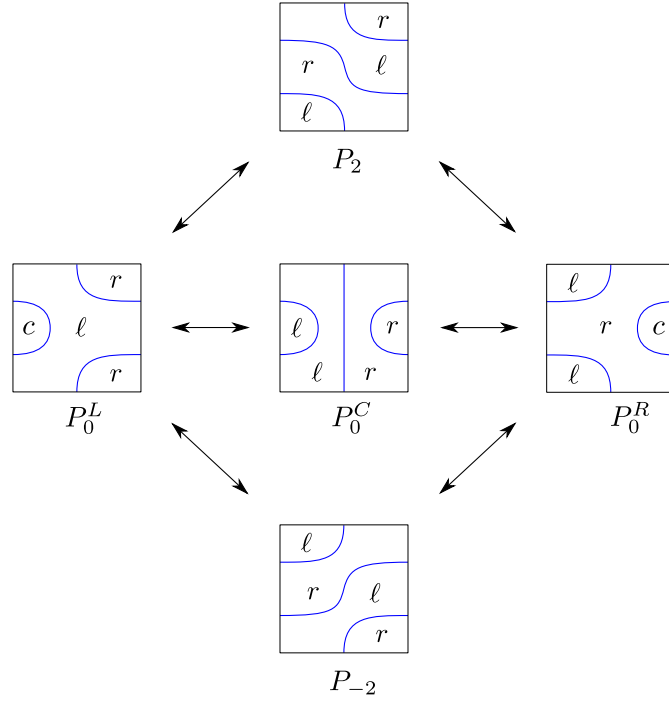


FIGURE 26. Planar 3-tangles in the disk. Pairs of planar tangles connected by arrows are related by saddles.

B.1. Chain homotopy equivalence for $P_2(\ell, r)$. For a planar 3-tangle $P_2(\ell, r)$, diagram (18) has the form

$$(19) \quad \begin{array}{c} \left(\begin{array}{c} (W_0, L_0) \otimes A^{\otimes(k+1)} \\ (W_0, L_2) \otimes A^{\otimes k} \end{array} \right) \begin{array}{c} \xleftarrow{d^0, H^0} \\ \xrightarrow{d^1, H^1} \end{array} \left(\begin{array}{c} (W_0, L_0) \otimes A^{\otimes k} \\ (W_0, L_0) \otimes A^{\otimes k} \end{array} \right) \\ F^0 \uparrow \downarrow G^0 \\ (W_0, L_2) \otimes A^{\otimes k}, \end{array}$$

where $k = \ell + r$. We define linear maps

$$\begin{array}{lll} \mathbb{1}_{\sigma\alpha} : (W_0, L_0) \rightarrow (W_0, L_2), & \alpha_0 \mapsto \sigma_{2,0}, & \beta_0 \mapsto 0, \\ \mathbb{1}_{\sigma\beta} : (W_0, L_0) \rightarrow (W_0, L_2), & \alpha_0 \mapsto 0, & \beta_0 \mapsto \sigma_{2,0}, \\ \mathbb{1}_{\alpha\sigma} : (W_0, L_2) \rightarrow (W_0, L_0), & \sigma_{2,0} \mapsto \alpha_0, & \tau_{2,0} \mapsto 0, \\ \mathbb{1}_{\beta\sigma} : (W_0, L_2) \rightarrow (W_0, L_0), & \sigma_{2,0} \mapsto \beta_0, & \tau_{2,0} \mapsto 0, \\ \mathbb{1}_{\tau\tau} : (W_0, L_2) \rightarrow (W_0, L_2), & \sigma_{2,0} \mapsto 0, & \tau_{2,0} \mapsto \tau_{2,0}. \end{array}$$

The differentials in diagram (19) are

$$d^0 = \begin{pmatrix} 0 & \mathbb{1}_{\beta\sigma} I_{\ell+r} \\ 0 & \mathbb{1}_{\beta\sigma} I_{\ell+r} \end{pmatrix}, \quad d^1 = \begin{pmatrix} (a_0 \dot{\eta} + c_0 \eta) I_{\ell+r} & a_0 \dot{\eta} I_{\ell+r} \\ 0 & 0 \end{pmatrix}.$$

The homotopy equivalences in diagram (19) are

$$F^0 = \begin{pmatrix} \mathbb{1}_{\alpha\sigma} \eta I_{\ell+r} + \mathbb{1}_{\beta\sigma} \eta I_{\ell} \Sigma_r \\ \mathbb{1}_{\tau\tau} I_{\ell+r} \end{pmatrix}, \quad G^0 = \begin{pmatrix} \mathbb{1}_{\sigma\alpha} \epsilon I_{\ell+r} & \mathbb{1}_{\tau\tau} I_{\ell+r} \end{pmatrix}.$$

The homotopy in diagram (19) is

$$H^0 = \begin{pmatrix} \mathbb{1}_{\alpha\beta} \epsilon I_{\ell+r} + \mathbb{1}_{\alpha\alpha} \epsilon I_{\ell} \Sigma_r & 0 \\ (a_0 \epsilon + \mathbb{1}_{\alpha\beta} \epsilon) I_{\ell+r} + \mathbb{1}_{\alpha\alpha} \epsilon I_{\ell} \Sigma_r & 0 \end{pmatrix}, \quad H^1 = \begin{pmatrix} 0 & 0 \\ \mathbb{1}_{\sigma\beta} I_{\ell+r} & 0 \end{pmatrix}.$$

The differentials for a saddle that splits a circle in region ℓ from the arc component are

$$d_+ = a_0 \dot{\eta} I_{\ell+r}, \quad \tilde{d}_+ = \begin{pmatrix} a_0 \mathbb{1} \dot{\eta} I_{\ell+r} + c_0 \mathbb{1} \dot{\eta} I_{\ell} \Sigma_{r_e} I_{r_n} & 0 \\ 0 & d_+ \end{pmatrix}.$$

The differentials for a saddle that splits a circle in region r from the arc component are

$$d_+ = a_0 I_{\ell+r} \dot{\eta}, \quad \tilde{d}_+ = \begin{pmatrix} a_0 \mathbb{1} I_{\ell+r} \dot{\eta} + c_0 \mathbb{1} I_{\ell+r} \eta + c_0 \mathbb{1} I_{\ell_n} \Sigma_{\ell_e} I_r \dot{\eta} & 0 \\ 0 & d_+ \end{pmatrix}.$$

The differentials for a saddle $P_2(\ell_n + \ell_e, r) \rightarrow P_0^R(\ell_n, r, \ell_e)$ are

$$d_{R2} = \mathbb{1}_{\beta\sigma} I_{\ell_n} \tau_{\ell_e, r}, \quad \tilde{d}_{R2} = \begin{pmatrix} (a_0 \dot{\eta} \mathbb{1} + c_0 \eta \mathbb{1}) I_{\ell_n} \tau_{\ell_e, r} + c_0 \dot{\eta} \mathbb{1} I_{\ell_n} (\tau_{\ell_e, r} \circ \Sigma_{\ell_e} I_r) & 0 \\ 0 & d_{R2} \end{pmatrix}.$$

The differentials for a saddle $P_2(\ell, r_e + r_n) \rightarrow P_0^L(r_e, \ell, r_n)$ are

$$d_{L2} = \mathbb{1}_{\beta\sigma} \tau_{\ell, r_e} I_{r_n}, \quad \tilde{d}_{L2} = \begin{pmatrix} a_0 \dot{\eta} \mathbb{1} \tau_{\ell, r_e} I_{r_n} + c_0 \dot{\eta} \mathbb{1} (\tau_{\ell, r_e} \circ I_{\ell} \Sigma_{r_e}) I_{r_n} & 0 \\ 0 & d_{L2} \end{pmatrix}.$$

Differentials that split one circle into two circles or merge two circles into one circle commute with F^0 and G^0 due to the identities in equation (7).

B.2. Chain homotopy equivalence for $P_0^R(\ell, r, c)$. For a planar 3-tangle $P_0^R(\ell, r, c)$, diagram (18) has the form

$$(20) \quad \begin{array}{c} \left(\begin{array}{c} (W_0, L_0) \otimes A^{\otimes(k+2)} \\ (W_0, L_0) \otimes A^{\otimes k} \end{array} \right) \xrightleftharpoons[d^1, H^1]{d^0, H^0} \left(\begin{array}{c} (W_0, L_0) \otimes A^{\otimes(k+1)} \\ (W_0, L_0) \otimes A^{\otimes(k+1)} \end{array} \right) \\ F^0 \uparrow \downarrow G^0 \\ (W_0, L_0) \otimes A^{\otimes k} \end{array}$$

where $k = \ell + r + c$. The differentials in diagram (20) are

$$d^0 = \begin{pmatrix} 0 & a_0 \dot{\eta} I_{\ell+r+c} \\ 0 & a_0 \dot{\eta} I_{\ell+r+c} \end{pmatrix}, \quad d^1 = \begin{pmatrix} a_0 \Delta I_{\ell+r+c} & a_0 \mathbb{1} \dot{\eta} I_{\ell+r+c} \\ 0 & 0 \end{pmatrix}.$$

the homotopy equivalences in diagram (20) are

$$F^0 = \begin{pmatrix} a_0 \eta \dot{\eta} I_{\ell+r+c} + a_0 \dot{\eta} \eta I_{\ell} \Sigma_r I_c + \mathbb{1}_{\beta\beta} \dot{\eta} \eta I_{\ell+r} \Sigma_c + \mathbb{1}_{\alpha\beta} \dot{\eta} \eta I_{\ell+r+c} + \mathbb{1}_{\beta\alpha} (\eta \dot{\eta} I_{\ell+r} \Sigma_c + \dot{\eta} \eta I_{\ell} \Sigma_r \Sigma_c) \\ 0 \end{pmatrix},$$

$$G^0 = \begin{pmatrix} a_0 \dot{\epsilon} \dot{\epsilon} I_{\ell+r+c} + \mathbb{1}_{\beta\alpha} \dot{\epsilon} \dot{\epsilon} I_{\ell+r} \Sigma_c & 0 \end{pmatrix}.$$

The homotopy in diagram (20) is

$$H^0 = \begin{pmatrix} a_0 (\epsilon \mathbb{1}) I_{\ell+r+c} + \mathbb{1}_{\alpha\beta} (\mathbb{1}_{ee} \circ m) I_{\ell+r+c} + a_0 (\mathbb{1}_{ee} \circ m) I_{\ell} \Sigma_{r+c} & 0 \\ a_0 (\mathbb{1}_{ex} \circ m) I_{\ell+r+c} + \mathbb{1}_{\alpha\beta} (\mathbb{1}_{ee} \circ m) I_{\ell+r+c} + a_0 (\mathbb{1}_{ee} \circ m) I_{\ell} \Sigma_{r+c} & 0 \end{pmatrix},$$

$$H^1 = \begin{pmatrix} 0 & 0 \\ 0 & a_0 \epsilon I_{\ell+r+c} \end{pmatrix}.$$

The differentials for a saddle that splits a circle in region ℓ from the (left) of the arc component are

$$d_+ = a_0 \dot{\eta} I_{\ell+r+c} + c_0 \dot{\eta} I_{\ell} \Sigma_{r_e} I_{r_n+c}, \quad \tilde{d}_+ = \begin{pmatrix} a_0 \mathbb{1} \dot{\eta} I_{\ell+r+c} + c_0 \mathbb{1} \dot{\eta} I_{\ell} \Sigma_{r_e} I_{r_n+c} & 0 \\ 0 & d_+ \end{pmatrix}.$$

The differentials for a saddle that splits a circle in region r from the right of the arc component are

$$d_+ = a_0 I_{\ell} \dot{\eta} I_{r+c} + c_0 I_{\ell} \eta I_{r+c} + c_0 I_{\ell_n} \Sigma_{\ell_e} \dot{\eta} I_{r+c},$$

$$\tilde{d}_+ = \begin{pmatrix} a_0 \mathbb{1} I_{\ell} \dot{\eta} I_{r+c} + c_0 \mathbb{1} I_{\ell} \eta I_{r+c} + c_0 \mathbb{1} I_{\ell_n} \Sigma_{\ell_e} \dot{\eta} I_{r+c} & 0 \\ 0 & d_+ \end{pmatrix}.$$

The differentials for a saddle that splits a circle in region r from the left of the arc component are

$$d_+ = a_0 I_{\ell+r} \dot{\eta} I_c + c_0 I_{\ell+r} \dot{\eta} \Sigma_{c_e} I_{c_n}, \quad \tilde{d}_+ = \begin{pmatrix} a_0 (\eta \dot{\epsilon} \mathbb{1} I_{\ell+r} \dot{\eta} + \dot{\eta} \dot{\epsilon} \mathbb{1} I_{\ell+r} \eta + \dot{\eta} \epsilon \mathbb{1} I_{\ell+r} \dot{\eta}) I_c & 0 \\ 0 & d_+ \end{pmatrix}.$$

The differentials for a saddle that splits a circle in region c from the (right) of the arc component are

$$\begin{aligned} d_+ &= a_0 I_{\ell+r+c} \dot{\eta} + c_0 I_{\ell+r+c} \eta + c_0 I_{\ell+r_n} \Sigma_{r_e} I_c \dot{\eta}, \\ \tilde{d}_+ &= \begin{pmatrix} a_0(\eta \dot{\epsilon} \mathbb{1} I_{\ell+r+c} \dot{\eta} + \dot{\eta} \dot{\epsilon} \mathbb{1} I_{\ell+r+c} \eta + \dot{\eta} \epsilon \mathbb{1} I_{\ell+r+c} \dot{\eta}) & 0 \\ 0 & d_+ \end{pmatrix}. \end{aligned}$$

The differentials for a saddle $P_0^R(\ell, r, c) \rightarrow P_2(\ell + c, r)$ are

$$d_{2R} = \mathbb{1}_{\sigma\alpha} I_{\ell} \tau_{r,c}, \quad \tilde{d}_{2R} = \begin{pmatrix} (a_0 \dot{\epsilon} \mathbb{1} + c_0 \epsilon \mathbb{1}) I_{\ell} \tau_{r,c} + c_0 \dot{\epsilon} \mathbb{1} I_{\ell} (\tau_{r,c} \circ I_r \Sigma_c) & 0 \\ 0 & d_{2R} \end{pmatrix}.$$

The differentials for a saddle $P_0^R(\ell, r_e + r_n, c) \rightarrow P_0^C(\ell + r_e, r_n + c)$ are

$$\begin{aligned} d_{CR} &= a_0 \dot{\eta} I_{\ell+r_e+r_n+c} + c_0 \dot{\eta} I_{\ell} \Sigma_{r_e} I_{r_n+c} + c_0 \dot{\eta} I_{\ell+r_e+r_n} \Sigma_c, \\ \tilde{d}_{CR} &= \begin{pmatrix} a_0 \dot{\eta} \tau_{1,1} I_{\ell+r_e+r_n+c} + c_0 \dot{\eta} \tau_{1,1} I_{\ell} \Sigma_{r_e} I_{r_n+c} & 0 \\ 0 & d_{CR} \end{pmatrix}. \end{aligned}$$

The differentials for a saddle $P_0^R(\ell, r, c) \rightarrow P_{-2}(\ell + c, r)$ are

$$d_{-2R} = \mathbb{1}_{\tau\alpha} I_{\ell} \tau_{r,c}, \quad \tilde{d}_{-2R} = \begin{pmatrix} (a_0 \dot{\epsilon} \mathbb{1} + c_0 \epsilon \mathbb{1}) I_{\ell} \tau_{r,c} + c_0 \dot{\epsilon} \mathbb{1} I_{\ell} (\tau_{r,c} \circ I_r \Sigma_c) & 0 \\ 0 & d_{-2R} \end{pmatrix}.$$

Differentials that split one circle into two circles or merge two circles into one circle commute with F^0 and G^0 due to the identities in equation (7).

B.3. Chain homotopy equivalence for $P_0^L(c, \ell, r)$. For a planar 3-tangle $P_0^L(c, \ell, r)$, diagram (18) has the form

$$\begin{array}{ccc} \left(\begin{array}{l} (W_0, L_0) \otimes A^{\otimes(k+2)} \\ (W_0, L_0) \otimes A^{\otimes k} \end{array} \right) & \begin{array}{c} \xrightarrow{d^0, H^0} \\ \xleftarrow{d^1, H^1} \end{array} & \left(\begin{array}{l} (W_0, L_0) \otimes A^{\otimes(k+1)} \\ (W_0, L_0) \otimes A^{\otimes(k+1)} \end{array} \right) \\ F^0 \uparrow \downarrow G^0 & & \\ (W_0, L_0) \otimes A^{\otimes k} & & \end{array}$$

where $k = c + \ell + r$. The differentials in diagram (21) are

$$d^0 = \begin{pmatrix} 0 & (a_0 \dot{\eta} + c_0 \eta) I_{c+\ell+r} \\ 0 & (a_0 \dot{\eta} + c_0 \eta) I_{c+\ell+r} \end{pmatrix}, \quad d^1 = \begin{pmatrix} (a_0 \mathbb{1} \dot{\eta} + c_0 \mathbb{1} \eta) I_{c+\ell+r} & a_0 \Delta I_{c+\ell+r} \\ 0 & 0 \end{pmatrix}.$$

The homotopy equivalences in diagram (21) are

$$\begin{aligned} F^0 &= \begin{pmatrix} (\mathbb{1}_{\alpha\beta} \dot{\eta} \eta + \mathbb{1}_{\alpha\alpha} \eta \eta) I_{c+\ell+r} + \mathbb{1}_{\alpha\alpha} \dot{\eta} \eta \Sigma_c I_{\ell+r} + (a_0 \dot{\eta} \eta + \mathbb{1}_{\beta\alpha} \eta \eta) I_{c+\ell} \Sigma_r + \mathbb{1}_{\beta\alpha} \dot{\eta} \eta \Sigma_c I_{\ell} \Sigma_r \\ 0 \end{pmatrix}, \\ G^0 &= \begin{pmatrix} (a_0 \dot{\epsilon} \dot{\epsilon} + \mathbb{1}_{\beta\alpha} (\epsilon \dot{\epsilon} + \dot{\epsilon} \epsilon)) I_{c+\ell+r} + \mathbb{1}_{\beta\alpha} \dot{\epsilon} \dot{\epsilon} \Sigma_c I_{\ell+r} & 0 \end{pmatrix}. \end{aligned}$$

The homotopies in diagram (21) are

$$\begin{aligned} H^0 &= \begin{pmatrix} (\mathbb{1}_{\beta\beta} (\mathbb{1}_{ex} \circ m) + \mathbb{1}_{\alpha\beta} \eta \dot{\epsilon} \dot{\epsilon}) I_{c+\ell+r} + a_0 m I_{c+\ell} \Sigma_r & 0 \\ (\mathbb{1}_{\alpha\alpha} \mathbb{1} \epsilon + \mathbb{1}_{\beta\beta} \epsilon \mathbb{1} + \mathbb{1}_{\alpha\beta} \eta \dot{\epsilon} \dot{\epsilon}) I_{c+\ell+r} + a_0 m I_{c+\ell} \Sigma_r & 0 \end{pmatrix}, \\ H^1 &= \begin{pmatrix} 0 & 0 \\ a_0 \epsilon I_{c+\ell+r} + (a_0 \dot{\epsilon} + \mathbb{1}_{\beta\alpha} \epsilon) I_{c+\ell} \Sigma_r & 0 \end{pmatrix}. \end{aligned}$$

The differentials for a saddle that splits a circle in region c from the left of the arc component are

$$d_+ = a_0 \dot{\eta} I_{c+\ell+r} + c_0 \dot{\eta} I_{c} \Sigma_{\ell_e} I_{\ell_n+r}, \quad \tilde{d}_+ = \begin{pmatrix} a_0(\eta \dot{\epsilon} \mathbb{1} \dot{\eta} + \dot{\eta} \dot{\epsilon} \mathbb{1} \eta + \dot{\eta} \epsilon \mathbb{1} \dot{\eta}) I_{c+\ell+r} & 0 \\ 0 & d_+ \end{pmatrix}.$$

The differentials for a saddle that splits a circle in region ℓ from the right of the arc component are

$$d_+ = (a_0 I_c \dot{\eta} + c_0 I_c \eta) I_{\ell+r} + c_0 I_{c_n} \Sigma_{c_e} \dot{\eta} I_{\ell+r}, \quad \tilde{d}_+ = \begin{pmatrix} a_0(\eta \dot{\epsilon} \mathbb{1} I_c \dot{\eta} + \dot{\eta} \dot{\epsilon} \mathbb{1} I_c \eta + \dot{\eta} \epsilon \mathbb{1} I_c \dot{\eta}) I_{\ell+r} & 0 \\ 0 & d_+ \end{pmatrix}.$$

The differentials for a saddle that splits a circle in region ℓ from the left of the arc component are

$$d_+ = a_0 I_{c+\ell} \dot{\eta} I_r + c_0 I_{c+\ell} \dot{\eta} \Sigma_{r_e} I_{r_n}, \quad \tilde{d}_+ = \begin{pmatrix} a_0 \mathbb{1} I_{c+\ell} \dot{\eta} I_r + c_0 \mathbb{1} I_{c+\ell} \dot{\eta} \Sigma_{r_e} I_{r_n} & 0 \\ 0 & d_+ \end{pmatrix}.$$

The differentials for a saddle that splits a circle in region r from the (right) of the arc component are

$$d_+ = a_0 I_{c+\ell+r} \dot{\eta} + c_0 I_{c+\ell+r} \eta + c_0 I_{c+\ell_n} \Sigma_{\ell_e} I_r \dot{\eta}, \\ \tilde{d}_+ = \begin{pmatrix} a_0 \mathbb{1} I_{c+\ell+r} \dot{\eta} + c_0 \mathbb{1} I_{c+\ell+r} \eta + c_0 \mathbb{1} I_{c+\ell_n} \Sigma_{\ell_e} I_r \dot{\eta} & 0 \\ 0 & d_+ \end{pmatrix}.$$

The differentials for a saddle $P_0^L(c, \ell, r) \rightarrow P_2(\ell, r + c)$ are

$$d_{2L} = \mathbb{1}_{\sigma\alpha} \tau_{c,\ell} I_r, \quad \tilde{d}_{2L} = \begin{pmatrix} a_0 \dot{\epsilon} \mathbb{1} \tau_{c,\ell} I_r + c_0 \dot{\epsilon} \mathbb{1} (\tau_{c,\ell} \circ \Sigma_c I_\ell) I_r & 0 \\ 0 & d_{2L} \end{pmatrix}.$$

The differentials for a saddle $P_0^L(c, \ell_n + \ell_e, r) \rightarrow P_0^C(c + \ell_n, \ell_e + r)$:

$$d_{CL} = a_0 \dot{\eta} I_{c+\ell_n+\ell_e+r} + c_0 \eta I_{c+\ell_n+\ell_e+r} + c_0 \dot{\eta} \Sigma_c I_{\ell_n+\ell_e+r} + c_0 \dot{\eta} I_{c+\ell_n} \Sigma_{\ell_e} I_r, \\ \tilde{d}_{CL} = \begin{pmatrix} a_0 \mathbb{1} \dot{\eta} I_{c+\ell_n+\ell_e+r} + c_0 \mathbb{1} \eta I_{c+\ell_n+\ell_e+r} + c_0 \mathbb{1} \dot{\eta} I_{c+\ell_n} \Sigma_{\ell_e} I_r & 0 \\ 0 & d_{CL} \end{pmatrix}.$$

The differentials for a saddle $P_0^L(c, \ell, r) \rightarrow P_{-2}(\ell, r + c)$ are

$$d_{-2L} = \mathbb{1}_{\tau\alpha} \tau_{c,\ell} I_r, \quad \tilde{d}_{-2L} = \begin{pmatrix} a_0 \dot{\epsilon} \mathbb{1} \tau_{c,\ell} I_r + c_0 \dot{\epsilon} \mathbb{1} (\tau_{c,\ell} \circ \Sigma_c I_\ell) I_r & 0 \\ 0 & d_{-2L} \end{pmatrix}.$$

Differentials that split one circle into two circles or merge two circles into one circle commute with F^0 and G^0 due to the identities in equation (7).

B.4. Chain homotopy equivalence for $P_0^C(\ell, r)$. For a planar 3-tangle $P_0^C(\ell, r)$, diagram (18) has the form

$$(21) \quad \begin{array}{ccc} \begin{pmatrix} (W_0, L_0) \otimes A^{\otimes(k+3)} \\ (W_0, L_0) \otimes A^{\otimes(k+1)} \end{pmatrix} & \begin{array}{c} \xrightarrow{d^0, H^0} \\ \xleftarrow{d^1, H^1} \end{array} & \begin{pmatrix} (W_0, L_0) \otimes A^{\otimes(k+2)} \\ (W_0, L_0) \otimes A^{\otimes(k+2)} \end{pmatrix} \\ & \begin{array}{c} \uparrow F^0 \\ \downarrow G^0 \end{array} & \\ & (W_0, L_0) \otimes A^{\otimes(k+1)}, & \end{array}$$

where $k = \ell + r$. We define a 3-fold product map

$$m_3 : A^{\otimes 3} \rightarrow A, \quad m_3 = m \circ \mathbb{1} m.$$

The differentials in diagram (21) are

$$d^0 = \begin{pmatrix} 0 & a_0 \Delta I_{\ell+r} \\ 0 & a_0 \Delta I_{\ell+r} \end{pmatrix}, \quad d^1 = \begin{pmatrix} a_0 \mathbb{1} \Delta I_{\ell+r} & a_0 \Delta \mathbb{1} I_{\ell+r} \\ 0 & 0 \end{pmatrix}.$$

The homotopy equivalences: in diagram (21) are

$$F^0 = \begin{pmatrix} a_0 \mathbb{1} \eta I_{\ell+r} + \mathbb{1}_{\alpha\beta} (\mathbb{1} \eta \mathbb{1} \circ \Delta) I_{\ell+r} + a_0 (\mathbb{1} \eta \mathbb{1} \circ \Delta) I_\ell \Sigma_r \\ 0 \end{pmatrix}, \\ G^0 = \begin{pmatrix} a_0 (\mathbb{1} \dot{\epsilon} \dot{\epsilon} + \dot{\epsilon} \mathbb{1} \dot{\epsilon} + \dot{\epsilon} \dot{\epsilon} \mathbb{1}) I_{\ell+r} & 0 \end{pmatrix}.$$

The homotopy in diagram (21) is

$$H^0 = \begin{pmatrix} (a_0 \mathbb{1} \mathbb{1} \epsilon + \mathbb{1}_{\alpha\beta} m_3 \eta) I_{\ell+r} + a_0 m_3 \eta I_\ell \Sigma_r & 0 \\ (a_0 \mathbb{1} (\mathbb{1}_{e_x} \circ m) + \mathbb{1}_{\alpha\beta} m_3 \eta) I_{\ell+r} + a_0 m_3 \eta I_\ell \Sigma_r & 0 \end{pmatrix}, \quad H^1 = \begin{pmatrix} 0 & 0 \\ 0 & a_0 \mathbb{1} \epsilon I_{\ell+r} \end{pmatrix}.$$

The differentials for a saddle that splits a circle in region ℓ from the left or right of the circle containing the left arc is

$$d_+ = a_0 (\eta \dot{\epsilon} \dot{\eta} + \dot{\eta} \dot{\epsilon} \eta + \dot{\eta} \epsilon \dot{\eta}) I_{\ell+r}, \quad \tilde{d}_+ = \begin{pmatrix} a_0 (\eta \dot{\epsilon} \mathbb{1} \dot{\eta} + \dot{\eta} \dot{\epsilon} \mathbb{1} \eta + \dot{\eta} \epsilon \mathbb{1} \dot{\eta}) I_{\ell+r} & 0 \\ 0 & d_+ \end{pmatrix}.$$

The differentials for a saddle that splits a circle in region ℓ from the (left) of the arc component are

$$d_+ = a_0 \mathbb{1} \dot{\eta} I_{\ell+r} + c_0 \mathbb{1} \dot{\eta} I_{\ell} \Sigma_{r_e} I_{r_n}, \quad \tilde{d}_+ = \begin{pmatrix} a_0 \mathbb{1} \mathbb{1} \dot{\eta} I_{\ell+r} + c_0 \mathbb{1} \mathbb{1} \dot{\eta} I_{\ell} \Sigma_{r_e} I_{r_n} & 0 \\ 0 & d_+ \end{pmatrix}.$$

The differentials for a saddle that splits a circle in region r from the (right) of the arc component are

$$d_+ = a_0 \mathbb{1} I_{\ell+r} \dot{\eta} + c_0 \mathbb{1} I_{\ell+r} \eta + c_0 \mathbb{1} I_{\ell_n} \Sigma_{l_e} I_r \dot{\eta}, \\ \tilde{d}_+ = \begin{pmatrix} a_0 \mathbb{1} \mathbb{1} I_{\ell+r} \dot{\eta} + c_0 \mathbb{1} \mathbb{1} I_{\ell+r} \eta + c_0 \mathbb{1} \mathbb{1} I_{\ell_n} \Sigma_{l_e} I_r \dot{\eta} & 0 \\ 0 & d_+ \end{pmatrix}.$$

The differentials for a saddle that splits a circle in region r from the left or right of the circle containing the right arc are

$$d_+ = a_0 (\eta \dot{\epsilon} I_{\ell+r} \dot{\eta} + \dot{\eta} \dot{\epsilon} I_{\ell+r} \eta + \dot{\eta} \epsilon I_{\ell+r} \dot{\eta}), \\ \tilde{d}_+ = \begin{pmatrix} a_0 (\mathbb{1} \mathbb{1} \eta \dot{\epsilon} I_{\ell+r} \dot{\eta} + \mathbb{1} \mathbb{1} \dot{\eta} \dot{\epsilon} I_{\ell+r} \eta + \mathbb{1} \mathbb{1} \dot{\eta} \epsilon I_{\ell+r} \dot{\eta}) & 0 \\ 0 & d_+ \end{pmatrix}.$$

The differentials for a saddle $P_0^C(\ell_n + \ell_e, r_n + r_e) \rightarrow P_0^R(\ell_n, \ell_e + r_n, r_e)$ are

$$d_{RC} = a_0 \dot{\epsilon} I_{\ell_n + \ell_e + r_n + r_e} + c_0 \dot{\epsilon} I_{\ell_n} \Sigma_{l_e} I_{r_n + r_e} + c_0 \dot{\epsilon} I_{\ell_n + \ell_e + r_n} \Sigma_{r_e}, \\ \tilde{d}_{RC} = \begin{pmatrix} a_0 \dot{\epsilon} \tau_{1,1} I_{\ell_n + \ell_e + r_n + r_e} + c_0 \dot{\epsilon} \tau_{1,1} I_{\ell_n} \Sigma_{l_e} I_{r_n + r_e} & 0 \\ 0 & d_{RC} \end{pmatrix}.$$

The differentials for a saddle $P_0^C(\ell_e + \ell_n, r_e + r_n) \rightarrow P_0^L(\ell_e, \ell_n + r_e, r_n)$:

$$d_{LC} = a_0 \dot{\epsilon} I_{\ell_e + \ell_n + r_e + r_n} + c_0 \epsilon I_{\ell_e + \ell_n + r_e + r_n} + c_0 \dot{\epsilon} \Sigma_{l_e} I_{\ell_n + r_e + r_n} + c_0 \dot{\epsilon} I_{\ell_e + \ell_n} \Sigma_{r_e} I_{r_n}, \\ \tilde{d}_{LC} = \begin{pmatrix} a_0 \mathbb{1} \mathbb{1} \dot{\epsilon} I_{\ell_e + \ell_n + r_e + r_n} + c_0 \mathbb{1} \mathbb{1} \epsilon I_{\ell_e + \ell_n + r_e + r_n} + c_0 \mathbb{1} \mathbb{1} \dot{\epsilon} I_{\ell_e + \ell_n} \Sigma_{r_e} I_{r_n} & 0 \\ 0 & d_{LC} \end{pmatrix}.$$

Differentials that split one circle into two circles or merge two circles into one circle commute with F^0 and G^0 due to the identities in equation (7).

B.5. Chain homotopy equivalence for $P_{-2}(\ell, r)$. For a planar 3-tangle $P_{-2}(\ell, r)$, diagram (18) has the form

$$(22) \quad \begin{array}{ccc} \begin{pmatrix} (W_0, L_0) \otimes A^{\otimes(k+1)} \\ (W_0, L_{-2}) \otimes A^{\otimes k} \end{pmatrix} & \begin{array}{c} \xrightarrow{d^0, H^0} \\ \xleftarrow{d^1, H^1} \end{array} & \begin{pmatrix} (W_0, L_0) \otimes A^{\otimes k} \\ (W_0, L_0) \otimes A^{\otimes k} \end{pmatrix} \\ & \begin{array}{c} \uparrow F^0 \\ \downarrow G^0 \\ \Downarrow \end{array} & \\ & (W_0, L_{-2}) \otimes A^{\otimes k}, & \end{array}$$

where $k = \ell + r$. We define linear maps

$$\begin{array}{lll} \mathbb{1}_{\tau\alpha} : (W_0, L_0) \rightarrow (W_0, L_{-2}), & \alpha_0 \mapsto \tau_{-2,0}, & \beta_0 \mapsto 0, \\ \mathbb{1}_{\tau\beta} : (W_0, L_0) \rightarrow (W_0, L_{-2}), & \alpha_0 \mapsto 0, & \beta_0 \mapsto \tau_{-2,0}, \\ \mathbb{1}_{\alpha\tau} : (W_0, L_{-2}) \rightarrow (W_0, L_0), & \sigma_{-2,0} \mapsto 0, & \tau_{-2,0} \mapsto \alpha_0, \\ \mathbb{1}_{\beta\tau} : (W_0, L_{-2}) \rightarrow (W_0, L_0), & \sigma_{-2,0} \mapsto 0, & \tau_{-2,0} \mapsto \beta_0, \\ \mathbb{1}_{\sigma\sigma} : (W_0, L_{-2}) \rightarrow (W_0, L_{-2}), & \sigma_{-2,0} \mapsto \sigma_{-2,0}, & \tau_{2,0} \mapsto 0. \end{array}$$

The differentials in diagram (22) are

$$d^0 = \begin{pmatrix} 0 & \mathbb{1}_{\beta\tau} I_{\ell+r} \\ 0 & \mathbb{1}_{\beta\tau} I_{\ell+r} \end{pmatrix}, \quad d^1 = \begin{pmatrix} (a_0 \dot{\eta} + c_0 \eta) I_{\ell+r} & a_0 \dot{\eta} I_{\ell+r} \\ 0 & 0 \end{pmatrix}.$$

The homotopy equivalences in diagram (22) are

$$F^0 = \begin{pmatrix} \mathbb{1}_{\alpha\tau} \eta I_{\ell+r} + \mathbb{1}_{\beta\tau} \eta I_{\ell} \Sigma_r \\ \mathbb{1}_{\sigma\sigma} I_{\ell+r} \end{pmatrix}, \quad G^0 = \begin{pmatrix} \mathbb{1}_{\tau\alpha} \dot{\epsilon} I_{\ell+r} & \mathbb{1}_{\sigma\sigma} I_{\ell+r} \end{pmatrix}.$$

The homotopy in diagram (22) is

$$H^0 = \begin{pmatrix} \mathbb{1}_{\alpha\beta} \dot{\epsilon} I_{\ell+r} + \mathbb{1}_{\alpha\alpha} \dot{\epsilon} I_{\ell}\Sigma_r & 0 \\ (a_0\epsilon + \mathbb{1}_{\alpha\beta} \dot{\epsilon})I_{\ell+r} + \mathbb{1}_{\alpha\alpha} \dot{\epsilon} I_{\ell}\Sigma_r & 0 \end{pmatrix}, \quad H^1 = \begin{pmatrix} 0 & 0 \\ \mathbb{1}_{\tau\beta} I_{\ell+r} & 0 \end{pmatrix}.$$

The differentials for a saddle that splits a circle in region ℓ from the arc component are

$$d_+ = a_0 \dot{\eta} I_{\ell+r}, \quad \tilde{d}_+ = \begin{pmatrix} a_0 \mathbb{1} \dot{\eta} I_{\ell+r} + c_0 \mathbb{1} \dot{\eta} I_{\ell}\Sigma_{r_e} I_{r_n} & 0 \\ 0 & d_+ \end{pmatrix}.$$

The differentials for a saddle that splits a circle in region r from the arc component are

$$d_+ = a_0 I_{\ell+r} \dot{\eta}, \quad \tilde{d}_+ = \begin{pmatrix} a_0 \mathbb{1} I_{\ell+r} \dot{\eta} + c_0 \mathbb{1} I_{\ell+r} \eta + c_0 \mathbb{1} I_{\ell_n} \Sigma_{\ell_e} I_r \dot{\eta} & 0 \\ 0 & d_+ \end{pmatrix}.$$

The differentials for a saddle $P_{-2}(\ell_n + \ell_e, r) \rightarrow P_0^R(\ell_n, r, \ell_e)$ are

$$d_{R-2} = \mathbb{1}_{\beta\tau} I_{\ell_n} \tau_{\ell_e, r}, \quad \tilde{d}_{R-2} = \begin{pmatrix} (a_0 \dot{\eta} \mathbb{1} + c_0 \eta \mathbb{1}) I_{\ell_n} \tau_{\ell_e, r} + c_0 \dot{\eta} \mathbb{1} I_{\ell_n} (\tau_{\ell_e, r} \circ \Sigma_{\ell_e} I_r) & 0 \\ 0 & d_{R-2} \end{pmatrix}.$$

The differentials for a saddle $P_{-2}(\ell, r_e + r_n) \rightarrow P_0^L(r_e, \ell, r_n)$ are

$$d_{L-2} = \mathbb{1}_{\beta\tau} \tau_{\ell, r_e} I_{r_n}, \quad \tilde{d}_{L-2} = \begin{pmatrix} a_0 \dot{\eta} \mathbb{1} \tau_{\ell, r_e} I_{r_n} + c_0 \dot{\eta} \mathbb{1} (\tau_{\ell, r_e} \circ I_{\ell}\Sigma_{r_e}) I_{r_n} & 0 \\ 0 & d_{L-2} \end{pmatrix}.$$

Differentials that split one circle into two circles or merge two circles into one circle commute with F^0 and G^0 due to the identities in equation (7).

REFERENCES

- [1] A. Alekseev, A. Malkin, and E. Meinrenken. Lie group valued moment maps. *J. Differential. Geom.*, 48:445–495, 1998.
- [2] M. Asaeda, J. H. Przytycki, and A. S. Sikora. Categorification of the Kauffman bracket skein module of I -bundles over surfaces. *Algebr. Geom. Topol.*, 4(2):1177–1210, 2004.
- [3] M. F. Atiyah and R. Bott. The Yang–Mills equations over Riemann surfaces. *Phil. Trans. R. Soc. Lond. A*, 308:523–615, 1982.
- [4] D. Auroux. A beginner’s introduction to Fukaya categories. *arXiv preprint arXiv:1301.7056*, 2013.
- [5] D. Bar-Natan. Khovanov’s homology for tangles and cobordisms. *Geom. Topol.*, 9:1443–1499, 2005.
- [6] P. Bellingeri. On presentations of surface braid groups. *J. Algebra*, 274:543–563, 2004.
- [7] D. Boozer. Holonomy perturbations of the Chern–Simons functional for lens spaces. *Indiana Univ. Math. J.*, 70:2065–2106, 2021.
- [8] D. Boozer. Khovanov homology via 1-tangle diagrams in the annulus. *arXiv preprint arXiv:2102.10748*, 2021.
- [9] A. Cattabriga and M. Mulazzani. (1,1)-knots via the mapping class group of the twice punctured torus. *Adv. in Geom.*, 4:263–277, 2004.
- [10] B. Gabrovšek. The categorification of the Kauffman bracket skein module of \mathbb{RP}^3 . *Bull. Austral. Math. Soc.*, 88(3):407–422, 2013.
- [11] S. Gervais. A finite presentation of the mapping class group of a punctured surface. *Topology*, 40:703–725, 2001.
- [12] W. M. Goldman. The symplectic nature of fundamental groups of surfaces. *Adv. in Math.*, 54:200–225, 1984.
- [13] M. Hedden, C. Herald, and P. Kirk. The pillowcase and perturbations of traceless representations of knot groups. *Geom. Topol.*, 18(1):211–287, 2014.
- [14] M. Hedden, C. Herald, and P. Kirk. The pillowcase and traceless representations of knot groups II: a Lagrangian–Floer theory in the pillowcase. *J. Symplect. Geom.*, 18(3):721–815, 2018.
- [15] M. Hedden, C. M. Herald, M. Hogancamp, and P. Kirk. The Fukaya category of the pillowcase, traceless character varieties, and Khovanov cohomology. *Trans. Amer. Math. Soc.*, 373:8391–8437, 2020.
- [16] V. Jones. A polynomial invariant for knots via von Neumann algebras. *Bull. Amer. Math. Soc.*, 12:103–111, 1985.
- [17] M. Khovanov. A categorification of the Jones polynomial. *Duke Math. J.*, 101(3):359–426, 2000.
- [18] P. Kronheimer and T. Mrowka. Khovanov homology is an unknot-detector. *Publ. Math. Inst. Hautes Études Sci.*, 113:97–208, 2011.
- [19] P. Kronheimer and T. Mrowka. Knot homology groups from instantons. *J. Topol.*, 4:835–918, 2011.
- [20] P. Kronheimer and T. Mrowka. Filtrations on instanton homology. *Quantum Topol.*, 5:61–97, 2014.
- [21] C. Labruère and L. Paris. Presentations for the punctured mapping class groups in terms of Artin groups. *Algebr. Geom. Topol.*, 1:73–114, 2001.
- [22] L. Rozansky. A categorification of the stable $SU(2)$ Witten–Reshetikhin–Turaev invariant of links in $S^2 \times S^1$. *arXiv preprint arXiv:1011.1958*, 2010.
- [23] P. Seidel. *Fukaya categories and Picard–Lefschetz theory*. Zürich Lectures in Advanced Mathematics, European Mathematical Society (EMS), Zürich, 2008.
- [24] N. F. Vargas. Geometry of the moduli of parabolic bundles on elliptic curves. *Trans. Am. Math.*, 374:3025–3052, 2021.
- [25] M. Willis. Khovanov homology for links in $\#^r(S^2 \times S^1)$. *Michigan Math. J.*, 70(4):675–748, 2021.